RESTORATION OF THE SOUTH AFRICAN POWER SYSTEM AFTER A BLACKOUT INCIDENT

by

Uriel Patrick Heideman

Submitted in partial fulfilment of the requirements for the degree
Master of Engineering (Electrical Engineering)

in the

Department of Electrical, Electronic and Computer Engineering
Faculty of Engineering, Built Environment and Information Technology

UNIVERSITY OF PRETORIA

February 2022

SUMMARY

RESTORATION OF THE SOUTH AFRICAN POWER SYSTEM AFTER A BLACKOUT INCIDENT

by

Uriel Patrick Heideman

Supervisor: Professor Ramesh Bansal

Department: Electrical, Electronic and Computer Engineering

University: University of Pretoria and University of Sharjah

Degree: Master of Engineering (Electrical Engineering)

Keywords: Power system restoration, battery energy storage, power system stability, turbine governor models, power system modelling and simulation

Power system restoration after a blackout incident requires an integrated effort between the generation, transmission and distribution utilities. Restoration planning of the South African interconnected power system (SA IPS) primarily focuses on establishing the generation pool and transmission grid with little focus on the distribution utility requirements. These requirements are the load size for connection, power factor support and the effect of the source voltage within the interconnected power system (IPS). All the focus, as mentioned above, is essential for the distribution utility to plan for IPS restoration. In understanding the operating voltage, load power factor requirements and size of the load that may connect, the distribution utility can align with the generation and transmission expectations. The SA IPS is unique compared to utilities within Europe, the United Kingdom and North America. The challenges stem from not having firm interconnecting tie lines from neighbouring countries to support the restoration of the SA IPS. The SA IPS primarily supports the interconnecting regions. This research intends to highlight the SA IPS vulnerabilities that may cause further delays when implementing restoration initiatives. The intention is to assist with the best course of action during the system restoration stage. The simulation assessment uses a simplified case model in DIgSILENT Powerfactory for the evaluation.

ACKNOWLEDGEMENT

I wish to acknowledge the support of my family, my wife, Rosanne, my daughter Mischka, and my newly born baby boy, Asher, who were both born during the pandemic, which was a challenging time for us. We had no support from family during the pandemic as they were far away and could only express their support and guidance through phone calls and video conferencing. It would not have been possible to complete this thesis if it was not for the help of my family.

I wish to express my sincere gratitude to Professor Ramesh Bansal for accepting to assist me with completing this thesis. Thank you for providing me with the flexibility to work independently and always being professional in providing guidance when the journey became challenging. On many occasions, I was provided with submission extensions, even when I sometimes did not communicate my personal and work-related challenges to him.

LIST OF DEFINITIONS

cold load pickup	The cold-load pickup is a combination of the loss of load diversity effect and motor in-rush currents. The amount of cold load pickup depends upon the nature of the connected load [1].
disturbance	A disturbance in a power system is a sudden change or a sequence of changes in one or more of the power system's parameters [1].
Ferranti effect	The Ferranti rise effect is a long-term overvoltage condition associated with high voltage lines due to lightly loaded conditions [1].
frequency	The utility frequency, (power) line frequency or mains frequency, is the nominal frequency of the oscillations of alternating current (AC) in an electric power grid transmitted from a power station to the end-user [1].
frequency stability	Refers to a power system's ability to maintain steady frequency following a severe incident, resulting in a significant imbalance between generation and load [2, 3].
oscillatory instability	A power system is oscillatory unstable for a particular steady-state operating condition if following a disturbance, and its instability results from insufficient damping torque [2, 3].
rotor angle stability	Angle stability studies whether a power system maintains its magnetic bonds. A power system is stable if its generators keep solid magnetic bonds with the system and one another [2, 3].
steady-state stability	For a particular operating condition, the power system is in a steady-state condition. If, following any minor disturbance, it reaches a steady-state condition identical to the pre-disturbance state [2, 3].

transient stability	A power system is transiently stable for a particular steady-state operating condition and a specific disturbance if, following that disturbance, it reaches an acceptable steady-state condition [2, 3].
voltage stability	Voltage stability is the ability of a power system to maintain adequate voltage magnitudes so that when the nominal system load increases, the MW transferred to that load will increase [2, 3].

LIST OF ABBREVIATIONS

ACE	area control error
AGC	automatic generation control
BESS	battery energy storage system
BMS	battery management system
CC	constant current
CCL	constant current load
CCTV	closed-circuit television
CI	constant impedance
CLPU	cold load pickup
CP	constant power
CPL	constant power load
DER	distributed energy resources
DSM	demand-side management
EHV	extra-high voltage
EMS	energy management system
EPRI	electric power research institute
FERC	Federal energy regulatory commission
FFR	fast frequency response
FR	frequency response
GRA	generic restoration actions
GRM	generic restoration milestones
GRS	generic restoration strategies
IPS	interconnected power system
NERC	North American electric reliability corporation
NERSA	National energy regulator of South Africa
NMD	notified maximum demand
NR	Newton Raphson
NRS	national rationalised standard
NSC	negative sequence current

NSV	negative sequence voltage
OPF	optimal power flow
PCS	power conversion system
Pdf	probability distribution function
pf	power factor
PS	power system
pu	per unit
REIPP	renewable energy independent power producer
REIPPP	renewable energy independent power procurement programme
ROCOF	rate of change of frequency
SA	South Africa
SA IPS	South African interconnected power system
SADC	Southern African development community
SAPP	South African power pool
SCADA	supervisory control and data acquisition
SIL	surge impedance loading
SSC	supervisory system control
TSO	transmission system operator
UFLS	under frequency load shedding
UPS	uninterruptible power supply
UVLS	under-voltage load shedding
VR	voltage response

LIST OF SYMBOLS

e_cP	Exponential load model parameter for the active power component
e_cQ	Exponential load model parameter for the reactive power component
I	Current
I_p	Fraction of constant current load for the real power component
I_q	Fraction of constant current load for the reactive power component
J	Jacobian Matrix
k_{pu}	Exponential load model parameter for the active power component
k_{qu}	Exponential load model parameter for the reactive power component
Θ	Displacement angle (theta)
P	Real power
P_0	Active power initial value
P_p	Fraction of constant power load for the real power component
P_q	Fraction of constant power load for the reactive power component
Q	Reactive power
Q_0	Reactive power initial value
R	Resistance
S	Apparent power
U	Voltage
U_n	Nominal voltage
V	Voltage
Y	Admittance
Z_p	Fraction of constant impedance load for the real power component
Z_q	Fraction of constant impedance load for the reactive power component

TABLE OF CONTENTS

LIST OF FIGURES

LIST OF TABLES

CHAPTER 1 INTRODUCTION

1.1 PROBLEM STATEMENT

1.1.1 Context of the problem

Electricity is the heartbeat of any country's economy, and in the unlikely event of a power system blackout, the consequences are dire [4, 5]. A power system blackout happens due to multiple cascading failures of the designed interconnected power system (IPS) preventative barriers. The result is a total disconnection of the generation pool from the transmission grid and distribution networks [4–8]. Modern-day power system design can withstand most of the sustained and transient faults on an IPS [9, 10]. Various preventative and response mechanisms are in place to enhance overall IPS resilience. Even though a considerable amount of reliability planning goes into the design, operation and maintenance of the IPS, there is no guarantee that a system-wide outage would not occur [11]. Various literature suggests that most blackouts happened during stable system conditions where thermal and voltage measurements were well within the specified compatibility limits [12, 13].

The IPS has many components, each having different means of interaction. Each element has operational limits, and once breached, it results in the disconnection of components or, in specific instances, the failure of components. The loss may occur in a localised area and propagate to the rest of the power system resulting in a total collapse of the IPS [14–16]. In many power systems, transient and sustained faults occur within the IPS [7, 14, 17]. These failures affect the long-term reliability of the assets and terminal equipment impacted by the fault. It may result in the consequent build-up to a risk of failure to critical assets and

equipment. The subsequent impact of blackouts may result in the loss of life due to the dependency from the various sectors on the availability of a firm electricity supply [18, 19].

It is prudent to have restoration plans and procedures in place that are current and aid the efficient and effective restoration of the power system [20]. Literature review informs that the frequency of blackouts in the United States has been once every thirteen years for the past 30 years. The probability distribution function (pdf) of blackout sizes has a power tail, suggesting that the likelihood of blackouts are high based on the size of the power system [5, 16, 17]. A further increase in complexity of operations and maintenance power systems results from the introduction of renewable energy resources to most grids in the world with the drive of moving to purely renewable grids providing sustainable energy with little or no impact on the environment [13, 17].

The power tail pdf proves true for the North American, Sweden, Norway, New Zealand and China blackouts [6, 21]. In 2003, five significant blackouts occurred worldwide in this year alone. From 2002 to 2012, 14 significant outages occurred in total [12, 19, 22, 23]. The occurrences have not slowed down, with more recent cases such as the Brazil blackout (2019) [24] and Jakarta blackout (2019) [25] resulting in 21735MW and 19120MW disconnected, respectively. In addition, on 2 August 2019, the Indian power grid experienced a near-miss event, almost resulting in a blackout incident [26]. A more recent contributing challenge in power systems is digitalised grids resulting in the grid collapsing due to a well-coordinated cyberattack [27–29].

1.1.2 South African context of the problem

Since 2008, the declaration of a national emergency by the transmission system operator (TSO) within the SA IPS forced load-shedding practices. The demand outstripped the supply, and due to challenges in the ageing of generation fleet, inadequate load forecast planning, and strong economic growth, the problems worsened [30]. Since then, the South African (SA) consumer has experienced frequent load shedding interruptions that have significantly staggered the economic development within SA [31]. In addition to having

inadequate generation resources, there are also unreliable generation resources commercially connected to the SA IPS. The implemented maintenance philosophy further worsened generation fleet availability [32]. In 1999, Graeber published a document [33] outlining the Southern African development community (SADC). Over the past 15-year period, if SADC committed to utilising energy efficiency practices, savings could have materialised. There was a surplus of energy within the SADC, including the energy contribution from SA. However, this picture has changed within nine years, as discussed by Bohlmann et al. [30], resulting in frequent power interruptions.

Due to delays in the Medupi and Kusile projects and suffering significant financial losses, the SA government opted to invest in the Renewable energy independent power procurement program (REIPPP) that the Department of Energy drives and implements. As observed in the Eskom IRP 2019, the SA government decided to incorporate renewable energy in grid practices [34]. The current energy model does not maximise renewable energy resources at all voltage levels within the IPS, and the drive of this program seeks to address this shortcoming [34–36]. Taking all the mentioned initiatives and challenges into consideration, as projects continued, generation fleet performance worsened, and load shedding is looming within the SA IPS as the system reserve margin remains tightly constrained [31]. The SA IPS often provides energy, frequently breaching operational limits with a questionable reserve margin. The Medupi and Kusile project significantly reduced the operational and capital expenditure (OPEX and CAPEX) available to the utility, affecting generation maintenance, national refurbishment and capital project budgets [30, 31, 37]. These mentioned elements provide a significant risk within the current operational practice of maintaining supply and demand equilibrium.

1.1.3 Research gap

The SA TSO has a system restoration plan that considers the generation pool and transmission grid. The documented grid code requirement under the Transmission system operation code (version 9) [38] adopted a top-down restoration plan based on the power system's topology. Still, there is no elaboration of the restoration requirements during the

various restoration stages noting that the distribution utility has heterogeneous load resources [38]. Furthermore, there is no standardised approach for the restoration stages.

Further analysis to determine the impact on the distribution sectors provides comfort in understanding the risk associated with the preparation, system restoration and load restoration stages. This research contribution intends to define an integrated optimal restoration solution that will ensure the efficient and effective restoration of the SA IPS without violating the power system adequacy and stability. The research will provide a guideline for distributors to follow when restoring the SA IPS.

1.2 RESEARCH GOALS

There are various risks and opportunities when restoring the SA IPS. The load size contributes to the restoration procedure risk impacting the overall system frequency and provides reactive power support assisting with voltage management on the IPS. The goal is to develop a solution that effectively manages the system frequency and reactive power constraints within the IPS. It is done by determining the optimal load selection and restoration route selection.

1.3 RESEARCH OBJECTIVE AND QUESTIONS

This research aims to understand and answer five questions, namely:

(i) To determine through simulation the optimal amount of load to be connected to the SA IPS during the restoration stages without triggering severe frequency excursion, voltage collapse or voltage oscillations.

(ii) To determine the system's operating voltage with the optimal power factor selected for the connecting load.

(iii) Analyse the impact on the turbine-generator system prime movers response and justify how the connected load assists in maintaining power system stability.

(iv) To assess if the UFLS relays should remain armed on the network during restoration conditions.

(v) Determine the support provided through battery energy storage (BESS) technology and recommend optimal strategies for the deployment of the resource.

1.4 RESEARCH APPROACH

Restoration principles follow similar restoration milestones when restoring the power system. These restoration milestones are classified as generic restoration milestones (GRMs). A literature review investigates the definition, stages of failure and the various restoration stages. Furthermore, information on the possible risks and identifying the necessary mitigations is analysed. In this approach, the following assumptions apply to the simulation assessment:

(i) There is no turbine-generator islanding within the simulation system.

(ii) The system restart originates from the blackstart state using certified blackstart facilities.

(iii) There are no power system reserves to assist with managing the frequency on the IPS during the system restoration condition.

(iv) Automatic voltage regulation is disabled. The system's voltage is managed manually to provide a unified system view during the various simulation tests.

(v) UFLS schemes are enabled to confirm the impact as the load systematically connects to the IPS.

(vi) Design models and parameters will be utilised for the simulation model.

(vii) Assets and equipment are assumed to operate within design parameters for the transmission systems.

(viii) The power system is assumed to be prepared ready for restoration.

The IPS technical constraints and risks worsen during the preparation phase by creating radial feeds for specific load types connecting to the power system. The primary focus is on the electrical model parameters. It incorporates the generator model, transmission grid and distribution customer load. In each of the classified restoration stages, the system inertia changes. For various stages, simulations will provide the required information on the size of the load that may connect to the IPS during system restoration.

1.5 RESEARCH CONTRIBUTION

The research contribution intends to determine an optimal restoration solution that will ensure that the SA IPS is restored efficiently without violating the power system adequacy and stability and understanding the operating limits and constraints during the various stages of restoration.

1.6 RESEARCH OUTPUTS

Target journal: IEEE Transactions on Power Systems
Preliminary title: Restoration of the South African power system after a blackout incident

1.7 ORGANISATION OF THESIS

In Chapter 2, a literature study covers the construct of the SA IPS, the definition of a blackout, the stages of blackout progression and IPS restoration. In addition, the restoration objectives are unpacked. Chapter 3 introduces the challenges experienced during the various stages of restoration, and chapter 4 covers the IPS stability requirements during restoration conditions. In chapter 5, information on the solution methodology for system restoration is discussed. Chapter 6 presents the results of the initial phases of power system restoration to determine restoration rules with associated principles. Chapter 7 shows the results of the impact that different conductor lengths and typical design configurations have on the initial stages of restoration. Chapter 8 presents the results of the simplified model and BESS system analysing the initial stages of restoration, and chapter 9 provides the results for the energisation of the simulation model resembling the SA IPS construct. Chapter 10 concludes all information for the conducted studies and provide scope for future work.

CHAPTER 2 A LITERATURE STUDY OF BLACKOUTS

2.1 CHAPTER OVERVIEW

The electrical power system is the most critical infrastructure as reliable and sustainable electrical grids are essential drivers for economic growth within a country [28]. Power systems operate and are maintained to withstand almost all severe disturbances [12, 18, 38]. When incidents occur, to arrest a rapid or slow frequency decline, voltage decline or system separation, various preventative measures help avoid any further damning consequences that may cascade to a power system blackout [20, 39]. The existing preventive measures provide an acceptable level of assurance compared to industry standards but do not entirely guard against a complete power system blackout [20]. It is vital to have restoration plans in place that are current and to ensure operators' training on restoration plans for effective and efficient restoration of the IPS. In having a restoration plan, the impact to a country's economy, loss of life, impact to the company assets and the environment is minimised to an extent [18, 20, 39].

This chapter discusses the construct of the SA IPS with the associated load mix under section 2.2. The definition of a blackout is unpacked under section 2.3, with the stages of cascading failure, pre-condition to a blackout incident, and the events that could cause a regional or national blackout. Section 2.4 discuss the restoration enhancements for the prevention and response to a regional or national blackout, and section 2.5 discuss the various stages of restoration before the chapter summary under section 2.6.

2.2 THE SOUTH AFRICAN INTERCONNECTED POWER SYSTEM

2.2.1 Background

The construct and composition of the SA IPS intend to highlight the installed generation capacity and assets, to show the size of the transmission grid and distribution network, and finally to summarise the composition of the energy mix within the SA IPS. Information on the length of the critical backbone corridors utilised for system restoration helps appreciate the generation pool and transmission grid challenges experienced. In the analysis, the transmission grid's backbone supports system restoration. There is no information on the impact of different load sizes, possible configurations and the consequence of transmission lines transfer capability and length on the overall restoration of the SA IPS. In not having this information, the decision-making process on the route selection for operators is complex and uncertain, and operators rely on experience to answer the questions.

2.2.2 The generation penetration in the SA IPS

The commercial, operational generation capacity within the SA IPS is approximately 45535MW. The generation capacity includes various energy sources of which conventional thermal plants constitute the more significant portion, equalling roughly 83% in total, amounting to 36822MW [34, 35]. The coal-fired power plants in South Africa consume a capacity of approximately 50000 tons of coal per day. They can produce around 20000 tons of ash per day [32]. Other sources of energy are nuclear (4.1%), pumped storage (6%), gas (5.3%), hydro (1.3%) and wind energy (0.22%) [34], with the operating frequency of the SA IPS strictly managed at 50Hz [30, 38, 40]. The conventional thermal generation plants have six to ten power station units per generation station. Each unit provides 90MW to 600MW of power with the bigger plants, Kusile and Medupi, planned for 2015 [32]. It puts South Africa amongst the largest coal-fired stations in the world [41]. The nuclear power station Koeberg provide 970MW (gross) and 930MW (net) to the power grid. Different hydro technologies each provide different net outputs to the grid, having other capacity options [34]. The SA IPS also has a renewable energy independent power producer (REIPP)

contingent that has increased over the past four years since its inception. The energy contribution since 2019 is approximately 4498MW (installed capacity) [34, 35]. The current operational practices are that REIPP will automatically island if zero voltage and frequency detection occur at the connection point. Table 2.1 summarises the cumulative installed capacity, including commercial plants within the SA IPS.

Table 2.1. Total installed generation capacity (MW) for Eskom [35]

Internal and External	**2019**	**2020**	**2021**	**2022**	**2023**
Eskom installed	45535	46784	46387	46693	45771
REIPP installed	4498	5555	6282	6282	6282
Total	50033	52339	52669	52975	52053

The capacity options for power stations are separated into a baseload, mid merit and peaking resources [35]. The different philosophies seek to cater to all possible capacity constraints for various times and seasons during the day and night to support anticipated and unanticipated supply and demand constraints [34, 38, 42]. The baseload composition is approximately 38339MW. The mid merit and peaking comprise of 600MW of hydro, 2724MW of pumped storage and 2409MW of open-cycle gas turbine (OCGTs) stations, based on Eskom's integrated report of 2019 [34, 35]. The contracted peaking and mid merit stations provide the emergency reserve margin during operation constraint periods. They provide support during constraint periods (peaking period), where reactive power and frequency management becomes challenging based on the demand and generation availability observed from forecasts and actual operational information from the TSO [35]. The renewable contingent in the SA IPS is approximately 10% compared to the SA IPS' installed capacity. These resources are far from the blackstart facilities and generation pool, with most of these resources located in Free State, North Cape, Western Cape and Eastern Cape province [35].

The control of the system frequency is a balancing act. The system operator uses planned load curtailment, instantaneous and supplemental reserves, and demand-side management to support the IPS frequency, ensuring adequate management and operation of the IPS [35, 43]. Apart from the Eskom installed energy sources, there are also firm and non-firm supply agreements with metropolitan and bulk supply municipalities to provide additional interconnected support. SA IPS delivers approximately 45% of Southern African power pools' (SAPP) electricity through transmission and distribution corridors interconnected to Botswana, eSwatini, Lesotho, Mozambique, Namibia, Zambia and Zimbabwe [34, 35]. The non-Eskom installed capacity contingent amounts to 4369MW from various supply resources embedded within multiple transmission and distribution networks [33, 44]. The majority of the coal resources are located in the northeastern area of the SA IPS, within Mpumalanga province. The power grid geographically overlaps Gauteng, Limpopo, Kwa-Zulu Natal and Free State regions [34]. The contractually certified hydro stations are located in the eastern part of the SA IPS, within the Kwa-Zulu Natal province.

2.2.3 Transmission and distribution grids

The entire transmission and distribution power grid in the SA IPS has 387,633km of high, medium and low voltage lines and cable network systems. These lines and conductors transfer electrical energy to the end customer using a cumulative substation capacity of 297,512MVA, shared between transmission and the distribution utilities [34]. The transmission and distribution networks operate and are maintained within acceptable design criteria to ensure system adequacy, reliability and security [38, 42]. Compliance management by implementing various grid code practices assures reliable energy to consumers with different load types [42]. The existing 400kV and 765kV transmission infrastructure covers and flows through all major towns in the SA IPS, with n-1 reliability for most parts of the transmission backbone grid [34, 42]. The strategically positioned hydro, wind, and nuclear station nodes assist with reactive power and voltage management, as the SA IPS' interconnected design is based on the old conventional philosophies [34, 38, 42] (i.e. source located far from load).

2.2.4 The SA consumer energy mix

The SA energy consumption splits into various energy mixes serving different load types. Industry customers consume approximately 52% of the total electricity generated. The consumption is restricted to the contractual notified maximum demand (NMD) [41]. This contractual obligation applies to all customers within the SA IPS. The second more considerable portion of the consumption is the residential sector at 23%, then the commerce and public services at 17%, with the agricultural and transportation sector consuming 3% and 2% respectively [34, 41]. The energisation of the vast network requires voltage support management within manageable operational limits under lightly loaded conditions [45, 46]. The long transmission lines under lightly loaded conditions will be more capacitive and challenging to manage during restoration conditions. As the grid becomes more extended with the limited load that may connect to the SA IPS, the Ferranti challenges will worsen [2].

2.3 THE DEFINITION OF A POWER SYSTEM BLACKOUT

2.3.1 Background

A power system blackout is defined as the total disconnection of generation resources from the transmission grid, impacting many consumers for an extended duration [47, 48]. A power system blackout classifies as a high impact low likelihood event [13, 49] and is measured using three measures, namely [50],

- the amount of unserved energy lost (MWh),
- the amount of power lost (MW) and
- the number of customers interrupted.

Adibi et al. [39] have defined this criterion for reporting significant incidents under regulating authorities in the United States power grids outlining the interruption duration, customers impacted, and megawatts lost.

2.3.2 History of power system blackouts

From 2002 until 2013, the United States has experienced five significant disruptions, and Europe experienced seven severe outages. In developing economies, Brazil has experienced four significant outages, India and Russia have experienced two and three, respectively [9]. In most cases, before the occurrence of a blackout, the power system impacted was operating close to stability limits [18]. When running too close to the stability limits, the rate of change of frequency (ROCOF) may be too high or too sensitive, and under frequency load shedding relays are easily triggered [51]. The average frequency of (national, regional or localized) blackout occurrence in the United States is 13 days. This number has not changed over the past 30 years [17]. Observations of significant blackout occurrences in developed and developing economies in the world appear in Table 2.2.

Table 2.2. The history of power system blackouts [9]

When	Where	Lost load (MW)	Affected persons /areas	Duration (hours)	Initial cause
2012-06-30	India	35670	3.7 billion	19	substation fault
2012-07-31	India	50000	6 billion	7.5	power system instability
2011-02-04	Brazil	8000	40 million	8	transmission lines outage
2009-11-10	Brazil	24436	50 million	4	heavy rainfall with lightning
2007-04-26	Columbia	11700	all over country	3	an outage of power plant
2006-11-04	Western Europe	17000	50 million	1.5	transmission lines outage
2006-09-24	Pakistan	no data	10 million	>5	transmission line maintenance
2006-06-01	China	2150	10 million	3	transmission lines outage
2005-09-12	USA	no data	50 million	4.5	incorrect operation

When	Where	Lost load (MW)	Affected persons /areas	Duration (hours)	Initial cause
2005-06-22	Switzerland	no data	rail network collapse	4	transmission lines fault
2003-09-28	Italy	27702	57 million	20	transmission lines outage
2003-09-23	Switzerland & Denmark	1800	5 million	8	transmission equipment failed
2003-08-14	USA & Canada	61800	50 million	29	transmission lines outage
2002-01-21	Brazil	23766	the whole country	4	transmission lines outage

Momentary (transient) or prolonged (sustained) interruptions occur frequently. All these interruptions, however long the duration, have a lasting impact on the failure rate of equipment or networks that could contribute to more severe cascading failures in the IPS in the future [20, 39]. It is imperative to do frequent network risk assessments post the occurrences of these incidents to determine the lasting impact. Thorough risk assessments on the impacted equipment, with the implementation of the necessary mitigations, will improve the overall integrated resilience of the IPS [19].

2.3.3 Stages of cascading failure

In all instances, blackouts start with an initiating event that cascades to the rest of the IPS [6, 21]. The first event triggers multiple in-between events, affecting the overall stability of the IPS. The initiating event may originate from slow steady-state failures or fast transient events until the final state of complete failure is achieved [18, 19]. Figure 2.1 demonstrates a simplified overview of blackout progression phases until the state of power system restoration.

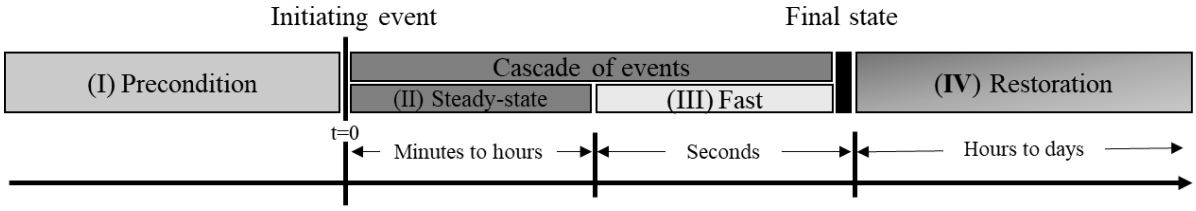

Figure 2.1. Phases of blackout progression (Taken from [18]**,** © 2018 IEEE)

The steady-state sequence lasts from minutes to hours, whereas the fast onset of multiple cascading failures happens within seconds. One of the most notable recorded outages that followed the phases of slow and fast progression occurred in India during the 30th and 31st of July 2012 with a load interruption of 76403MW [10].

2.3.4 Preconditions to blackout incident

The precondition state of the power system is the behaviour before the initial incident; this power system state represents the normalised condition of the IPS [18]. The transmission and distribution grid codes prescribe the normal and abnormal operating conditions based on equipment rate A, B and C limits for assets such as transformers and lines [52]. The system operators manage the overall system to the highest degree of security to ensure that, in most circumstances, the power system is operated within the designed reliability criteria as intended [38, 42]. In most cases, unaccounted risks force the transition to a cascade of incidents. From the pre-condition state, breaches in operational limits result in protection operation, helping to transition back to a state of equilibrium. As these transitions happen, a self-healing process occurs. However, when the self-healing does not arrest the stability challenges, management of the frequency, voltage and power angle becomes extremely difficult, resulting in the transition of cascaded failure. Other devices such as generators, boilers, and turbines also have prescribed operating limits, and failure limits are triggered due to the loss experienced on the IPS [38, 53].

2.3.5 Cascading events transitioning to a nationwide blackout

Cascading failures cause power system blackouts originating from an initial event usually caused by a fault or multiple faults (e.g. single-phase, two-phase or three-phase faults). Low preventative maintenance, severe weather conditions, human errors or asset theft and damage further exacerbate the risk of failure [12, 28, 47]. The two main factors involved in a cascading loss are deterministic and probabilistic. The deterministic factors are breaches in the overarching stability conditions such as the system voltage, frequency and rotor-angle. The triggers or flags would be defined as overloading, over-current faults, low voltage risks, and under-frequency loadshedding relay activation [47, 54, 55].

The lack of operator situational awareness influences the probabilistic aspects. The condition is a result of the failure of critical supporting systems, backup systems, remote terminal unit (RTU) communication, energy management systems (EMS), and the inability to control the system voltage due to critical asset failures and failure of emergency standby capability [47]. The simultaneous breach of probabilistic and deterministic factors will lead to a nationwide power system failure [47, 55]. Based on the stability parameters, once a significant imbalance occurs, the impact is on the frequency, voltage or power angle. A breach in the thermal limit influences all three stability parameters resulting in continuous tripping if the system does not self-heal. The impact exacerbates supply and demand imbalances, resulting in over and under frequency incidents on the IPS. In addition, it affects preventative measures such as loadshedding or stability control if not adequately implemented.

2.4 RESTORATION DURING A BLACKOUT

2.4.1 Background to blackout restoration

The primary objective of utilities is to provide power to the consumer. If there is an interruption, utilities must restore the supply to unserved load efficiently and adequately, managing all associated risks [35, 38, 40, 42]. When the power system is in a state of restoration, the consequences of not having a restoration plan have a prolonged impact on

the restoration duration [56–58]. The restoration plan provides predefined steps to restore the IPS, minimising reoccurring interruptions due to uncertainty in the actions implemented. The restoration of the IPS divides into key critical steps [59, 60]. The task is not straightforward and relatively complex due to restoration challenges encountered per restoration stage, each of which is influenced to the restoration stage [20, 39, 61]. Even though developing restoration plans is a prudent measure in preparing for a blackout, covering all restoration procedures is an impossible task due to multiple possible scenarios that may also change on the day. However, logical and pragmatic restoration plans, principles, rules, route selection and confirmation through stability studies ensure confidence in restoring the IPS [56, 62].

2.4.2 Enhancements to power system reliability

Recognising and accepting that power system blackouts do occur, the reliability planning criteria is revised continuously to ensure effectiveness [63]. It is to provide a positive cost-benefit analysis based on the expansion plans and design proposals for the device installed to show future profits due to reliability improvements ensuring continuity of supply. Also, the overall power system continuously has flexibility in operations and maintenance and supports the connection of prospective customers for future revenue streams [38, 42].

In the SA IPS context, a widespread power system blackout constitutes a disaster. Under the Disaster management act [Act 57 of 2002], as a responsible electricity supplier, each utility must ensure the availability of an updated and exercised contingency plan in the event of a large-scale interruption. The contingency plan must ensure people's safety with minimal impact to consumers, assets and the environment [64]. The occurrence of blackouts has led to improvements under regulatory, economic and technical considerations [63]. From multiple unit trips to cascading line failures leading to system separation, the impact is always a substantial amount of customers without supply [12, 19, 28, 65].

Review and research by international independent regulatory authorities such as the Federal energy regulatory commission (FERC), the North American electric reliability corporation

(NERC) [4, 18], and for SA, the National energy regulator of South Africa (NERSA) [38, 43] assist with developing reliability guidelines and grid code enhancements. The learnings, through the investigations conducted by independent international organizations such as CIGRE and IEEE, streamline the best possible improvement for enhanced prevention and response [9]. Continuous benchmarking against global learnings ensure that utilities stay current with new technological advancements and education from around the world.

2.4.3 Reliability enhancement to the SA IPS

2.4.3.1 Preventative measures

The power system design can withstand most unplanned incidents. Due to the size and complexity of the IPS, the design incorporates n-1 firmness for the most critical parts of the power system [38, 42]. The TSO is responsible for managing the national frequency and voltage at all EHV busbars; this influences the power transfer capabilities within the various distribution networks. The TSO must ensure that the reactive power reserve margin is adequately maintained to support the exportation of real power to end users during all operational periods of the day [48]. In the case of a network or substation failure, the restoration plans will guide the TSO on the most effective restoration procedure to ensure efficient restoration of the failed asset or power grid [38, 42]. The future development plans must ensure future economic growth and future system security that support maintaining continuity of supply [42].

In the unlikely event of a transient or steady-state frequency incident, there are manual and automatic preventative measures in place that assists with the management of the national system frequency [38, 43]. The steady-state and dynamic manual response divides into various layers of protection such as the implementation of demand-side management (DSM) initiatives, load curtailment measures through pre-agreed customer contracts and through implementing the following loadshedding practices (stages 1 to 8):

(i) The TSO calls upon the implementation of manual load shedding by reducing between 1000MW to 4000MW (stage 1 to 4) on the IPS. This initiative is to arrest the anticipated and unanticipated mismatches between supply and demand [38, 43].

(ii) The TSO calls upon implementing contingency load shedding between 5000MW to 8000MW (stage 5 to 8) [38, 43].

(iii) Or lastly, the TSO implements unscheduled shedding on the IPS to arrest the system instability beyond stage 8 [38, 43].

The speed onset of a transient frequency incident is ordinarily quick, and the operator reaction time to a transient frequency incident is limited. A fast frequency response (FFR) mechanism, under frequency loadshedding (UFLS), is employed to assist with maintaining IPS security in the event of a transient frequency incident [13, 38, 42, 51]. The UFLS preventative barriers have multiple embedded layers of protection aligned to system frequency triggers set points. The UFLS protection scheme operates when the following frequency setpoints are triggered as specified in Table 2.3:

Table 2.3. Automatic load-shedding frequency scheme design [38]

f – trigger (Hz)	Relays reaction time (ms)	Stages classification	Reduction (%)
49.2	300	Customer Voluntary Automatic 1	3.3
49.1	300	Customer Voluntary Automatic 2	3.3
49.0	300	Customer Voluntary Automatic 3	3.3
48.8	500	Mandatory 1 (MAN 1)	10
48.5	500	Mandatory 2 (MAN 2)	10
48.2	500	Mandatory 3 (MAN 3)	10
47.9	500	Mandatory 4 (MAN 4)	10

If the frequency hovers between 49.7 and 49.5Hz for longer than 1 hour, a low-frequency alarm will emerge, providing situational awareness to the operator. From Table 2.3, the first frequency trigger, in the event of an incident, is set to 49.2 Hz resulting in 3.3% of the total demand being curtailed when triggered accurately. If all seven stages are activated, the result is a 50% load reduction from the IPS [38, 42, 43]. In the unlikely event that the UFLS

protective barriers function inadequately, a national frequency collapse will occur, resulting in a nationwide blackout incident [66]. Any frequency decline beyond 47.5Hz results in the automatic disconnection of generators from the IPS due to the built-in protection failsafe of these systems, avoiding severe damage as turbine-generator shafts begin to vibrate below 47.5Hz resulting in costly damages to the entire plant [67].

2.4.3.2 Response and Recovery measures

In addition to preventative measures, there are also response and recovery measures to assist with the power system's normalisation after a blackout incident. The generation pool primarily comprises fossil plant stations, as mentioned previously [34, 35]. Within the SA IPS, certified fossil-fired power plants provide islanding support during unhealthy system conditions. Fossil power plant stations are contracted to perform unit islanding according to grid code practices that support the system restart requirements [38, 42]. The operating philosophy around unit islanding is maintaining islanded fossil power plants in a hot state, allowing for the efficient synchronisation and restoration of the IPS due to loss of synchronisation after a blackout has occurred. It is a crucial response function in the restoration process and is regularly tested to ensure compliance and enhanced system resilience [12, 38, 42, 68]. If the islanding barrier is unavailable after a blackout, blackstart facilities enable the SA IPS to rebuild for normalisation. The boiler and turbine conditions can be within the following restart states, namely [39]:

(i) hot-restart system state.
(ii) hot-boiler-hot-turbine.
(iii) hot-boiler-cold-turbine.
(iv) cold-boiler-cold-turbine.
(v) a cold system state.

The mentioned conditions significantly hamper restart times if within the cold restart states. Testing of blackstart facilities is done as per the grid code requirements to ensure compliance, preparedness and resilience as with islanding facilities. These tests can be quite strenuous and are performed every three years [38, 42, 69].

2.5 VARIOUS RESTORATION STAGES

2.5.1 The Purpose of restoration stages

The restoration tasks guide transmission and distribution system operators on the critical functions performed to secure the power system and prepare the IPS for the system restoration stage [62]. With the separation of restoration tasks into the various restoration stages, it is crucial to understand the critical restoration tasks during each restoration stage. It is an essential part of the recovery and overall normalisation process [59]. The system restoration stage is the focal point for this thesis, requiring the establishment of the power system backbone, commonly referred to as the cranking path [56]. There are multiple interdependencies between the restoration tasks that will impact the overall stability of the IPS [59]. There must be a shared understanding and alignment to the tasks required to achieve and maintain overall power system stability [20, 39].

Apart from the restoration task issued from the technical plans, there should be instructions focussed on the preservation of DC and executing business continuity plans (BCP) for the conservation of standby services that support system restoration [39, 70, 71]. The execution of restoration actions should be minimised as any insignificant breaker operation, busbar preparation, and transformer preparation step drain stored energy from backup batteries as there is no AC supply available [72, 73]. It would be good to execute all instructions affecting system restoration from the centralised place or coordinate from a centralised location to streamline critical activities to avoid unnecessary operations impacting restoration activities [70, 72–74].

Restoration plans should be developed, exercised and maintained [20, 39], understanding all interdependencies between generation, transmission and distribution utilities as normalisation of the IPS is an integrated process [59]. Vulnerabilities in timing requirements for generation services must be tabled and understood as crucial coordination steps [75]. Problems exist with the power transfer capability from assets such as generators to transformers and reactive power compensation support to absorb large amounts of reactive

power, assisting with managing receiving end voltage [39, 60, 76, 77]. This section intends to outline the various restoration objectives restoration goals and to list the multiple steps for the normalisation of the SA IPS [60, 62].

2.5.2 Restoration goals and objectives

The goal after a blackout condition is restoring the IPS to the normalised state as observed before the interruption. This goal is a complex and integrated task between system operators, planners, strategic, tactical and onsite operational support teams [58, 60]. Having a sound thought through restoration plan requires that all logistical matters be addressed and aligned beforehand as it is an enabler for the successful, efficient restoration of an IPS [20, 39, 59, 60, 78]. Deliberate restoration steps help to accelerate the restoration process. Normalising the power system is achieved by establishing the critical path [58] and executing necessary actions during the preparation and system restoration stages.

There are various options of which Fink et al. [56] suggest the establishment of generic restoration actions (GRAs), Adibi et al. [60] offer generic restoration strategies (GRS) and under the current report from EPRI (2010) [62], proposed using GRMs. From the suggested restoration initiatives, generic actions exist between the mentioned strategies or steps that follow sequentially. These are executing system preparation and restoration actions and eventually transitioning to load restoration steps. From all required actions, the activities that frequently occur are the following six steps:

(i) Generator startup sequencing
(ii) Transmission path search
(iii) Load pickup sequencing
(iv) Optimal power flow (OPF) confirmation
(v) Confirmation of power system security
(vi) Move to the following restoration sequence

The first important consideration is determining the generator startup sequence, falling under the planning to restart criteria [20, 39, 71]. The generator unit startup sequence, typically

linked to blackstart facilities, provide the initial starting load through energising auxiliary systems load for the generator units [20, 59, 60]. The blackstart facilities provide the initial startup support for the startup sequence for the generator unit linked to the blackstart facility [20, 60, 70, 75]. The second consideration is selecting the optimal transmission path based on the load centre's distance, the reactive power constraints, the load type, and acceptable load size. Based on the considerations mentioned, the optimal transmission path is selected where voltage, reactive power and frequency are managed effectively after the energisation of the transmission path chosen [20, 39, 56, 59, 60, 62].

The third consideration is performing load pickup in steps to manage the system frequency, reactive power constraints and cold load pickup challenges [60, 75, 79–81]. The second and third considerations are interdependent. The load pickup requirements must be determined beforehand with specific rules for the size and type of the load that connect without causing a frequency excursion on the IPS [20, 71, 75, 82]. The fourth consideration is to determine if the IPS will solve OPF. The OPF is a steady-state assessment confirming that the voltages and thermal constraints are adequately managed. Once verified, the fifth consideration is confirmed through a momentary assessment of the stability parameters within the IPS. The subsequent restoration step commences, whereby the exact steps repeat (steps 1 to 5) in the sequence presented to ensure completeness [20, 21, 39, 83–85].

The mentioned steps simplify the required actions ensuring stability to the IPS. A more detailed analysis is necessary to guide on the limitations of the existing assets and equipment used for a comprehensive technical restoration plan [20, 39, 62, 69, 71]. The protection settings boundaries must be understood and adjusted for restoration conditions to avoid any further severe damage to assets [42]. It is essential to classify and understand the restoration stages and overall system normalisation [75]. Each restoration stage has different priority levels in load type and load size as a more stable IPS is achieved after the blackout incident [68]. The restoration stages after a blackout incident divide into the following steps shown in Figure 2.2.

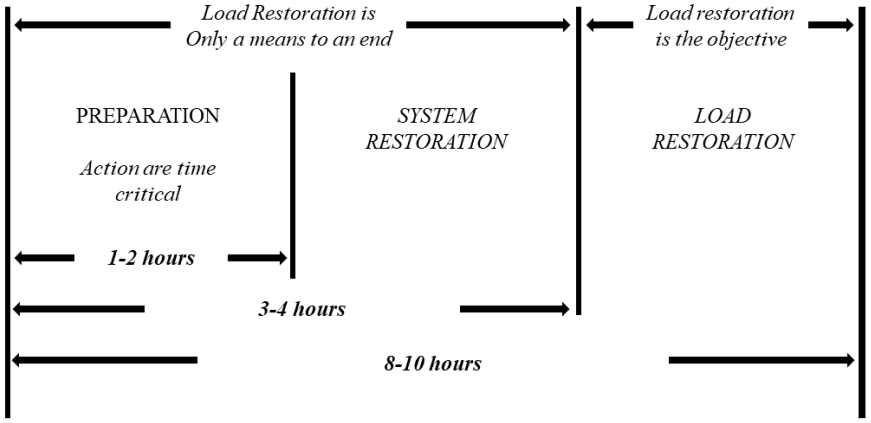

Figure 2.2. The restoration stages with revised tasks (Taken from [71]**,** © 2008 IEEE)

The restoration stages also provide information on the vulnerability within the IPS at a particular time. The operator will be more careful in connecting more significant load during system restoration when compared to load restoration, as when in load restoration, the IPS will be more stable through having multiple meshed configurations [71]. It is essential to understand these criteria through simulation to determine how far the power system's operating limits can stretch. The analysis of operating limits through simulation of transient and steady-state stability analysis provides further insight in chapters to follow [39, 60, 68, 69, 71, 75].

2.5.3 Preparation for system restoration

During the system preparation stages, to ensure adequate network preparation for system restoration, predetermined switching strategies provide the smooth transition to system restoration [56, 60, 73]. Before the commencement of system preparation, the distribution operator and TSO on the desk must assess the power system state after the cascading failure to determine if the restoration plan as developed can be executed [60]. This task will take some time as the system will have experienced excessive alarms from multiple protection devices triggered and sent to the SCADA systems [59, 60, 86].

The number of SCADA alarms under normalised system conditions is typically between 2000-5000 indications. During the cascading failure of IPS components, the SCADA alarms

that the operator and SCADA system must manage can be over 10000 alarms [70]. The power system is typically broken down into smaller restoration islands to manage grid reliability and resilience to provide options for the stable parallel restoration of the IPS [39, 60]. Decisions on the desks are guided by predetermined principles [59, 70, 78], such as the switching strategy of an "all open" or "controlled operation" may be followed, as discussed in Adibi et al. [70]. The all open approach purely rely on the available standby capability at the various stations as well as the operating staff and SCADA capability that is available to a utility.

2.5.4 System restoration

System restoration is when the blackstart facilities provide auxiliary power to the generation connected fleet. Stabilisation happens through using the power station house loads and energising specific customers to assist generators and turbines [20, 87, 88]. Tap changers at the generator step-up transformers and auxiliary transformers must be optimised to improve the power transfer capability to the end customer [56, 60, 68, 71]. As demonstrated in section 2.2 under the construct on the SA power system, the generation pool is typically far from the load centres. It indicates that reactive power management and voltage control is a significant challenge during the critical stages of system restoration, as there will be a limited amount of generation fleet connected to the IPS [89].

2.5.5 Load restoration

As the system transitions towards the load restoration stage, the system frequency bias is more robust, resulting in a more robust frequency response to the load connected. The somewhat healthy frequency bias allows for a more copious load to the IPS [68, 71]. A more stable restoration island exists from creating meshed networks and systems using transmission lines, transformers and energisation of more power station units. Increased power system fault levels allow for the startup of larger motorised loads on the power system, with manageable frequency deviations and voltage sag due to the inrush currents [20, 59,

78]. When the load restoration stage commences, it will be considerably better to manage assets' resource capability and the associated risk such as IPS failure.

2.6 CHAPTER SUMMARY

Based on the topology outlining the position of the generation station and possible blackstart position, an assumption is that the proposed restart of the SA power system will commence from the northeastern part of the SA IPS. The restoration of the remaining IPS is at a much later stage after achieving sufficient reliability and stability, falling within the system restoration stage. Careful analysis should determine the optimal restoration route considering various enabling factors to ensure the IPS restoration activities. Another assumption is that in the absence of the SA IPS, the SAPP will manage their localised supply requirements.

CHAPTER 3 POWER SYSTEM RESTORATION CHALLENGES

3.1 CHAPTER OVERVIEW

The restoration challenges are different during the restoration and recovery stages. In being proactive, underlying challenges identified provides a better understanding of the required actions on the day [4, 39, 60]. While offline analysis work through simulation offers a degree of preparedness, real-time simulation response assists with decision-making for the operators when the prepared simulation response does not cover unaccounted scenarios during a real-time system response [16, 57, 78, 82]. When restoring the IPS, fundamental problems frequently occur during the restoration process; these problems are reactive power balancing, load and generation balancing and the protection operation [20, 71, 82, 90, 91]. Each aspect forms part of a high-level description of the possible challenges during restoration conditions. The IPS construct, the equipment, and operational asset limitations influence the challenges experienced within the IPS. The response to various load types (e.g. leading or lagging power factor load types) connected to the grid contributes to the risks but may also provide possible mitigations [61, 70, 71].

This chapter outlines the various challenges during the preparation and system restoration stages. The first challenge introduced is reactive power balancing and management during the initial phases of restoration under section 3.2. Sections 3.3 and 3.4 discuss the load-generation balancing and coordination requirements within the IPS. The balancing and coordination act is a fundamental success factor when developing, exercising and executing a technical restoration plan. In section 3.5, the power system protection challenges are briefly touched on, and section 3.6 discuss the energy storage and auxiliary systems considerations

that support the effective and efficient restoration of the IPS. Section 3.7 provides a summary of the information discussed within this chapter.

3.2 REACTIVE POWER BALANCING AND MANAGEMENT

3.2.1 Background to reactive power balancing and management

Reactive power is a fundamental consideration supporting real power transfer from the generating station to the end-user or customer [38, 92]. Reactive power qualifies as an ancillary service due to the voltage security support provided in the IPS [93]. The lack of available reactive power contributed to IPS blackout causes, as demonstrated by Veloza et al. [92] due to the system experiencing a voltage collapse. Results on the impact of reactive power requirements on the SA IPS is provided in Chapter 7 using simplified models to determine principles for line design and conductor length selection.

3.2.2 Generator reactive power constraints

Sustained operation of the power systems is impossible unless generator frequencies and bus voltages are kept within strict limits [68, 71]. Automatic closed-loop controls meet these requirements under the operators' supervision [71, 94]. However, during the initial phases of restoration, when individual generators are up to speed, and large blocks of load are gradually connected, perturbations outside the range of operating limits are inevitable. Hence, hands-on control by system operators is necessary [60, 61]. Understanding power station generators maximum and minimum limits during the startup sequence are vital [60, 90, 91, 95]. Generators would typically operate between 40 and 60 per cent of their rated capacity due to the limited load available within the IPS during system restoration as the system is being rebuilt [85]. The actual limits significantly differ from the rated limits provided by manufacturers [71, 90]. The manual management, optimal setpoint adjustment and disconnection of certain automatic functions (e.g. AGC) from the IPS ensure the system and network operators [64].

3.2.3 Ferranti over-voltages and surge impedance loading

During the early stages of system preparation and system restoration, there are challenges with reactive power management due to the lack of generation resources within the IPS following a blackout [92]. Also, energised lines contribute to more severe Ferranti over-voltages that will impact primary plant assets and secondary plant equipment during the commencement of system restoration (e.g. insulator flashovers and other equipment damages) [45, 46]. The presence of negative sequence current (NSC) and negative sequence voltage (NSV) worsen through the existence of un-transposed transmission lines [46, 96, 97].

The circuit model is represented by series impedance (Z) and capacitive reactance (X_c) [3, 98]. As the network extends, Z and X_c also increase, resulting in increased voltages as, during system restoration, the IPS is lightly loaded. The coordination of restoration activities, balancing load and generation, and optimum generation startup sequence are intricate steps during the system preparation and restoration [20, 39, 60, 61, 78]. Transmission lines have two critical equipment limitations, the thermal limit and stability limit of the line. The thermal limit is a static factor based on the design of the transmission line, and the stability limit is a dynamic factor that changes as the length of the power system extends [99]. Figure 3.1 provides a simplified view of the two stability limits.

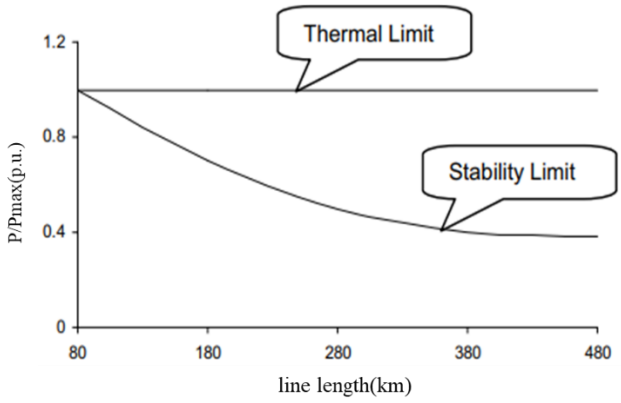

Figure 3.1. Thermal vs stability limit of EHV lines (Taken from [99]**,** © 2006 IEEE)

The inherent characteristic of transmission lines is that the equipment becomes more and more capacitive over longer distances, resulting in severe risks on the upstream IPS when active capacitive dampening is not present. The dynamic stability limit is also known as the surge impedance loading (SIL) [99].

3.3 LOAD AND GENERATION COORDINATION

The IPS frequency indicates the system's health in terms of supply and demand [38]. In the absence of a stable system frequency, and if the frequency drops below 47.5Hz, the risk is possible mechanical damage to turbine-generator machines [52]. For the distribution system operator and network operators, the primary dynamic contributor to the dynamic behaviour of the load is cold load pickup (CLPU) after an extended interruption duration [100, 101]. CLPU is an important consideration that affects the overall system frequency. The anticipation of CLPU during each stage of the restoration process is an important consideration that may affect the frequency stability of the IPS [81, 102–104]. The additional inrush contribution could significantly upset the state of equilibrium if not carefully managed [82]. In some instances, the effects of CLPU can result in an approximate increase in the steady-state expected load of 2 to 5 times (200% to 500%), resulting in a significant addition of unplanned additional load added to the IPS [105]. The gradual careful coordination of load during system restoration helps manage specific cases on the distribution network's MV side. Partial restoration assists in managing the large inrush currents [104].

3.4 LOAD AND GENERATION BALANCING

Based on assessments conducted around the IPS blackouts between 2005 and 2016 [18], the challenges identified were the load and generation balancing during restoration activities. NERC formed a diverse reliability committee to ensure continuous integration [4, 21]. In the construct of the SA IPS, the tie-line interconnection support is not available during the restoration of the IPS. Under normalised conditions, support is provided from the SA IPS to other neighbouring countries within the SADC. The initial stages of restoration will have changed the system, grid and network configuration into an abnormal state due to the

multiple failures. The number of generation units and subcomponents damaged during the cascaded loss is unknown [52]. It is imperative to understand the generator ramp rates and response support requirements from transmission and distribution utilities to align IPS balancing. The balancing and coordination of the power grid require interactive sessions, testing of simulation models [106], updating simulation models based on the existing operational performance tests performed at the power plants to ensure model calibration accuracy.

3.5 PROTECTION OPERATION CHALLENGES DURING POWER SYSTEM RESTORATION

Implementing IPS protection measures ensures power system protection against all faults. In measuring protection performance or accuracy, it is vital to ensure that the relays trip correctly at all times [52]. The IPS relays for protection operation is graded having various types of protection functionality and sensitivity selection ranging from overcurrent protection to under frequency load shedding, to name a few [38, 107]. Relays are equipped with specific functions and are selected and placed based on the role fulfilled [20, 39, 108]. In the event of a national blackout, protection components would have opened breakers, whereas other components auto-reclose breakers in the event of a fault and may have locked out. Auto-reclosing have to be disabled to avoid nuisance tripping [58], and the breakers that have been locked out have to be reset if they form part of the restoration plan. In some instances, field operators prepare the power system due to the protection philosophies applied to components [109].

Protection challenges exist due to grid configuration changes linked to a total systems failure affecting protection performance accuracy [59]. For a complete technical restoration plan, protection engineers must incorporate blackout-planning scenarios that support system restoration to ensure that during the transition to system normalisation, the installed relays function effectively. It may require additional planning incorporated into the operational restoration plans, which is purely an extra layer of protection should the restoration of the IPS be prolonged for unaccounted reasons [13, 20, 39]. It becomes riskier if there is no

situational awareness on the IPS. The protection concerns in the absence of restoration planning solutions are distance, differential and excitation protection systems in generation, transmission and distribution systems. The evaluation of wrongful tripping of protection relays is to avoid performance challenges during system restoration and load restoration conditions [13, 20, 39].

The second challenge is the presence of excessive standing phase angles during system restoration. It is a critical step in the management of rotor angle stability. Extreme standing phase angles usually exist between interconnecting tie lines. The constant load torque is adjusted by regulating the generator real power output to manage the risk of significant phase angles [20, 39, 108]. Lastly, due to unsymmetrical conductor spacing in the IPS, unacceptable negative sequence currents (NSC) exist. It is vital to determine the correct amount of load as the system is rebuilt to limit the impact of NSC as this will cause additional trips in various components in the power system (i.e. generators, lines and transformers) [20, 39, 71, 108].

3.6 ENERGY STORAGE AND AUXILIARY SYSTEMS ENERGIZATION

In a normalized power system configuration, all equipment such as breakers, substation essential loads, current transformers and voltage transformers receive an AC supply source from the grid. The AC source of supply provides a charging current to the installed batteries in substations from the auxiliaries of the station transformers. In the absence of AC supply from the grid, the installed batteries will provide standby support to substations restored (supporting breaker protection), with other essential loads coupled such as remote terminal units, substation lighting, electric fencing and CCTV surveillance, to name a few [42, 60, 70].

Other systems remotely located away from the substation, such as telecommunication infrastructure, also receive an AC source of supply from the grid [72, 73]. The telecommunication infrastructure is also equipped with backup batteries ensuring the necessary redundancy of the telecommunication link to the SCADA system. The SCADA

systems within a power system are equipped with a UPS, backup batteries and diesel generators, providing backup support in the absence of grid supply. It is vital to incorporate standard operating procedures for the preservation of DC within the IPS restoration plan, as well as supporting and enabling infrastructure that allows for efficient restoration after a blackout. The DC preservation practices should form part of the technical restoration plan during system preparation, and instructions should be executed from the control centre and monitored from the SCADA systems [36, 64, 72].

3.7 CHAPTER SUMMARY

Challenges exist for load restored to the IPS. The system is in a state of low-frequency bias with inadequate inertia to manage the connection of larger loads as FFR resources will not be available. The avoidance of unintended frequency excursions is managed by carefully selecting load size. The distribution network should be restored gradually to ensure stability in the system frequency response and effectively manage CLPU. The analysis of multiple setpoints within the simulation model assist with the extraction of the optimal mode of operation for system frequency and voltage during system restoration. It will help with the imminent Ferranti challenges on the IPS during system restoration. Restoration plans and procedures should incorporate standard operating procedures to preserve DC to ensure operating efficiency during system restoration.

CHAPTER 4 STABILITY REQUIREMENTS DURING RESTORATION CONDITIONS

4.1 CHAPTER OVERVIEW

The various stability requirements provide insight into the integrated coordination and decision-making during the system restoration stage. The transmission and distribution grid code outline the stability requirements providing the principles applicable for the studies performed. NERSA provides insight into the voltage compatibility limits, voltage dips and dip duration parameters to be cognisant of during system restoration. This section intends to describe the multiple stability criteria and to highlight the focus areas for the simulations, which will be the inertial response and voltage stability requirements.

Section 4.2 of this chapter introduce the definition of power system stability, unpacking the classification of stability. In section 4.3, the details on the frequency stability requirements for high and low-frequency excursions provide insight into the limitations within the frequency band for the SA IPS. Section 4.4 go into the requirements for voltage stability, looking at the steady-state conditions for stability. Lastly, section 4.5 briefly introduce and discuss the concept of rotor angle stability before the chapter summary under section 4.6.

4.2 DEFINITION OF POWER SYSTEM STABILITY

The definition of power system stability is the ability of an electrical power system for a given initial operating condition to regain a state of equilibrium after being subjected to a disturbance [53]. Numerous recorded significant blackouts were due to cascaded failure of

equipment, triggered by the breach of operational stability limits over short or extended periods [10, 12, 13]. Typically, under an n-2 loss for multiple transmission EHV line components, the risk significantly increases. To prevent a cascading incident, performing various stability assessments, calibrating the integrated IPS protection devices to provide assurance, ensure compliance to reliability and resilience enhancements stipulated in the transmission and distribution grid codes [38, 42]. Figure 4.1 describes the representation of the multiple components and subcomponents assessed for IPS stability.

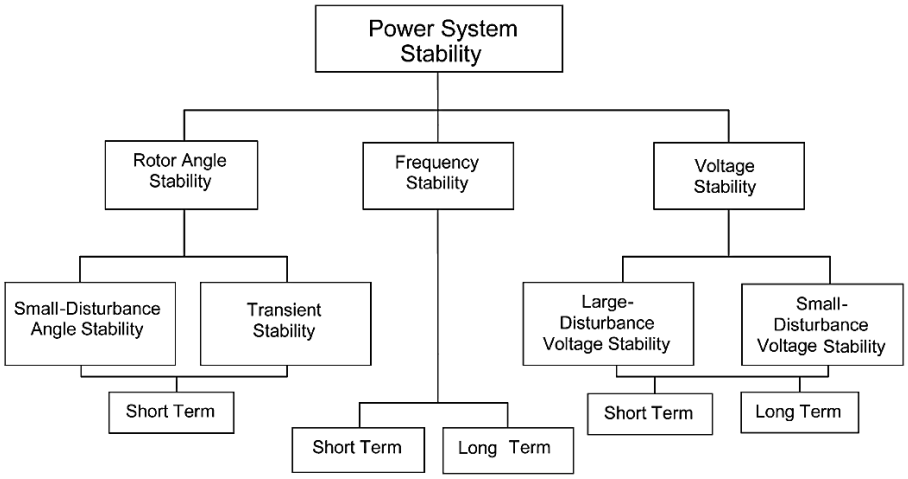

Figure 4.1. Classification of power system stability (Taken from [53]**,** © 2004 IEEE)

The reliability planning criteria requires a single level (n-1) of redundancy for all critical assets such as transformers and lines within the SA IPS [42]. The same applies to reliability standards and guidelines [5, 13, 49]. The requirement may not be applicable in areas with limited impact to a specific localised region. In areas where the event risk is significant, additional firmness caters for n-2 incidents [38, 42].

4.3 REVIEW OF FREQUENCY STABILITY

The frequency stability barrier of protection may experience short term or long term stability challenges that require consideration. Cases of short term and long term instability challenges occurred in the North American, Scandinavian and European blackout incidents [12]. Provisions made using various layers of protection for frequency instability protect the IPS. It is also a grid code requirement to ensure adequate maintenance of the protection

barriers. The system frequency provides a dipstick on the IPS' health. It gives crucial situational awareness information on the supply and demand state at any given time within the IPS.

The TSO manages the system frequency at 50Hz. Any frequency excursion outside of the positive and negative bandwidth of ±2.5% ($51.25 \leq f \leq 48.75$Hz) results in the System operator's intervention [38]. Frequency control relies not solely on the total inertial response but also on primary, secondary and tertiary response measures [110, 111]. The response measures are grouped into various criteria to provide distinction and a merit-order response based on resource capability [73]. During transient or steady-state instability incidents, if system frequency declines, it experiences an arrest, rebound and recovery period within the frequency band. Assistance provided through primary, secondary and tertiary frequency support measures supports the frequency response periods within the frequency band [110, 112, 113]. The mixed response grouping supplied in Figure 4.2 shows the response period aligned to the control measures.

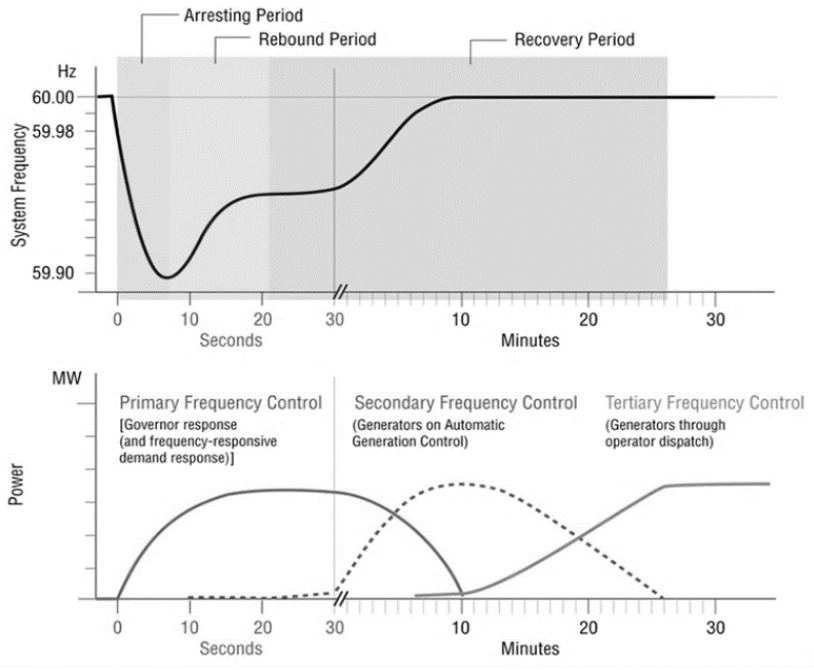

Figure 4.2. Frequency decline and recovery periods (Taken from [113]**,** © 2019 IEEE)

The explanation of the various frequency decline periods is as follow:

- **Primary frequency control**: The primary control response measures are the stored rotating inertia, turbine governor control and demand-side management initiatives such as specialised protection schemes (e.g. UFLS and UVLS) [38]. The resource deployment is within seconds of the interruption to arrest a rapid frequency decline. During the simulation of frequency decline, measures in place must try to avoid a drop in the frequency rate to 47.0Hz due to the risk of damaging vibrations on the generation plant [38, 42, 112–114].
- **Secondary frequency control**: This measure includes balancing services with fast-acting reserves, such as hydro. It comprises both spinning and non-spinning reserves. A typical service deployment happens when calculating the area control error (ACE) between interconnecting tie lines. Systems supporting ACE are AGC services and SCADA systems contractually authorising to dispatch the procured secondary frequency control resources [38, 42, 112–114].
- **Tertiary frequency control**: This measure includes deploying reserve resources within minutes for utilisation. The procured reserve resources provide the required energy and IPS security during emergency conditions. In some instances, the utilisation of larger conventional plants occurs within the tertiary frequency band. The scheduling and dispatch instructions of resources originate from the TSO's EMS [38, 42, 112–114].

4.3.1 Generator frequency operational limits during system restoration

The current design requirements for the SA IPS' governing system suggest that all units rated above 50MVA be equipped with governing capabilities that respond to the minimum operating limits. The conditions also stipulate that the system must ensure 100% active power output within the frequency band. The tripping times and frequency limits of importance are when the frequency drops below the continuous operating range, as stipulated in Figure 4.3. The minimum operating range for system frequency is between 49.0Hz and 51.0Hz [42].

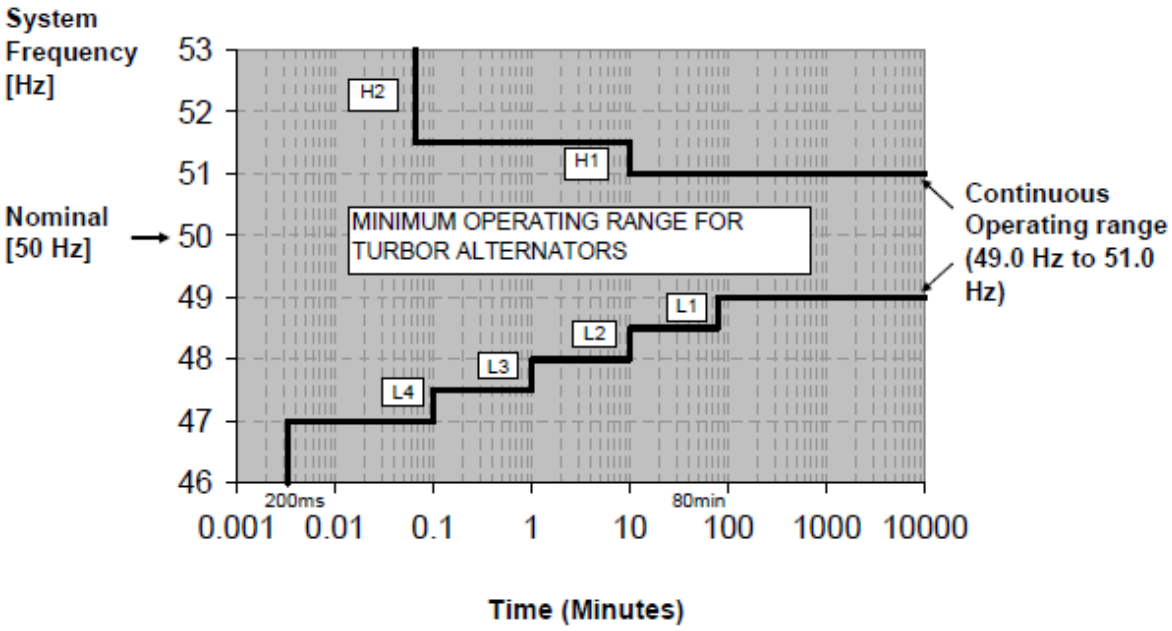

Figure 4.3. The minimum operating range for turbo alternators [42]

4.3.2 Generator high-frequency operational limits during system restoration

For over-frequency conditions, the design criteria allow for a withstand time of approximately 10 minutes between a frequency band of 51.0Hz and 51.5Hz (H1) over the generation service plant life. However, during operating conditions, if the frequency goes above 51Hz for 1 minute, islanding protection will disconnect the affected generation plant from the SA IPS if contracted for islanding [42].

The plant design allows the plant to operate above 51.5Hz (H2) for 1 minute. The operational limits for an H2 scenario trigger a disconnection of plant or islanding of plant after 4 seconds to protect generation assets against the over-speed of the turbine and generator machines. These limits provide a guideline on the operational limitations at each generation station and provide insight into the high-frequency limit setpoint [42].

4.3.3 Generator low-frequency operational limits during system restoration

The low-frequency design criteria vary in the frequency band with different tripping requirements. The first criteria are when the frequency ranges between 49.0Hz and 48.5Hz (L1). In this scenario, the IPS supports an operating period of 80 minutes within this respective frequency band. No generator tripping allows active and reactive frequency management to achieve stability within the IPS [42]. The second consideration is the low-frequency ranges between 48.5Hz and 48.0Hz (L2). The system design allows for operation in the L2 band for 10 minutes. If operated within this frequency range for more than 1 minute, the generation station affected can island or trip from the IPS to protect the asset [42].

The third consideration is when the frequency reaches a band between 48.0Hz and 47.5Hz (L3). Based on the plant's design, if the frequency is within the band mentioned above for longer than 1 minute, the generator will disconnect. If the frequency is within the L3 band for 10 seconds, the generator can island or trip from the IPS [42]. For frequency ranges between 47.5Hz and 47.0Hz (L4), the generation plant trips after 6 seconds and 200ms, respectively. At 47.0Hz, the station will be at risk and must trip very fast to ensure further damage to plant assets is avoided [42].

4.4 REVIEW OF VOLTAGE STABILITY

4.4.1 Background to voltage stability

Voltage management goes hand in hand with the optimisation of reactive power resources. Previous sections in this report mention shortages of reactive power during the early stages of system restoration. As a result, the management of system voltage for the IPS is more challenging when compared to a normalised IPS. Reactive power management simulations determine the optimal tap position on the generator transformer in the plant and the tap position of the EHV and HV transformers. In understanding the reactive power risk, the

operator on the desk would feel more comfortable making technical judgement calls on the challenges associated with the distances from the source to load [20, 39, 59, 62, 69–71].

4.4.2 Voltage dips and compatibility limits

4.4.2.1 Voltage compatibility limits

When loads, lines, transformers and generators connect to the IPS, voltage dips exist as a result. It is essential to understand the compatibility limits and the effect on equipment connected to the IPS [40, 43]. If there is a breach in the compatibility limits for an extended duration, the impact could result in equipment damage before energisation, resulting in unnecessary restoration delays to the IPS. The maximum deviation for the declared voltage is specified in Table 4.1.

Table 4.1. Maximum deviation from standard or declared voltages [40]

Voltage level (V)	Limit (%)
< 500V	15%
≥ 500V	10%

4.4.2.2 Voltage dip duration and depth

Voltage dip duration and depth is essential consideration during the system restoration stage of the IPS. If not considered, equipment damage may occur during system restoration. The classification of these dips falls into five categories, namely, Y-type, S-type, T-type, X-type and Z-type dips. The National rationalised standard (NRS) 048 part 2 provides information by looking at the indicator from the quality of supply performance perspective [40]. During the normal and abnormal operating conditions, the impact on the connected equipment is the same for both needs [71, 85].

The NRS standard applies to the analysis when assessing the impact of dips due to the type of load, size of load and equipment (e.g. transformers) connecting to the IPS. Table 4.2

provides a view of the transient parameters observed during the evaluation of voltage dips duration and depth of the dip experienced.

Table 4.2. Categorisation of voltage dips [40]

Dip category	Values of duration and depth		Definition
Y	duration	> 20 ms to 3 s	Dip definition (20 ms to 3 s) Y.
	depth	30 %, 20 %, 15 %	The minimum plant compatibility requirement (this covers a significant number of short duration dips).
X1	duration	> 20 ms to 150 ms	Typical zone 1 clearance (no pilot wire).
	depth	30 % to 40 %	Desired plant immunity – as this spans many dips caused by remote faults on the licensee network.
X2	duration	> 20 ms to 150 ms	Typical zone 1 clearance (no pilot wire).
	depth	40 % to 60%	Dips potentially cause drives to trip caused by remote faults on the licensee network.
S	duration	> 150 ms to 600 ms	Typical Zone 2 and accelerated clearance. Also, some distribution faults.
	depth	20 % to 60%	Plant compatibility (drives trip > 20 %) caused by remote faults on the licensee network
T	duration	> 20 ms to 600 ms	Zone 1 and zone 2 clearance times
	depth	60 % to 100 %	Plant compatibility (contactors trip > 60 %) caused by close-up faults on the licensee network
Z1	duration	> 600 ms to 3 s	Back-up and thermal protection clearance or long recovery times (transient voltage stability) or both
	depth	15 % to 30 %	Remote faults post-dip motor recovery without stalling
Z2	duration	> 600 ms to 3 s	Back-up and thermal protection clearance
	depth	30 % to 100 %	Closer faults potential motor stalling

4.5 A BRIEF REVIEW OF ROTOR ANGLE STABILITY

Rotor angle is the loss of synchronism between two synchronous generators or generator islands [53, 115]. In contrast, frequency stability is a widespread IPS characteristic and, if compromised, affect the entire IPS. Rotor angle stability may be localised or cause a cascaded incident within the IPS leading to widespread island instability [3]. Observed in the North American blackout incident is the loss of interconnected synchronisation [12].

The event often builds up to a more significant incident, eventually resulting in a complete failure of the power system. Rotor angle instability is due to massive power transfer quantities through a narrow corridor that may influence two significant islands within an IPS. The resultant is the loss of a generator or the regulating system's inability to adjust based on the supply and demand requirements on the IPS [52].

4.6 CHAPTER SUMMARY

For full frequency recovery, the entire period from the arresting period to the recovery period determine if the load connected does not cause a complete collapse, voltage oscillations or instability within the IPS. As there is manual management of the system frequency, resources supporting the primary, secondary and tertiary response is disabled. The design parameter for the generator plant disconnection uses a conservative approach within the frequency bands L1, L2 and L3.

Based on the specified voltage levels, it would be good to analyse scenarios for when the voltage is at 1.00 p.u. and 0.90 p.u. during the transient assessment. It would provide the worst-case upper and lower limit for the evaluation. The consideration of restart times is neglected, and the focus will be on the load size connection (this includes power factor and voltage selections) to the power system. The various inrush scenarios investigated and analysed determine the best course of action.

CHAPTER 5 METHODOLOGY FOR IPS RESTORATION

5.1 CHAPTER OVERVIEW

The solution methodology is analysed through various restoration scenarios to determine the optimal solution for an 11-bus IPS. The 11-bus IPS resembles a portion of the SA IPS, typically energised during testing, and this provides a realistic approach for the development of the restoration principles. On this specific corridor, load adjustment is flexible. Transient stability analysis assesses the impact on the system frequency and the source voltage response, whereas steady-state state analysis provides insight into the Ferranti risks experienced on the IPS. Each of the components, such as the generation plant and BESS control system model, uses the composite models to provide insight into the natural response of the currently installed assets. The automatic voltage regulation (AVR) and automatic generation control (AGC) supporting the inertial response is inactive, as the operator would typically perform active voltage management and generation control during a blackout scenario. The turbine-governor models (TGOV5 model in this instance) and BESS models with set-point parameters are shared in the appendix of this thesis report.

During the initial phases of restoration, the system operator is concerned with the response rate for power generation plants, the availability of reactive power resources in the IPS and maintaining interconnected stability as the load connects to the IPS [20, 39, 60]. As a large contingent of load connects to the IPS, already having low rotational inertia within the system, the IPS may suffer a frequency collapse forcing a complete restart of the generation

plant and restoration process. The frequency limit for generators at the high frequency and low-frequency ends are specified in the South African grid code (under the Network Code) and is used in the analysis as the design specifications for the stations within the IPS that is maintained accordingly [42]. Applying the power quality limits from the NRS 048-2 standard determines the compatibility limits. It ensures no harm to equipment and load connecting to the IPS as conventional limits would still apply [40].

Section 5.2 briefly introduces the aspects investigated in developing the solution. An overview of the simulation method used within the Powerfactory simulation model is provided in Section 5.3. Where Section 5.4 introduce the various test networks used within the Powerfactory simulation model, presenting all the scenarios with network configurations. Sections 5.5 briefly describe the used cases for BESS and how it is applied within the simulation model. Section 5.6 shows the load modelling used in the simulation that would support the scenarios is introduced. Section 5.7 summarises the information discussed within this chapter.

5.2 OVERVIEW OF THE SIMULATION CASE MODEL

5.2.1 The Newton-Raphson power flow method

OPF within a transmission and distribution system is a complex engineering task used to determine the most reliable and efficient power distribution within the power grid. The Newton-Raphson (NR) method assess the stability and convergence of the OPF within the IPS. The methodology requires initial conditions for voltage and angles within the power system. The use of the NR method requires that the power flow equations be written in a matrix format using the following equation known as the power mismatch equation [116, 117]:

$$\boldsymbol{F}(x) = 0 \tag{5.1}$$

The function contains injected active power and reactive power at each busbar, with the vector parameter consisting of δ_i and the voltage magnitude V_i. Under normal operating conditions, the initial angle and voltage magnitude are 0 degrees and 1.00 p.u. at the busbar; this also defines the slack bus [1, 116, 117]. The active and reactive power entering a bus is shown in (5.7) and (5.8), formulated from (5.2) to (5.6):

$$V_i = |V_i|\angle\delta_i = |V_i|(cos\delta_i + j\, sin\, \delta_i) \tag{5.2}$$

$$Y_{ii} = |Y_{ii}|\angle\theta_{ii} = |Y_{ii}|(cos\theta_i + j\, sin\, \theta_i) = G_{ii} + jB_{ii} \tag{5.3}$$

$$Y_{ij} = \left|Y_{ij}\right|\angle\theta_{ij} = \left|Y_{ij}\right|\left(cos\theta_{ij} + j\, sin\, \theta_{ij}\right) = G_{ij} + jB_{ij} \tag{5.4}$$

$$I_i = Y_{i1}V_1 + Y_{i2}V_2 + \cdots + Y_{in}V_n = \sum_{k=1}^{n} Y_{ik}\, V_k \tag{5.5}$$

$$P_i - jQ_i = V_i^* I_i = \sum_{k=1}^{n} |Y_{ik}\, V_i V_k|\, (cos\, \delta_i - j\, sin\, \delta_i)(cos\, \theta_{ik} + j\, sin\, \theta_{ik})\, (cos\, \delta_k + j\, sin\, \delta_k) \tag{5.6}$$

Therefore,

$$P_i = \sum_{k=1}^{n} |Y_{ik}V_iV_k|\, cos(\theta_{ik} + \delta_k - \delta_i) \tag{5.7}$$

$$Q_i = -\sum_{k=1}^{n} |Y_{ik}V_iV_k|\, sin(\theta_{ik} + \delta_k - \delta_i) \tag{5.8}$$

For the load flow calculations, (5.7) and (5.8) determine the net real and reactive power flow using a DIgSILENT Powerfactory simulation package. The Jacobian matrix is a first-order partial differential function that solves the corrections from the formulated Taylor series function. The Jacobian matrix equation uses multiple iterations to estimate the bus voltage and angles to calculate the mismatches. Equation (5.9) provides information on the formulated Jacobian matrix used to solve the corrections.

$$J\begin{bmatrix}\Delta\delta_2\\ .\\ .\\ .\\ \Delta\delta_n\\ \frac{\Delta|V_2|}{|V_2|}\\ .\\ .\\ .\\ \frac{\Delta|V_{1+n_p}|}{|V_{1+n_p}|}\end{bmatrix}=\begin{bmatrix}\Delta P_2\\ .\\ .\\ .\\ \Delta P_n\\ \Delta Q_2\\ .\\ .\\ .\\ \Delta Q_n\end{bmatrix} \tag{5.9}$$

The Jacobian matrix divides into submatrices whereby:

$$J=\begin{bmatrix}J_{11} & J_{12}\\ J_{21} & J_{22}\end{bmatrix} \tag{5.10}$$

The Jacobian matrix for each of the matrix elements divides into the following equations:

$$J_{11}=\begin{bmatrix}\frac{\partial P_2}{\partial\delta_2} & \cdots & \frac{\partial P_2}{\partial\delta_n}\\ \vdots & \ddots & \vdots\\ \frac{\partial P_n}{\partial\delta_2} & \cdots & \frac{\partial P_n}{\partial\delta_n}\end{bmatrix} \tag{5.11}$$

$$J_{12}=\begin{bmatrix}|V_2|\frac{\partial P_2}{\partial|V_2|} & \cdots & \left|V_{1+n_p}\right|\frac{\partial P_2}{\partial|V_2|}\\ \vdots & \ddots & \vdots\\ |V_2|\frac{\partial P_n}{\partial|V_2|} & \cdots & \left|V_{1+n_p}\right|\frac{\partial P_n}{\partial\left|V_{1+n_p}\right|}\end{bmatrix} \tag{5.12}$$

$$J_{21}=\begin{bmatrix}\frac{\partial Q_2}{\partial\delta_2} & \cdots & \frac{\partial Q_2}{\partial\delta_n}\\ \vdots & \ddots & \vdots\\ \frac{\partial Q_n}{\partial\delta_2} & \cdots & \frac{\partial Q_n}{\partial\delta_n}\end{bmatrix} \tag{5.13}$$

$$J_{22}=\begin{bmatrix}|V_2|\frac{\partial Q_2}{\partial|V_2|} & \cdots & \left|V_{1+n_p}\right|\frac{\partial Q_2}{\partial|V_2|}\\ \vdots & \ddots & \vdots\\ |V_2|\frac{\partial Q_n}{\partial|V_2|} & \cdots & \left|V_{1+n_p}\right|\frac{\partial Q_n}{\partial\left|V_{1+n_p}\right|}\end{bmatrix} \tag{5.14}$$

The number of buses is represented by n, the total number of P-Q buses is represented np, and the total of generator buses is represented by ng. The following equation then calculates the total number of buses:

$$n = np + ng + 1 \tag{5.15}$$

The Jacobian matrix dimensions for the calculation is determined using the following:

$$J_{11} = (n - 1) \times (n - 1) \tag{5.16}$$

$$J_{12} = (n - 1) \times np \tag{5.17}$$

$$J_{21} = np \times (n - 1) \tag{5.18}$$

$$J_{22} = np \times np \tag{5.19}$$

Once the size is determined, the equations are iteratively solved using DIgSILENT Powerfactory to determine the OPF within the IPS for the networks under study [116, 117].

5.2.2 RMS simulation philosophy

The simulation software package utilised is DIgSILENT Powerfactory version 2018 SP3. The package offers various simulation methods for multiple types of problem statements, of which the RMS simulation calculation methods is a solution applied to the dynamics of electromechanical, control and thermal devices [118]. The methodology helps calculate transient stability as the system normalization commences by setting up various scenarios based on the selected restoration route. Figure 5.1 depicts the RMS simulation process.

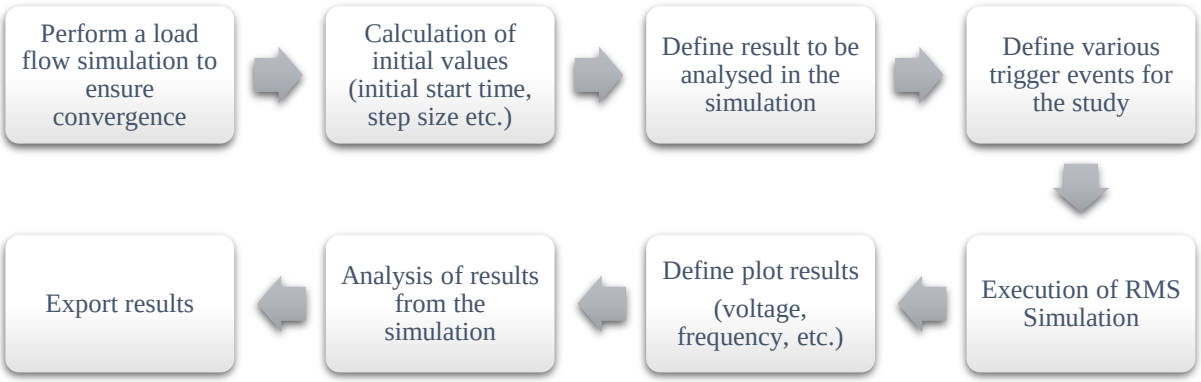

Figure 5.1. The RMS Simulation process (simulation steps followed)

The IPS has predefined static models for assets and terminal equipment. To perform dynamic simulations, the predefined static models have embedded dynamic control system models

that define the dynamic behaviour of the asset when subjected to transient events [118]. The RMS simulation option supports the dynamic response of the mathematical models linked to its associated asset (e.g. generation plants, synchronous machines and BESS systems). The simulation results from DIgSILENT export into excel format, where further data manipulation is applied to demonstrate the results (e.g. frequency vs time, voltage vs time) [118].

5.2.3 Model components for the simulation model

5.2.3.1 Turbine-governor model (TGOV5)

Turbine-governor models assist with regulating the rotational speed in response to changing load conditions [94]. The governor output signal manipulates the steam inlet valve (steam flow controller), which governs the steam flow to the turbine. The turbine and the droop control model resembles the IEEEG1 model [94], the most common model used to simulate steam turbines. The TGOV5 model extends from the IEEEG1 model, with additional parameters to determine the steam throttle pressure, a boiler pressure controller and a fuel controller. Also, controls supporting the electrical power, turbine inlet, position yields for the available mechanical energy for pressure and frequency error is added [94]. The TGOV5 model used within the DIgSILENT Powerfactory simulation model for the scenarios analysed is presented in Figure 5.2:

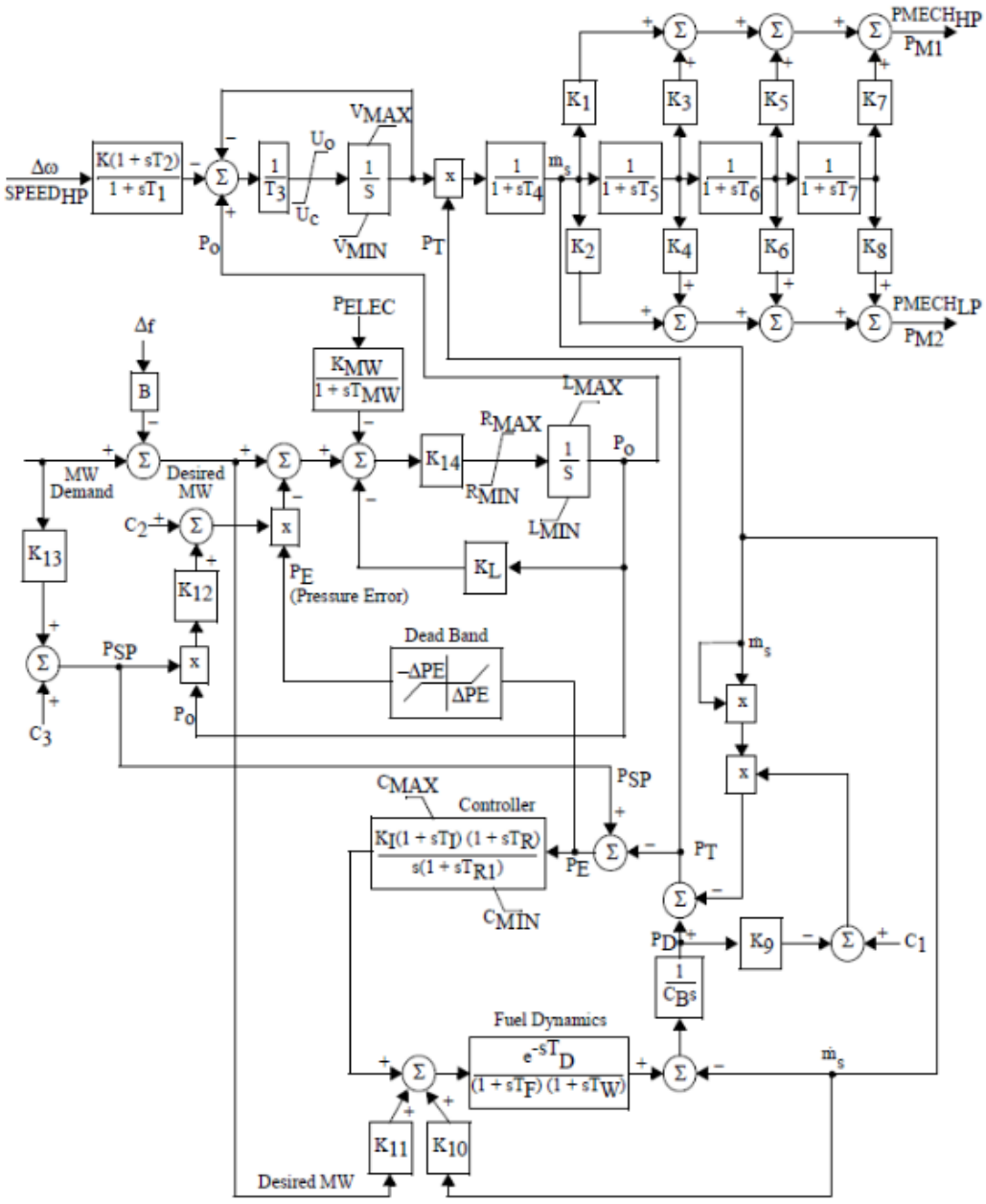

Figure 5.2. Turbine GOV5 model for the SA IPS (Taken from [94], © 2013 IEEE)

Finding the required parameters require continuous testing and calibration of TGOV5 parameters from generation operating personnel to ensure the accuracy of models during transient response conditions [94, 119]. Regular calibrations of the integrated systems provide a degree of confidence to the power system planning engineers. Due to the complex

integrated nature and size of the TGOV5 model, the calibration of input parameters is complicated [94].

5.3 THE RESTORATION SOLUTION METHODOLOGY

5.3.1 Background of the scenarios considered

The restoration steps divide into three main scenarios used to obtain principles that analyse the frequency response, load size, the power factor of the load and sending end voltage of the system. The first restoration step provides insight into the system restoration challenges within the IPS. The analysis is performed using a simplified network topology comprising of a thermal power plant, three transformers and two connecting transmission lines.

The second scenario determines the reactive power requirements based on typical conductors used within the SA IPS during the system restoration scenario, with the power system still in a vulnerable condition (i.e. having one generator to manage reactive power and load). The energizing conductor deliberately connects to the generation plant, with load energized afterwards to demonstrate the MVAr requirements for dampening the connected line and the connected load's support based on power factor selection. Following the steps under the two scenarios, the principles obtained is applied to the 11-bus model selected for the simulation.

The third scenario analyses the positive or negative contribution to various sizes of BESS technology. The restoration principles obtained from scenarios one and two provided information on the maximum load, power factor, the sending end voltage, and the principles applied throughout to give the most optimal solution when analysing the BESS technology. The load is adjusted, and the BESS size is correspondingly adjusted to highlight the support provided or challenges with deploying the resource during restoration conditions.

The fourth and final scenario analyses a simplified 11-bus grid portion within the SA IPS. The scenario divides into three sub-restoration strategies. The principles identified from the literature and actual simulation results obtained under scenarios one, two and three are tested

for adequacy. The various network corridors are gradually restored, iteratively assessing each restoration phase in terms of voltage impact, generation and load balancing, and frequency impact until stability scenarios are obtained.

5.3.2 The first restoration scenario consideration

The first restoration step intends to determine the impact on the weakest point of failure within the IPS. In doing this, the maximum limit for the connected load and contributing power factor for capacitive dampening is determined as a guideline. The energization is done based on the frequency setpoints of 50.40Hz and a maximum of 50.85Hz. The reason for the frequency selection is to be slightly lower than the 51Hz protection trigger in the upper band (over frequency), and the 50.40Hz setpoint provides a realistic in-between selection point, between 50.85Hz and 50Hz. Larger load size will be restricted if the operating frequency setpoint is 50Hz. The sending end voltage setpoints of 1.00 p.u. and 0.90 p.u. determine the optimal voltage as the load power factor adjusts from 0.98 to 0.85 for varying load sizes. The voltage level for the transmission study ranges from 400kV to 275kV. An overview of the simplified system considered is shown in Figure 5.3.

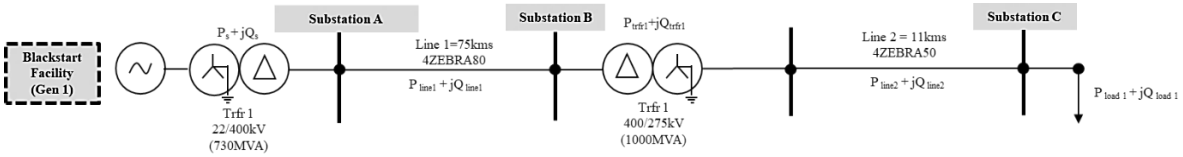

Figure 5.3. A simplified view of the IPS for the first restoration step

5.3.3 The second restoration scenario consideration

The second scenario analyses the impact of varying impedance distances of typical conductors assessing the reactive power consumption requirements with a load connected to the IPS. In the first scenario, selecting a realistic load type, good power factor, and source voltage set-point helped determine the load limitations. The system frequency increases to 50.85Hz, and the load impact is assessed to determine the system's inertial response. The typical conductors' distance is adjusted from 50km to 200km in increments of 50km to

evaluate the impact on system frequency and the reactive power absorption capability required by the blackstart facility. The connected maximum load of 50MW with a power factor of 0.90 p.f. provides insight into the challenges experienced using the adjusted distances. Figure 5.4 provides insight into the network topology for the IPS.

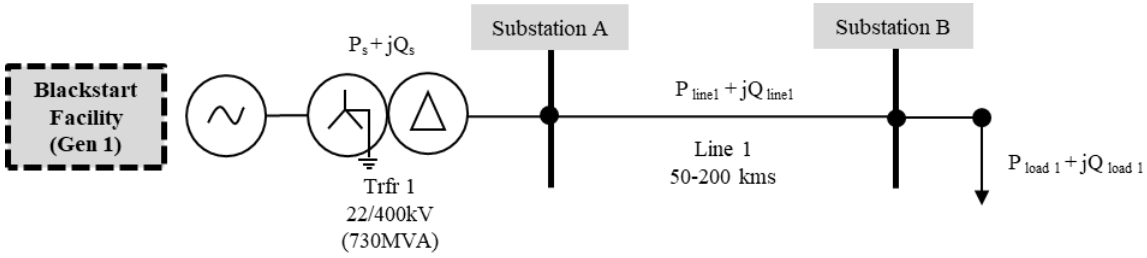

Figure 5.4. A simplified diagram for the connection of load and varying power factor

The line impedance connects directly to the generation source. The transmission system conductors typically have bi, tri and quad bundle configuration designs. Typical conductor sizes such as Bear, Bersfort, Dinosaur, Goat, Kingbird and Tern are used.

5.3.4 The third restoration scenario consideration

5.3.4.1 Background to the third restoration scenario

The second last consideration is using of BESS technology. The BESS size selection is from 10MVA in increments of 10MVA until 50MVA is achieved. The power factor for load sizes of 50MW is selected at 0.90 p.f. The intention is to determine if there is a positive impact on the frequency response. In addition, to assess the real and reactive power support provided when connecting BESS to the IPS. The third scenario uses the simplified IPS model under scenario one to determine the impact on system frequency voltage and the reactive power requirements for the power system. Comparing the results obtained in scenarios one and three highlights the benefits and challenges. The voltage for the IPS is 400kV. The control mode for the BESS module adjusted to reactive power management and the simplified view of the network topology used is that the assessment is shown in Figure 5.5

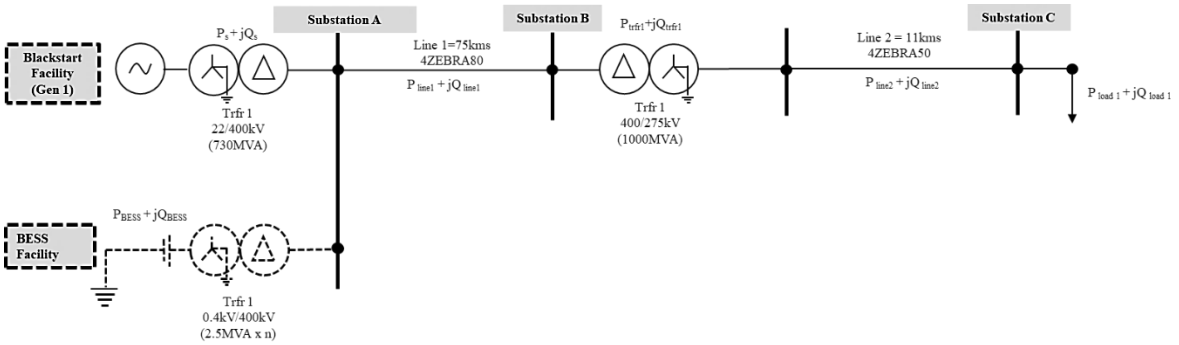

Figure 5.5. A simplified view of the IPS with the utilisation of BESS

5.3.5 The fourth restoration scenario consideration

5.3.5.1 Background to the fourth restoration scenario

The fourth scenario covers restoring a simplified 11-bus IPS model for the SA IPS. Information regarding restoration route and philosophy is selected based on principles identified from scenarios one, two and three. The result from scenarios one, two and three are applied as guidelines for the fourth restoration scenario. The system restoration is performed in phases allowing sufficient frequency recovery. Once the frequency is recovered successfully, the subsequent restoration step commences.

5.3.5.2 Restoration process and principles

The restoration of the power system must follow a set of predetermined rules when restoring the IPS. The predetermined rules must successfully restore the correct consumer loads to maintain system stability. The development of guiding principles under the various scenarios investigated provided the limitations on the existing installed assets when connected to the TGOV5 model. The system under study is the 400kV and 275kV transmission system. A step-up transformer provides the required step-up to 400kV at the generation plant. The network simulation model is prepared in the system restoration state, similar to actual events on the day of a significant interruption. When energizing a transformer with the associated load, the action is done by closing a single breaker. It means that when a conductor is energized, the conductor, transformer and load is energized in a single switching step. The

transformer selected is assumed as the auxiliary transformer, and once energised, all auxiliaries at the station is energised. All transformer taps settings are on nominal tap.

Another vital consideration is the overall impact on system voltage. The connected load help dampen the overall Ferranti effect. It is achieved by connecting lagging power factor loads (inductive loads). The most significant risk is selecting the correct voltage for the source voltage when the load connects to the power system through long transmission lines; the voltage selection should be at the lowest possible level. There will be a cascading impact on the system voltage due to Ferranti discharge as lines are connected to the IPS. The settling voltage is assessed to determine if the source voltage operates at a higher p.u. value. In line with the voltage requirements, the transformer automatic tap adjustment is disabled, and the tap setting is at the lowest position for the transformers selected. The management of the overall system voltage is from the sending end source voltage. The overall effect is better management of the Ferranti over-voltages on the IPS. Figure 5.6 provides an overview of the network topology under study.

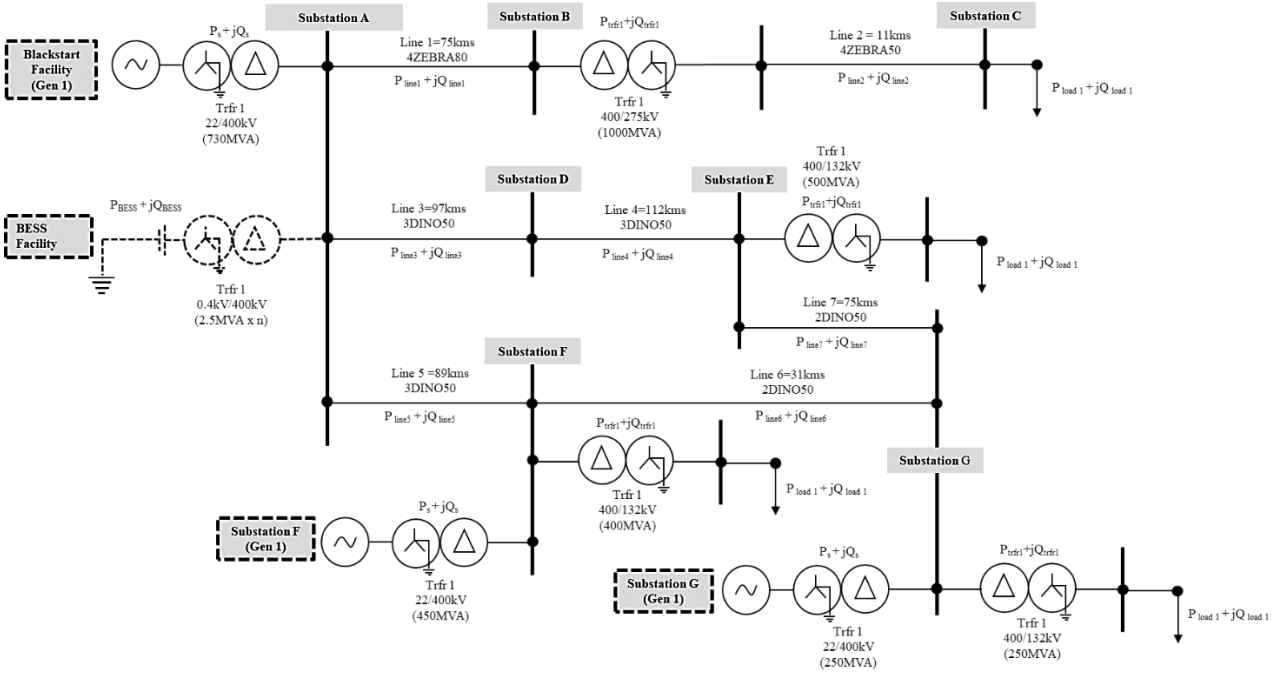

Figure 5.6. Overall network diagram of the 11-bus system

5.3.5.3 The first corridor energisation

The first restoration corridor incorporates the corridor under scenario 1, with an additional corridor energised. The corridor is line 5, substation F, the step-up transformer (22/400kV) at the generating station, and the step-down transformer (400/132kV) and with associated load linked. The time energisation adjustment is performed using the RMS simulation mode in DIgSILENT Powerfactory until the optimal restoration scenario is achieved. Figure 5.7 depicts a view of the network topology for the first restoration corridor under the fourth restoration scenario, with the additional corridor energised, highlighted in blue.

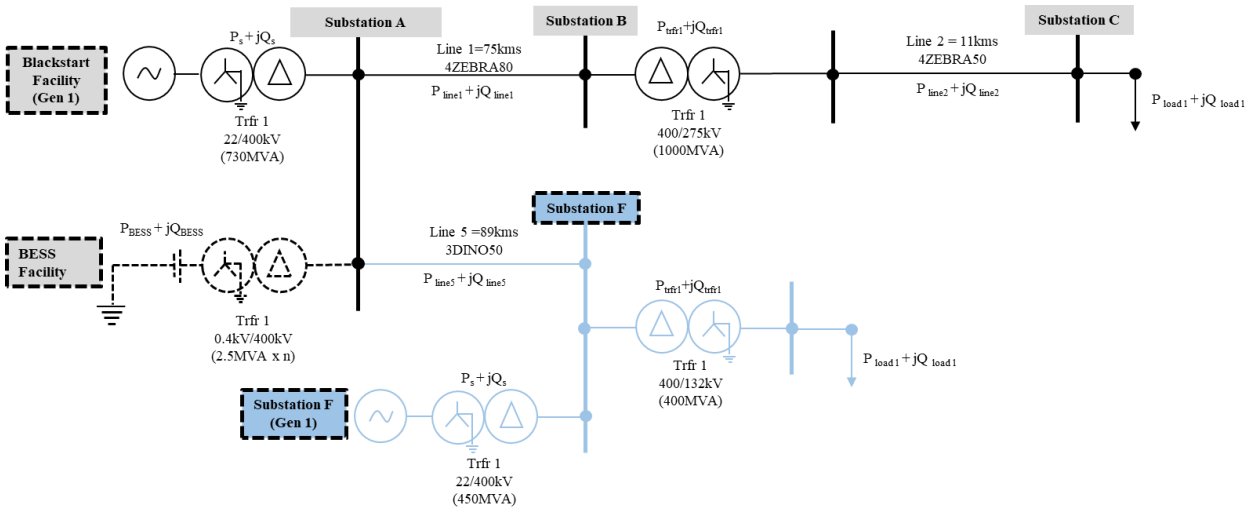

Figure 5.7. Network diagram for first restoration corridor

5.3.5.4 The second corridor energisation

The second restoration corridor incorporates the corridor energised in scenario 1, with an additional 400kV corridor energised. The corridor energised is line 3, substation D, line 4, substation E, a step-down transformer (400/132kV), with the associated load linked. As with the previous methodology, the energization time is adjusted using the RMS simulation mode in DIgSILENT Powerfactory until the optimal restoration scenario is achieved. Figure 5.8 provides the network for the second restoration corridor scenario, with the corridor energised, highlighted in blue.

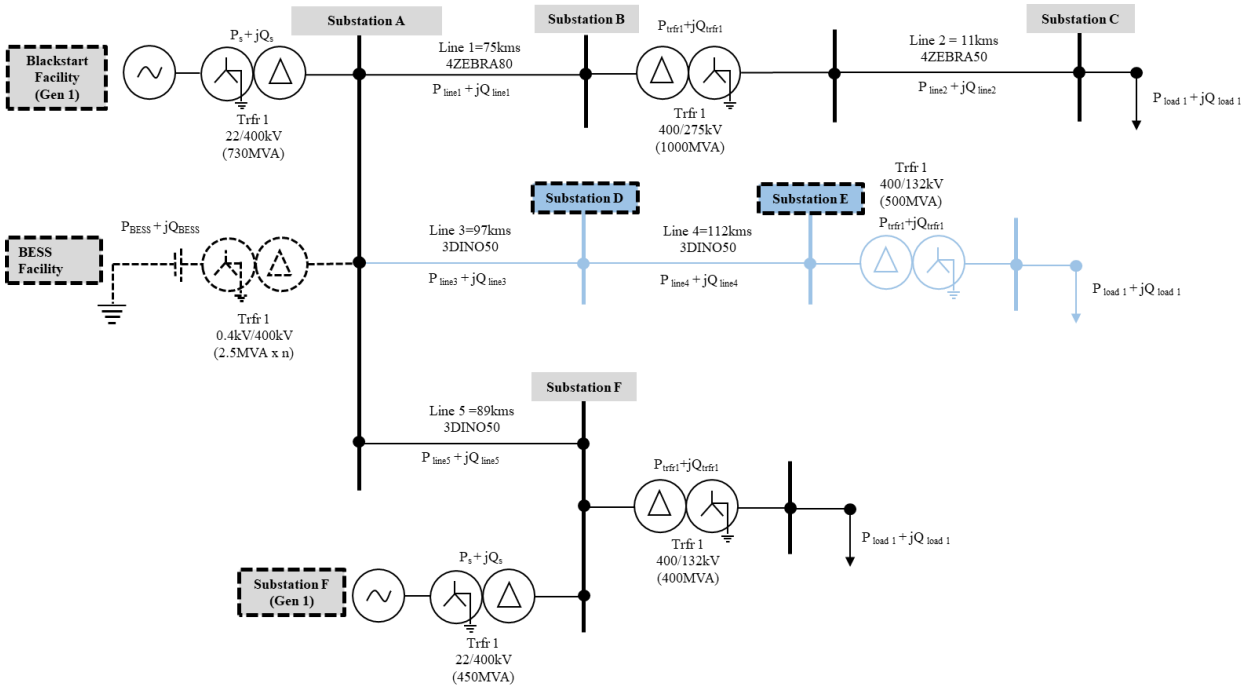

Figure 5.8. Network diagram for second restoration corridor

5.3.5.5 The third corridor energisation

The third scenario assesses the impact of energising all 11 busbars in total. It is a continuation of energising the first and second corridors from the previous scenarios. Yet again, the analysis of frequency and the sending end voltage is analysed. In this scenario, multiple iterations were performed to provide insight into the most optimal energisation sequence (timing and size of the load). A simplified view of the network for the final restoration corridor is shared in Figure 5.9, with the additional corridor highlighted in blue.

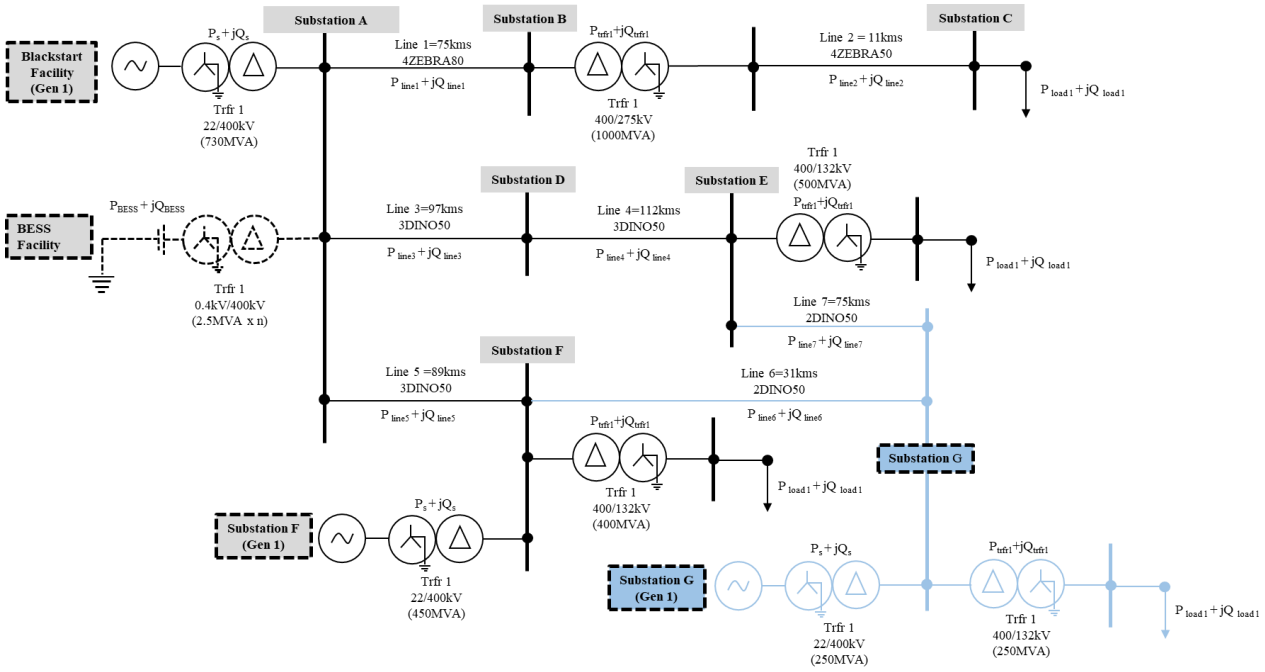

Figure 5.9. Network diagram for third restoration corridor

5.4 BATTERY ENERGY STORAGE TECHNOLOGY

5.4.1 Background to BESS

BESS is a reliable alternative for providing immediate inertia to the IPS. The BESS technology model divides into three main components, namely, the power conversion system (PCS), the supervisory system control (SSC) and the battery pack with the battery management system (BMS). The BMS and SSC support the optimal operation of the BESS system, and the PCS adjusts and dispatches the required energy as requested or contractually agreed upon within grid market operations [120]. BESS employed in power systems each has its unique benefit to the IPS. Typical functional employment for BESS is improving power quality challenges, providing grid support to the transmission and distribution utilities, and bulk power support in the capacity market as a procured ancillary service [121–123]. An overview of the application of BESS based on the type of technology, sizing and discharge time at rated power appear in Figure 5.10.

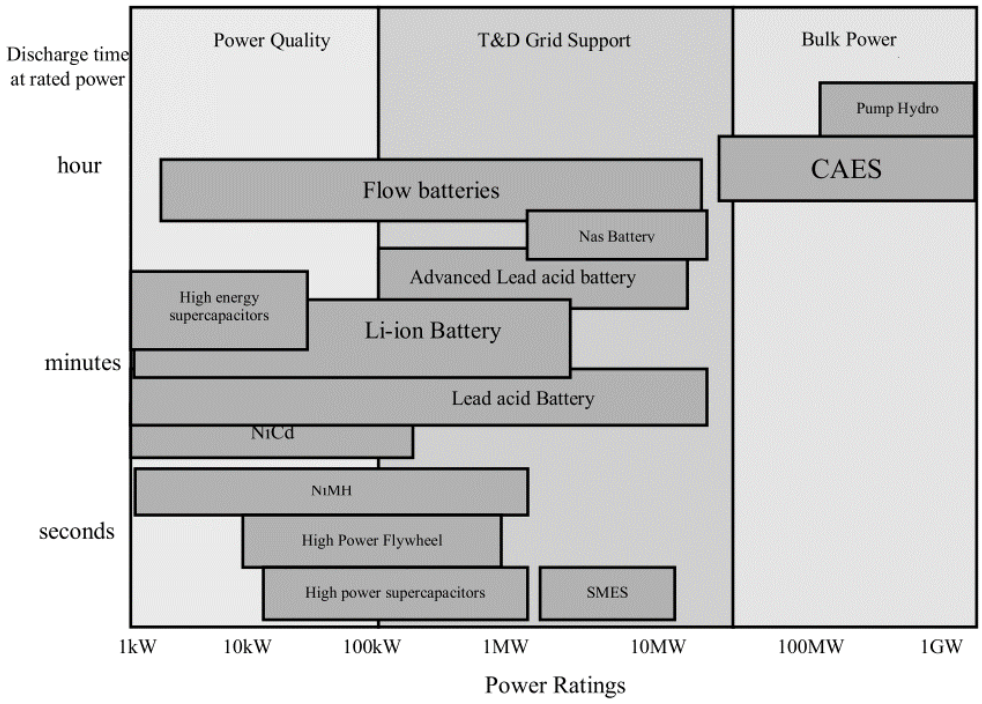

Figure 5.10. Use cases for BESS technology (Taken from [121]**,** © 2014 IEEE)

5.4.2 Use cases for BESS technology during power system restoration

5.4.2.1 BESS for fast frequency response (FFR)

BESS supports the system frequency and provides FFR for an instantaneous mismatch of a supply and demand within the IPS. The storage technology introduces virtual inertia to the power system and may be utilized to design microgrids or employed as a primary frequency control service, supporting positive frequency regulation. BESS technology also delivers higher efficiency and predictability than other distributed energy resources (DER). The technology employment provides a viable solution during blackout conditions and can support the inertial response within the frequency band [124, 125].

5.4.2.2 BESS for reactive power support

BESS significantly changes the dynamics in reactive power management in the IPS [122]. Transformers, loads, and conductors consume or provide reactive power support in the IPS.

To support dampening of the naturally generated reactive power within the IPS, for the transfer of real power, reactive power compensation through BESS, support the source generators in the IPS. As energy transmits along transmission lines, voltage degradation occurs at various IPS nodes. Deploying BESS within the IPS helps to reduce the impact of connecting larger loads with high reactive power consumption requirements [121]. In addition, it improves the real power transfer capability (power factor) limited by the natural reactive power support required due to the system's design. Lastly, the deployment will enhance the voltage distribution at various node points within the IPS. The mentioned constraints are also challenges experienced during blackout conditions, indicating that favourable support can be provided, limited to the design capability of the BESS technology employed [120, 121].

5.4.2.3 BESS for bulk power injection providing real power support

BESS, as a bulk power service, provides quick and efficient peak demand support during the peak periods within the load consumption curve. The rate of response is much faster than the ramping time for a conventional steam turbine system. The result is an almost instantaneous removal of real power from the IPS supporting the challenges experienced under blackout conditions if insufficient generation resources connect to the IPS during the system restoration stage [120, 121].

5.4.2.4 DIgSILENT Powerfactory BESS simulation model

The simulation model uses a battery pack size of 1MVA. The BESS system increases by increasing the parallel distribution of the resources within the simulation model to the desired size of the BESS resource. The incorporated battery capability curve under Figure 5.11 provides insight into the operational steady-state and transient limitations based on the size of the BESS system. The BESS reactive power support limitation of the device is specified in the system's design. The battery capability curve provides insight into the minimum and maximum reactive power and active power capability for the device under study.

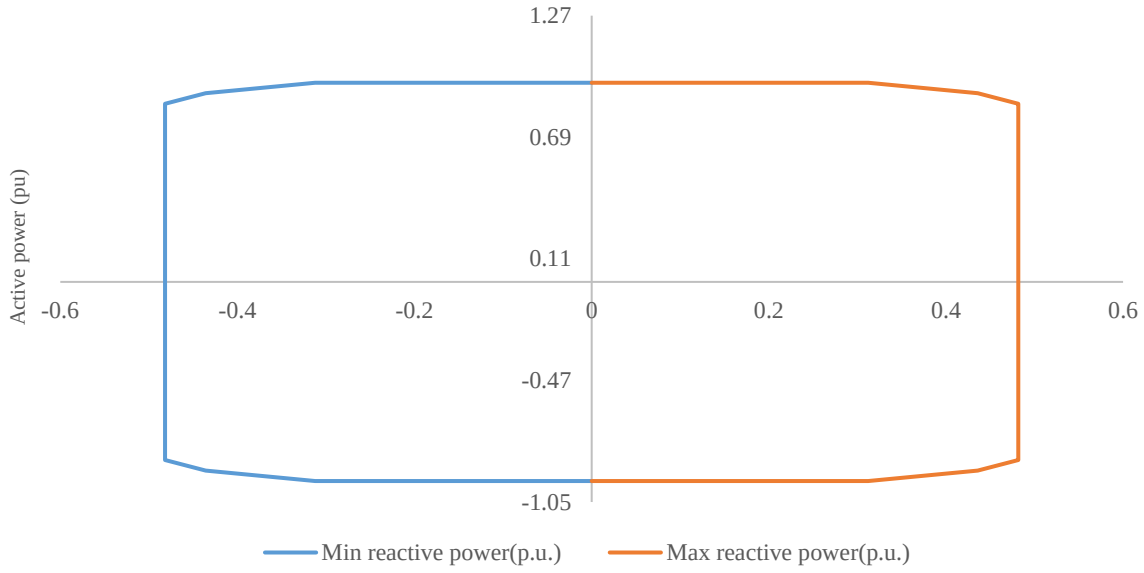

Figure 5.11. Battery capability curve – DIgSILENT Powerfactory model

5.5 VOLTAGE DEPENDENCY OF LOADS

5.5.1 Background on the voltage dependency of loads

The various load types should consider the voltage dependency of loads as voltage collapse is a dynamic phenomenon rather than static. Voltage dependency of loads is a critical stability consideration as the system is constructed during system restoration conditions, as the load modelling characteristics will have multiple constructs. The review helps achieve a more accurate result from the simulation study [126–128].

5.5.2 Load modelling considerations

Load modelling is performed using the exponential or polynomial functions to represent the real power and reactive power component. The load modelling functions represent the aggregated load response based on the frequency and voltage within the IPS. Typical load classes that exist are agricultural, residential, commercial and industrial load classes. Each of the mentioned load classes splits into various sub-component compositions (load components) such as heating, cooling, lighting and motorized compositions, to name a few.

Coefficients define the load components and depending on the mathematical function applied in a simulation (e.g. polynomial or exponential functions), it may comprise of reactive and real power coefficients or actual model parameters represented as percentages showing the aggregated load model. The exponential functions for the real power and reactive power functions are defined by (5.20) and (5.21) [126–128].

$$P = P_n \left(\frac{U}{U_n}\right)^{k_{pu}} \tag{5.20}$$

$$Q = Q_n \left(\frac{U}{U_n}\right)^{k_{qu}} \tag{5.21}$$

Furthermore, the polynomial equations for the real power and reactive power functions are represented by (5.22) and (5.23) [126–128].

$$P = P_n \left[Z_p \left(\frac{U}{U_n}\right)^2 + I_p \left(\frac{U}{U_n}\right)^2 + P_p\right] \tag{5.22}$$

$$Q = Q_n \left[Z_q \left(\frac{U}{U_n}\right)^2 + I_q \left(\frac{U}{U_n}\right)^2 + P_q\right] \tag{5.23}$$

5.5.3 DIgSILENT Powerfactory load modelling

Powerfactory has embedded exponential equations to calculate CPL, CCL and CIL behaviour [118]. The following two equations compute the real and reactive power using OPF:

$$P = P_0\left(aP\left(\frac{v}{v_0}\right)^{e_{aP}} + bP\left(\frac{v}{v_0}\right)^{e_{bP}} + (1 - aP - bP)\left(\frac{v}{v_0}\right)^{e\_cP}\right) \tag{5.24}$$

$$Q = Q_0\left(aQ\left(\frac{v}{v_0}\right)^{e\_aQ} + bQ\left(\frac{v}{v_0}\right)^{e\_bQ} + (1 - aQ - bQ)\left(\frac{v}{v_0}\right)^{e\_cQ}\right) \tag{5.25}$$

Load modelling requires setting the exponent values for the real power and reactive power equations to 0, 1 or 2. As load has multiple components, typical load model parameters for real and reactive power is presented in Table 5.1 [118, 127].

Table 5.1. Typical load model parameters [127]

Load component	e_cP/k_{pu}	e_cQ/k_{qu}
Battery charge	2.59	4.06
Fluorescent lamps	2.07	3.21
Constant impedance	2	2
Fluorescent lighting	1	3
Air conditioner	0.5	2.5
Constant current	1	1
Resistance space heater	2	0
Pumps, fans or other motors	0.08	1.6
Incandescent lamps	1.54	0
Compact fluorescent lamps	1	0.35
Small industrial motors	0.1	0.6
Large industrial motors	0.05	0.5
Constant power	0	0

Using the abovementioned exponent values, the real and reactive power equations for CPL, CCL and CIL further simplify into (5.26) to (5.31) for the real power and reactive power components, respectively [126, 127]. For CPL, the real and reactive power equations are as follow:

$$P = P_0 \tag{5.26}$$

$$Q = Q_0 \tag{5.27}$$

For CCL, the real and reactive power equations are as follow:

$$P = P_0 \left(\frac{v}{v_0}\right)^1 \tag{5.28}$$

$$Q = Q_0 \left(\frac{v}{v_0}\right)^1 \tag{5.29}$$

For CIL, the real and reactive power equations are as follow:

$$P = P_0 \left(\frac{v}{v_0}\right)^2 \tag{5.30}$$

$$Q = Q_0(\frac{v}{v_0})^2 \quad (5.31)$$

When performing OPF studies using DIgSILENT Powerfactory, convergence must be confirmed in the simulation model after successfully executing an OPF simulation. With the voltage dependency functionality enabled, (5.26) to (5.29) analyses the outcome of CPL and CCL types [118].

5.6 CHAPTER SUMMARY

The NR methodology and RMS simulation method will form the basis of the simulation studies. The simulation would explore three restoration scenarios to provide insight into the fourth scenario considered. The three scenarios consider a simplified model and extract critical principles and rules when analyzing the fourth scenario. For simplification, the load modelling is limited to CPL and CCL models.

The reactive power dampening support for CIL is limited by not having good power factor dampening capability due to the load-modelling construct (mostly resistive). Scenario three tests use cases for BESS during the initial stages of restoration. The third scenario determines the positive or negative contributions of BESS during the initial restoration stages. It will provide a better understanding of possible risks that would arise and provide insight into the applied mitigations.

The results obtained from the simulation assessment provides an opportunity to enhance the guiding principles within the Grid Code. Information that may be added or changed is the typical load types that may connect the IPS, the power factor support provided by the selected loads and the operating voltage range during system restoration. Information on the phasing of armed relays can provide further clarification during the risky restoration periods.

CHAPTER 6 RESULTS OF THE FIRST RESTORATION SCENARIO

6.1 CHAPTER OVERVIEW

This chapter analyses the first restoration scenario covering the simplified simulation model and presents the results. The simplified restoration scenario is when a blackstart facility energises the linked generation station with the associated main transmission stations and distribution load. The route selection allows for connecting a large load centre to the IPS. The initial requirements determine the maximum load connection based on size and power factor. The analysis seeks to determine the worst-case impact on the blackstart facility and to determine the power factors that support the IPS. Section 6.2 discuss the input parameters for the simulation model scenarios. Section 6.3 provide the transient state simulation results for the voltage response (VR) and frequency response (FR) for the scenario presented in section 6.2. An analysis is performed for each of the figures shown in section 6.2. Section 6.4 provides a chapter summary.

6.2 THE FIRST SCENARIOS CONSIDERED

The load type and size with the associated power factors, frequency and voltage setpoints are carefully adjusted to extract the required information to solve the restoration problem. The load adjustment starts with 20MW constant current (CCL) or constant power load (CPL) type and gradually increments by 10MW until 30MW is achieved. After the 30MW sizing, the load gradually increases by 2MW until the breached stability limit. The power factor remains fixed as the FR outcome as for any power factor adjustment with a selected load

size (e.g. 20MW), the same result is achieved in the FR. For an FR falling within the L2 (48.5 to 48.0Hz) and L3 (48.0 to 47.5Hz) band, a critical clearing time (CCT) of 10 minutes and 1 minute is applied, respectively. For frequency responses within the L4 (47.5Hz to 47.0Hz) band, a CCT of 6 seconds is used. Lastly, for a frequency lower than 47.0Hz, a CCT of 200ms is used. For a frequency adjustment of 50.85Hz, the load size again starts at 20MW. The frequency increments in orders of 10MW until a load size of 40MW is achieved. Beyond the 40MW load size, the load increases by 2MW until stability a stability breach is observed.

The voltage response analysis provides insight into possible reactive power support provided by the load connected through adjusting the load power factor. The VR scenarios investigate source voltage settings of 0.90 p.u. and 1.00 p.u., with no in-between adjustment, as principles are observed through analysing only the two scenarios. The frequency setpoint for the voltage scenario is 50.85Hz. The connection of load and transmission assets is explored within the first 10s window timeframe (i.e. within 0 to 10s, all switching concludes) to determine the overall impact and observe sufficient frequency recovery. The details on the adjustments and scenarios considered appear in Tables 6.1 and 6.2.

Table 6.1. Parameters for the frequency analysis scenarios

Scenario	Frequency setpoint (Hz)	Energisation time (s)	Load type	Source p.u. setpoint	Load size (MW)
6.3.1	50.40	6.0	CCL, CPL	0.90	20, 30, 32, 34
6.3.2	50.40	6.0	CCL, CPL	1.00	20, 30, 32, 34
6.3.3	50.85	7.0	CCL, CPL	0.90	20, 30, 40, 42, 44, 46, 48, 50, 52

Table 6.2. Parameters for the voltage analysis scenarios (1.00 p.u. and 0.90 p.u.)

Scenario	Load size (MW)	Source setpoint (p.u.)	Energisation time (s)	Load type	Power factor (lagging)
6.3.4	10, 20, 30, 40	1.00	5.0	CCL	0.98, 0.95, 0.90, 0.85
6.3.5	10, 20, 30, 40	0.90	5.0	CCL	0.98, 0.95, 0.90, 0.85

6.3 SCENARIO 1: TRANSIENT STATE SIMULATION RESULTS

6.3.1 FR for CCL and CPL at 50.40Hz and 0.90 p.u. source voltage

The following section covers the results from the FR simulation, analysing the impact of adjusting the frequency to 50.40Hz before energising load, presenting the effect of CPL and CCL types on the IPS. Figures 6.1 and 6.2 provide insight into the FR for CCL and CPL types at different load sizes.

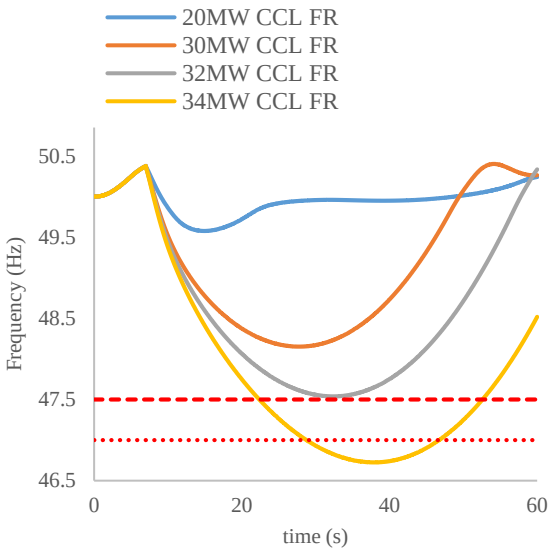

Figure 6.1. FR of CCL at 50.40Hz and 0.90 p.u. source voltage

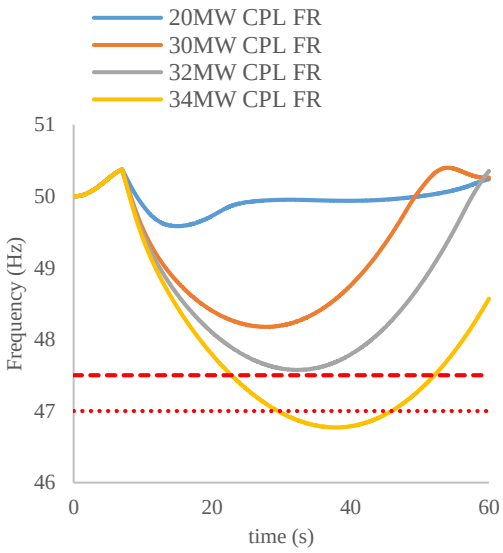

Figure 6.2. FR of CPL at 50.40Hz and 0.90 p.u. source voltage

The analysis indicates that under a frequency adjustment of 50.40Hz (seen under Figures 6.1 and 6.2), the maximum load that may be connected is 32MW when performing continuous load connection. The analysed scenario determines the weakest interconnection within the IPS due to analyzing the impact of one generator connected (energized by the blackstart facility). If more load connects, the generator station protection will be triggered disconnecting or islanding generation stations from the grid as the frequency remains under the 47Hz frequency limit for longer than 200ms. The difference in the frequency measurement between CCL and CPL is presented in the order mHz (10^{-3}) for the four scenarios analysed. A summary of this impact appears in Figures 6.3 and 6.4 for scenarios 1, 2, 3 and 4 (20MW, 30MW, 32MW and 34MW load connection scenarios).

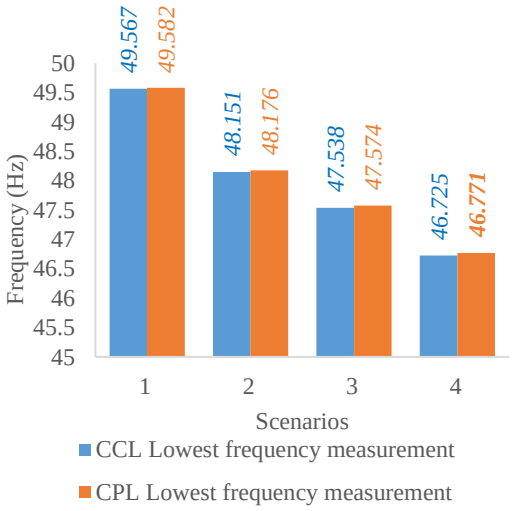

Figure 6.3. Calculated lowest FR measured for CCL and CPL

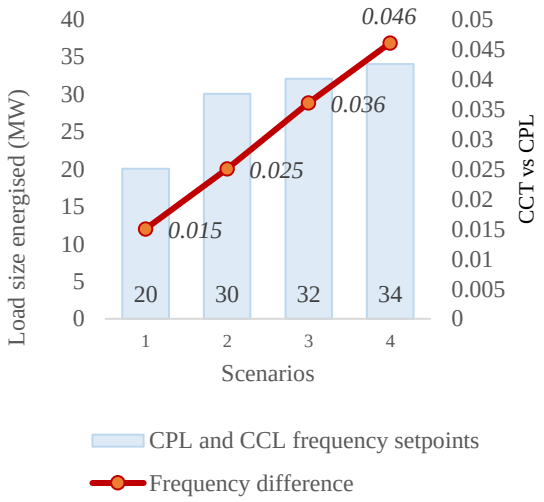

Figure 6.4. FR Difference calculation of CCL vs CPL

Based on Figure 6.3, the CCL result provides the worst FR compared to the CPL result. The difference in frequency measurements between CCL and CPL increases as the load increases under the scenarios analysed, as observed in Figure 6.4, with the maximum difference between CCL and CPL being 36mHz for 32MW load connected under scenario three within the assessment. Scenario 4 is where the station protection operates to disconnect or island the impacted system.

6.3.2 FR for CPL and CCL at 50.40Hz and 1.00 p.u. source voltage

The following section covers the results from the FR simulation, analysing the impact of adjusting the frequency to 50.40Hz before energising load, presenting the effect of CPL and CCL types on the IPS. The scenario presented in section 6.3.2 compared to the previous scenario under section 6.3.1 is that the sending end voltage is adjusted to 1.00 p.u. to determine if there are any differences in the results compared to the 0.90 p.u. result. Figures 6.5 and 6.6 provide insight into the FR for CCL and CPL types at different load sizes.

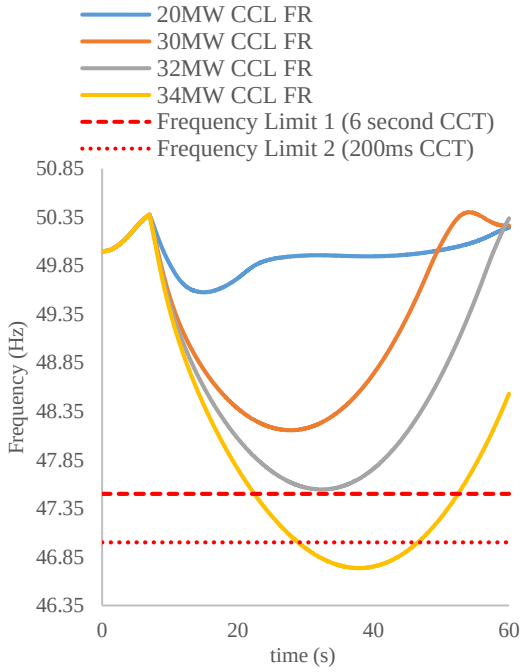

Figure 6.5. FR of CCL at 50.40Hz and 1.00 p.u. source voltage

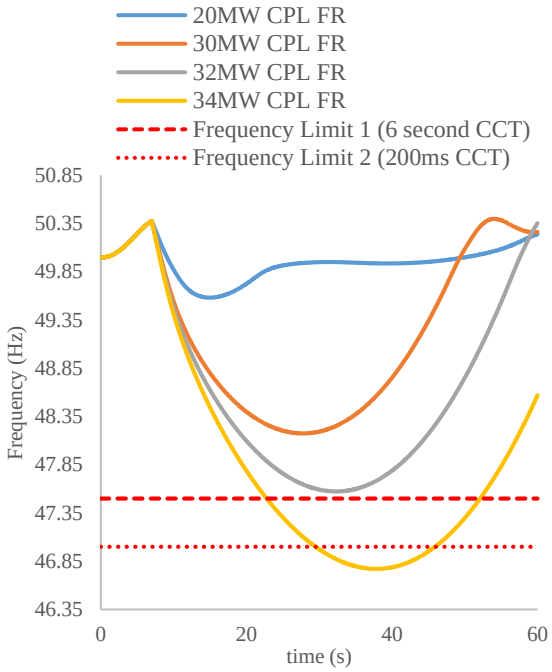

Figure 6.6. FR of CPL at 50.40Hz and 1.00 p.u. source voltage

From the analysis for a frequency adjustment to 50.40Hz at 1.00 p.u. sending end voltage (seen under Figures 6.5 and 6.6), the maximum load that may be connected is again 32MW. If more load connects, the station protection will be triggered to disconnect or island generation stations from the grid. The results from Figures 6.5 and 6.6 are similar to Figures 6.1 and 6.2. A load connection beyond 20MW will always trigger the subsequent UFLS stage if the relays remain armed within the IPS.

6.3.3 The FR for CCL and CPL at 50.85Hz and 0.9 p.u. source voltage

The following section covers the impact of connecting large amounts of load to the IPS, where the system frequency has increased to 50.85Hz. The scenario only analyses the effect of a sending end voltage of 0.90 p.u. A similar outcome is observed when comparing a 0.90 p.u. and 1.00 p.u. sending end voltages. Figures 6.7 and 6.8 provide the results for the FR.

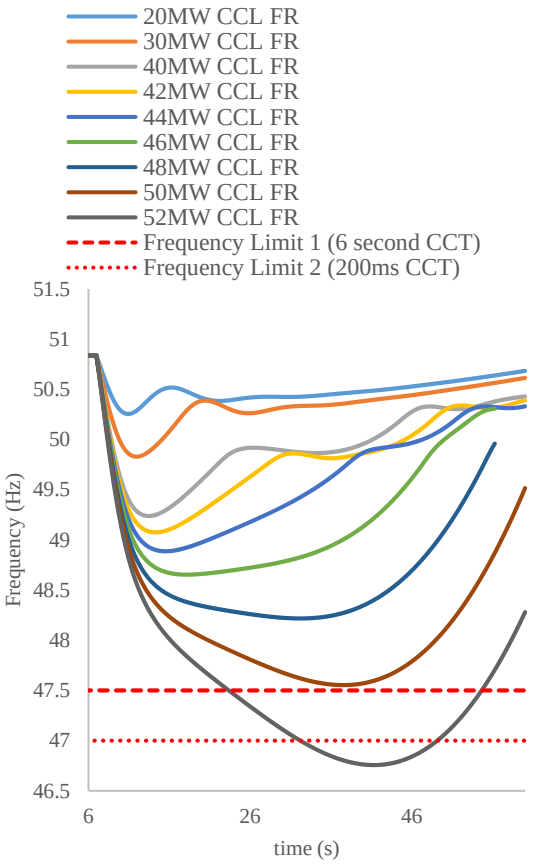

Figure 6.7. FR to CCL at 0.90 p.u. for frequency setpoint of 50.85Hz

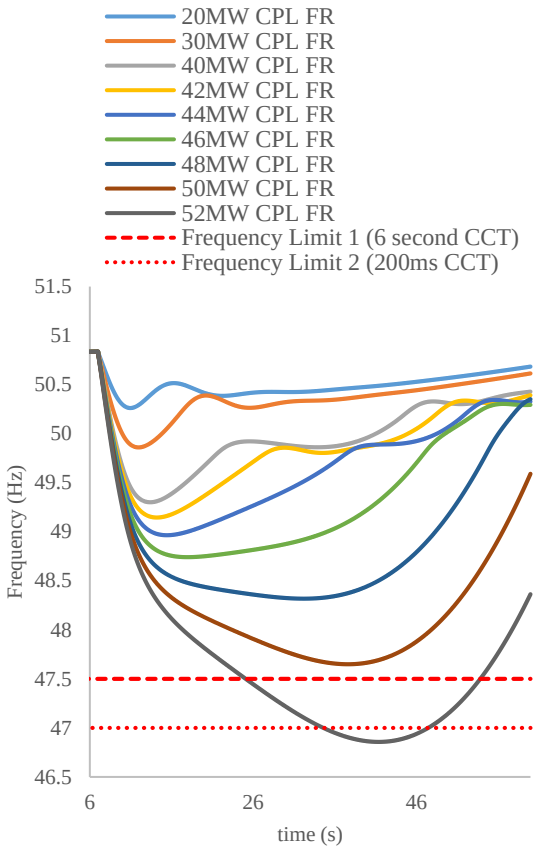

Figure 6.8. FR to CPL at 0.90 p.u. for frequency setpoint of 50.85Hz

The analysis indicates that under a frequency adjustment of 50.85Hz (seen under Figures 6.7 and 6.8), the maximum load that may be connected is 50MW when performing continuous load connection. When 52MW of load connects, the generation station protection is triggered, as the frequency drops below 47Hz for more than 200ms for CCL and CPL types. The system frequency significantly improves compared to the 50.40Hz scenario (18MW

increase in load). This consideration would substantially speed up the recovery efforts. The difference in the frequency measurement between CCL and CPL appear in Figures 6.9 and 6.10. A load connection beyond 30MW will always trigger the subsequent UFLS stage if the relays remain armed within the IPS.

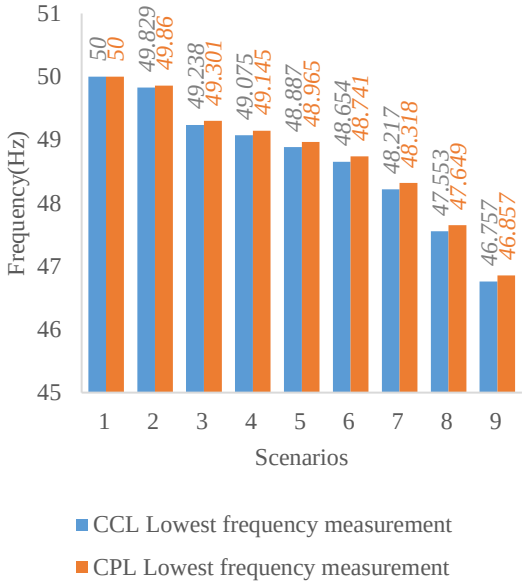

Figure 6.9. Calculated lowest FR measured for CCL and CPL

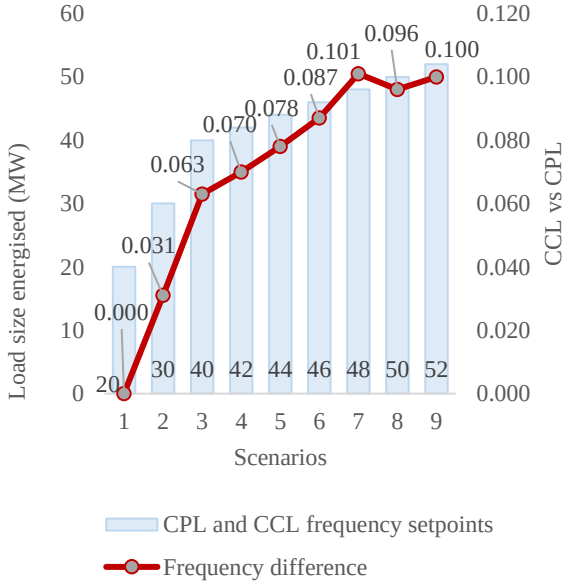

Figure 6.10. FR Difference calculation of CCL vs CPL

Figures 6.9 and 6.10 indicate that under a frequency adjustment slightly above 50.85 Hz, the frequency increases are more substantial for the load types and increases considered. For CCL, the lowest FR measured is 47.553Hz. The outcome of connecting 50MW is acceptable as this is well within the requirement. Careful structuring of the load blocks ensures that the load's portions gradually connect will manage the CLPU contribution not factored into the simulation. Another important contributing factor to the increased load is the voltage dependency response for the real power on the IPS. CCL reaches a higher initial response rise when compared to CPL. The real power peak impact on system frequency for CCL and CPL is presented in appendix 1 of this report.

6.3.4 The VR at 1.00 p.u. source voltage for CCL

The following section covers the VR curves for a sending end voltage of 1.00 p.u. with the transformers adjusted to their lowest tap setting. The power factor is changed for 10MW, 20MW, 30MW and 40MW load sizes to demonstrate the positive contribution to reactive power dampening. Figures 6.11 to 6.14 provide the results of the assessment.

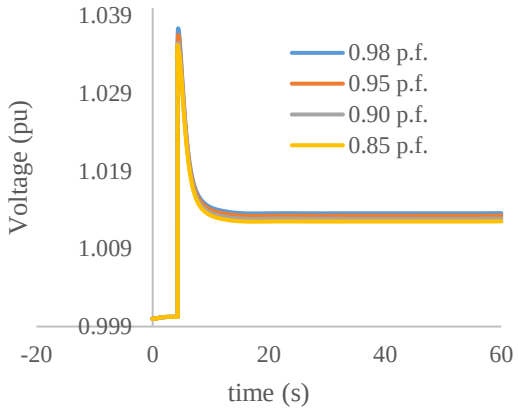

Figure 6.11. Source VR after energising 10MW at 1.00 p.u.

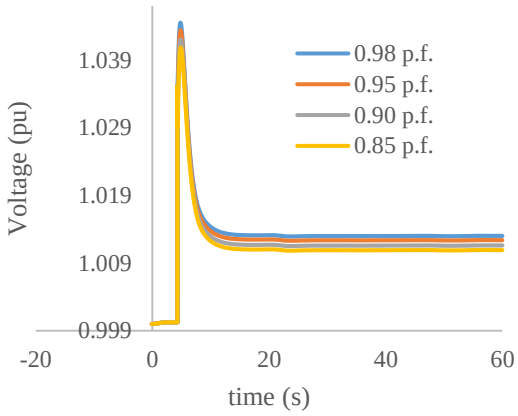

Figure 6.12. Source VR after energising 20MW at 1.00 p.u.

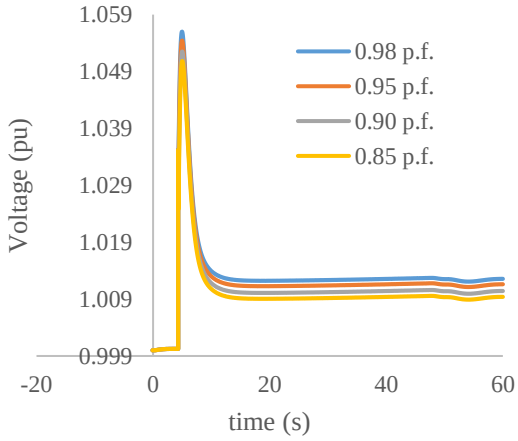

Figure 6.13. Source VR after energising 30MW at 1.00 p.u.

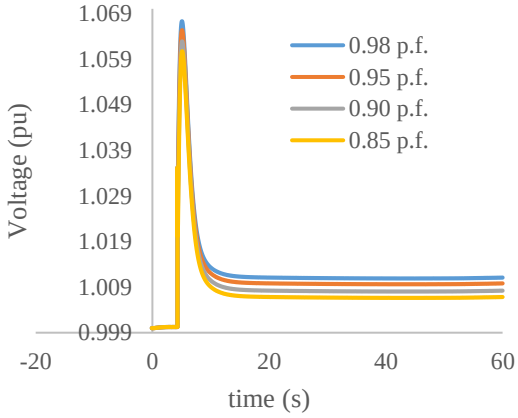

Figure 6.14. Source VR after energising 40MW at 1.00 p.u.

The source voltage selection of 1.00 p.u. provides little insight into Ferranti's inrush challenges experienced within a larger IPS (seen under Figures 6.11 to 6.14). The results show that the connected load supports the dampening of the voltage rise in the simplified

system, which will help the larger IPS. The observed increase in voltage becomes more pronounced as the network size increases as small loads connect to the IPS. Essentially the IPS is experiencing a lightly loaded condition as only a small load can connect to the IPS. It would be better to reduce the sending end voltage to its lowest possible setting. As the load increases, better reactive power dampening is observed at lower lagging power factors due to the support contribution provided by the bigger load blocks energized.

6.3.5 The VR at 0.90 p.u. source voltage for CCL

The final portion of the results covers the VR curves for a sending end voltage of 0.90 p.u. with the transformers adjusted to their lowest tap setting. The power factor is again adjusted for 10MW, 20MW, 30MW and 40MW load sizes to demonstrate the positive contribution to reactive power dampening. Figures 6.15 to 6.18 provide the results of the assessment.

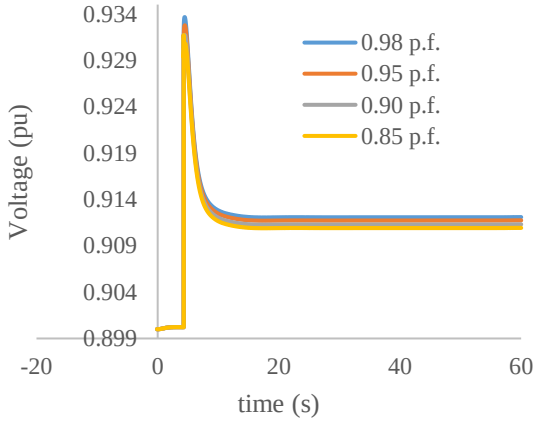

Figure 6.15. Source VR after energising 10MW at 0.90 p.u.

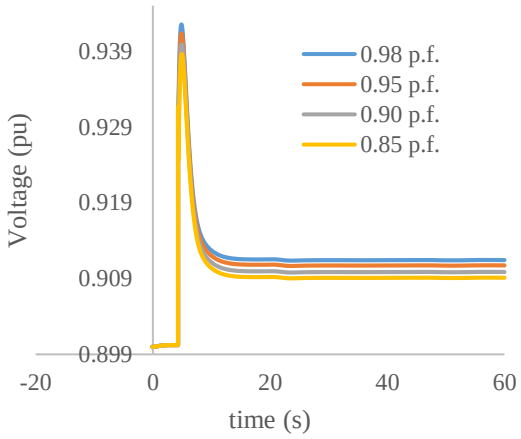

Figure 6.16. Source VR after energising 20MW at 0.90 p.u.

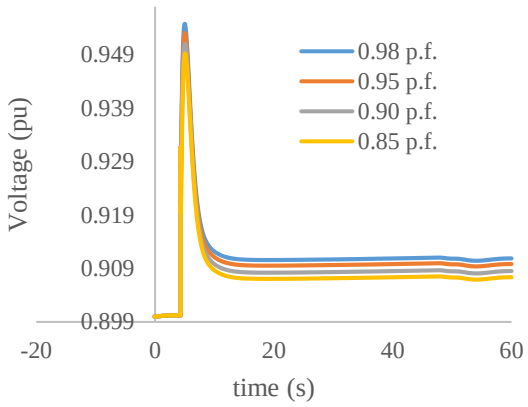

Figure 6.17. Source VR after energising 30MW at 0.90 p.u.

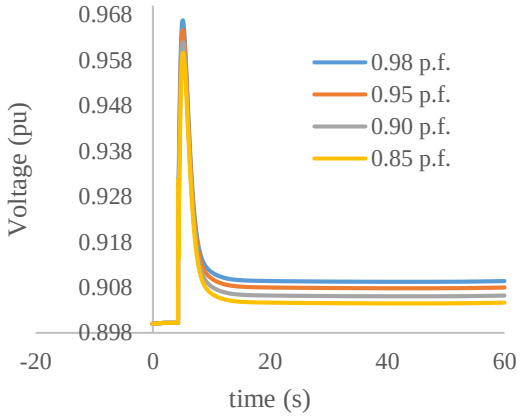

Figure 6.18. Source VR after energising 40MW at 0.90 p.u.

Having the voltage adjusted to 0.90 p.u., although the voltage would increase, the range to which the source voltage would increase is close to the sending end voltage setpoint, as seen under Figures 6.15 to 6.18. In managing the voltage risk, it is advisable to select a lower voltage set-point from the source end that must be tested through simulation such that the end of line voltage is acceptable. A lower power factor with increased load size assists dampening support, as observed in the previous scenario.

6.4 CHAPTER SUMMARY

Under restoration conditions, the operating frequency will not be at 50Hz, but slightly higher. Having a somewhat higher operating frequency allows for the connection of larger load sizes, which will speed up restoration and assist with significant dampening on the IPS. The lowest possible power factor supports the best dampening with the increased load size. The selection of a lower voltage setpoint helps Ferranti's challenges, as this will be more severe during system restoration conditions. However, voltage management is dynamic and will actively be managed to support the end of line voltage.

CHAPTER 7 RESULTS OF THE SECOND RESTORATION SCENARIO

7.1 CHAPTER OVERVIEW

In this chapter, a simplified network is analysed, considering the impact of longer EHV lines on the upstream generation system. The network does not consider the extended portion of the IPS from scenario 1. Instead, it has the reactive power support devices removed to confirm the impact of having only the sending end generator and transformer connected to establish how the system would deal with a scenario of varying conductor lengths and configurations. The lack of reactive power devices to support the IPS will demonstrate the absolute worst-case scenario when considering line lengths. The source generator manages the system voltage and reactive power requirements with the risks highlighted to determine principles for selecting conductor length. In this chapter, section 7.2 discuss the parameters used in the second scenario considered. In Section 7.3, the scenarios considered provide the FR, VR, and reactive power response requirements. Section 7.4 summarises the content of this chapter.

7.2 THE SECOND SCENARIO CONSIDERED

The second scenario analyses the impact of adjusting various typical transmission line lengths with standard design configurations for transmission lines within the SA IPS. The structures analysed is twin-, tri-, and quad-bundle design configurations. The line length adjusts from 50km to 200km, in increments of 50kms under the selected design configurations. The scenario simulation setpoints and adjustments summarise in Tables 7.1 and 7.2.

Table 7.1. Parameters for the frequency analysis scenarios

Scenario	Frequency setpoint (Hz)	Energisation time (s)	Load type	Load size (MW)	Power factor	Bundle configuration	Distance (km)	Conductor types
7.3.1	50.85	50	CCL	50	0.90	twin, tri, quad	50, 100, 150, 200	See appendix

Table 7.2. Parameters for the voltage analysis scenarios

Scenario	Voltage setpoint (p.u.)	Energisation time (s)	Load type	Load size (MW)	Power factor	Bundle configuration	Distance (km)	Conductor types
7.3.2	0.90	50	CCL	50	0.90	twin, tri, quad	50, 100, 150, 200	See appendix

7.3 SCENARIO 2: TRANSIENT STATE SIMULATION RESULTS

7.3.1 The FR and VR after the energization of 50MW CCL

The results from this section will assist the operator with decision-making. It also helps with determining the optimal route selection for the restoration problem. Factors considered are the generator design limits, more specifically, the reactive power absorption limit, the design of conductors and the length of the connecting system. The challenge with reactive power balancing is the ability of reactive power connected devices to dampen the overall system voltage. The FR and VR are important as they show the impact due to the connected load and distance from source to load, whereas the line lengths advise on the route selection highlighting the reactive power risk based on the design limitation from the generator connected. The results are presented, showing the FR, followed by the voltage response based on the length of the system.

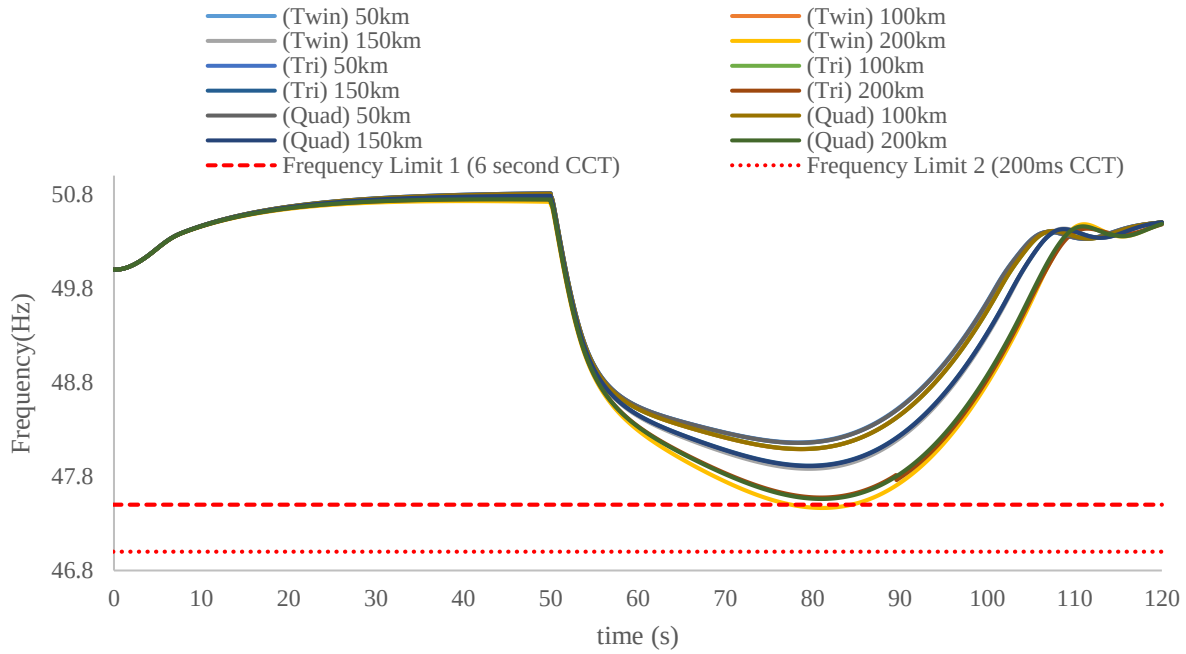

Figure 7.1. FR after energising 50MW CCL varying distance and design

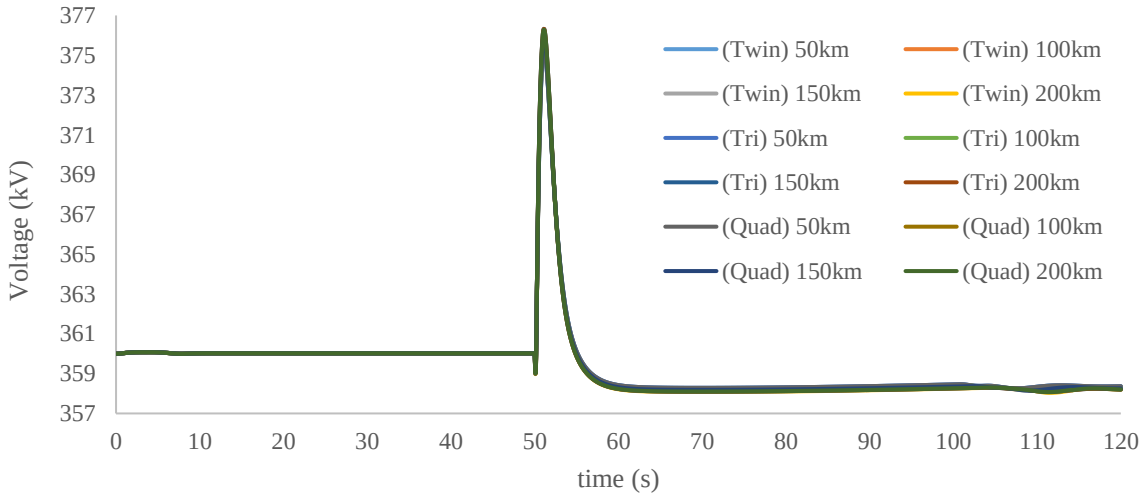

Figure 7.2. Source VR after energising 50MW CCL varying distance and design

Under Figure 7.1, as the frequency setpoint is adjusted to 50.85Hz, the scenario demonstrates that connecting a 50MW load block poses challenges to the generator's FR for lengths above 150km. Distances above 150km, the FR significantly worsen, and the time taken for system frequency recovery breaches the grid code specified criteria. Lengths kept as short as possible avoid risks, and for all bundle configurations, the same severe risk exists for the more considerable distances. The depth of the frequency dip is directly proportional to the length, and at shorter distances, faster recovery is observed. Connecting conductor lengths below

120km support the IPS adequately. From Figure 7.2, since the power factor remains constant, the VR would stay the same over varying distances.

7.3.2 The reactive power response after the energization of 50MW CCL using different design configurations

Principles to understand the reactive power risk is done using the physical assets connected to the power system through deliberately connecting the different line design configurations to the blackstart generator with the end of the line being in an open position. The maximum reactive power is determined and analysed at various conductor designs with varying distances. The dampening of reactive power is a combined effort supported by the generator and load connected to the IPS. The results present the reactive power response and maximum absorption requirements for the source generator.

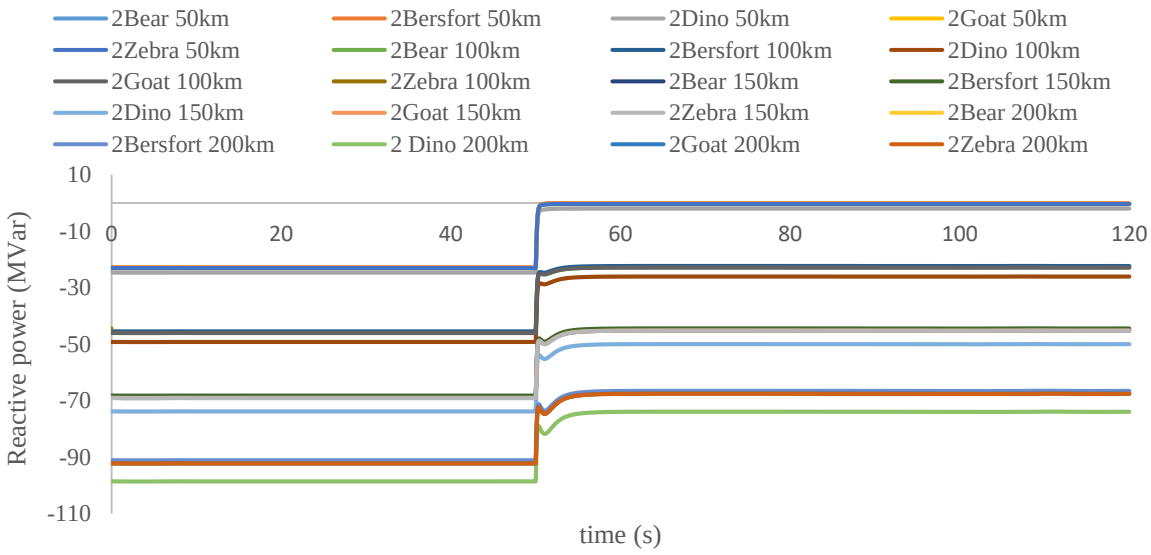

Figure 7.3. MVAr requirements after energising 50MW (twin bundle)

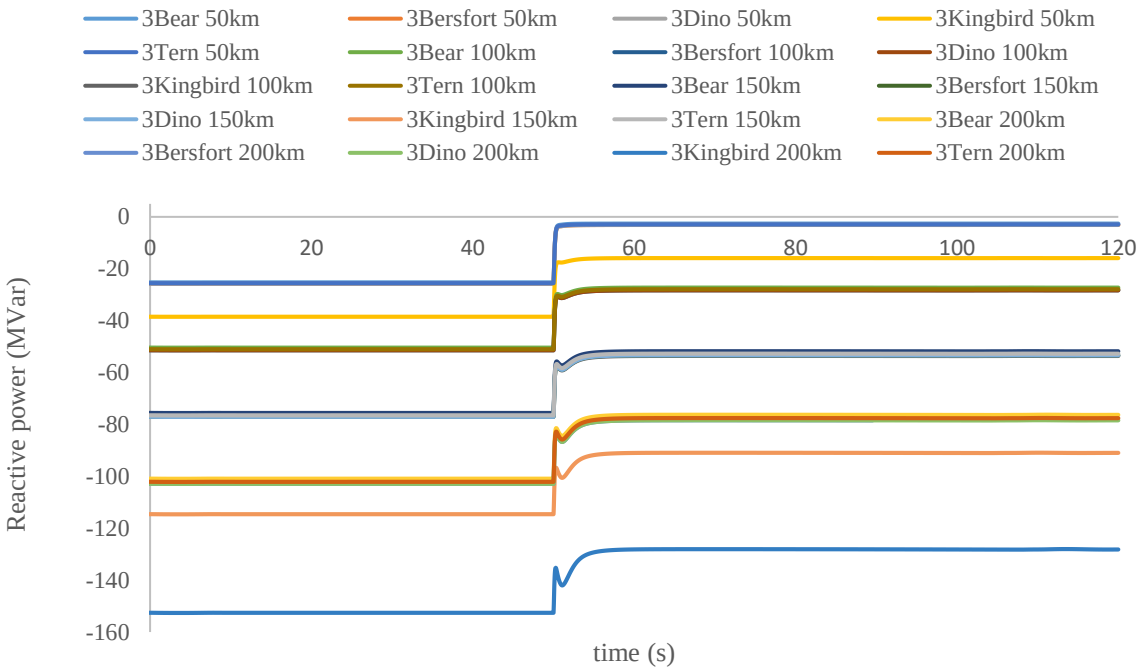

Figure 7.4. MVAr requirements after energising 50MW (tri-bundle)

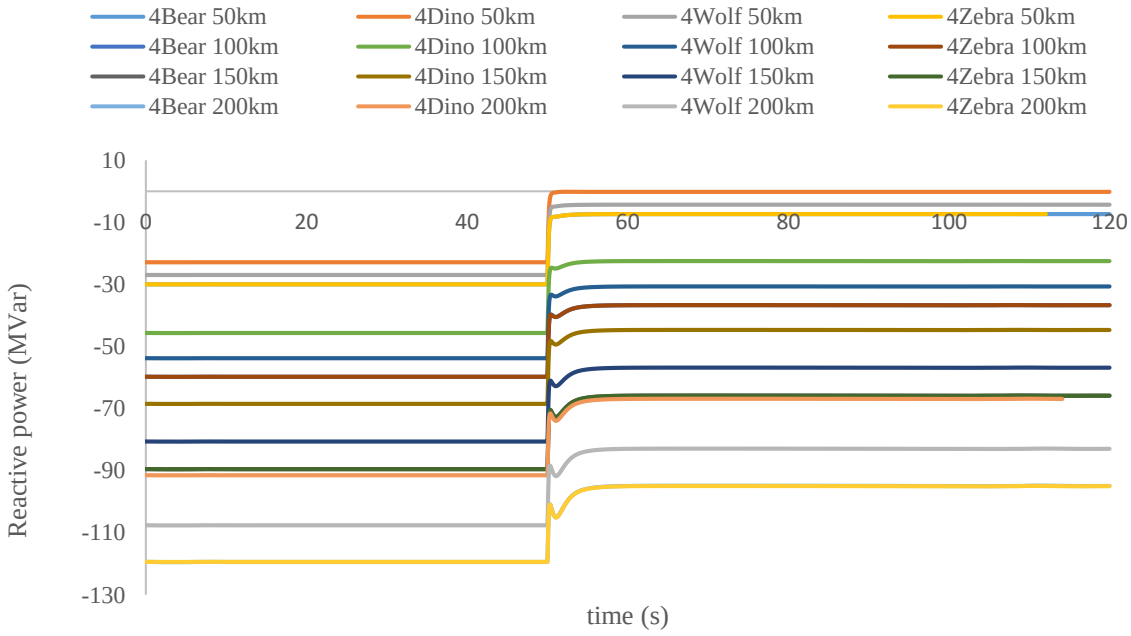

Figure 7.5. MVAr requirements after energising 50MW (quad-bundle)

In Figure 7.3, for the twin spacing design, the maximum starting point for the reactive power absorption is approximately 98MVAr. In Figure 7.4, for the tri-spacing design, the worst possible reactive power absorption is approximately 152MVAr. The last consideration is the quad bundle configuration, which required a maximum initial absorption capability of roughly 119MVAr, as seen in Figure 7.5. Twin spacing conductor design provides the least risk,

whereas, under tri- and quad-conductor spacing, the impact is more severe. The results also show a significant risk regarding the management of Ferranti over-voltages. For shorter distances (≤50km), the absorption of reactive power is close to zero, indicating that the cascaded impact of Ferranti is managed effectively. However, there will always be the absorption of reactive power, and the reactive settling power consumption point will shift as more load connects IPS and the system become extended. The challenges are exaggerated because of the relatively small load connecting to the IPS during the system restoration stage of power system restoration.

7.4 CHAPTER SUMMARY

Sizeable reactive power dampening is required. Shorter distances help cope better with 50MW load blocks and may even support more load. However, the selection of twin spacing configurations may not always be possible during the system restoration phase. At power stations, tri and quad design configurations exist due to the power evacuation requirements.

CHAPTER 8 RESULTS OF THE THIRD RESTORATION SCENARIO

8.1 CHAPTER OVERVIEW

In this chapter, the third scenario is investigated. The scenario considers the simplified network configuration used under scenario one, supported by BESS technology from the source end. The BESS technology location is arbitrarily selected at the source end and not optimised based on the network configuration. In addition, BESS resource switching optimisation is not done to accommodate the charge and discharge of the resource. Section 8.2 discuss the details of the scenario considered. The scenario analyses the impact of connecting varying BESS resource sizes to CCL type sizes. Section 8.3 provides the results and the analysis of the results for each of the figures presented. The results explore the FR and VR in the simplified system. Section 8.4 provides a chapter summary.

8.2 THE THIRD SCENARIO CONSIDERED

The IPS frequency setpoint is 50.15Hz with the source voltage set at 0.90 p.u. to analyse the possible support benefits from the BESS system. The load varies from 10MW to 50MW in increments of 10MW with a load power factor of 0.9. As the load adjusts, the BESS technology size adjusts from 10MVA to 50MVA in increments of 10MVA. It determines the impact of varying sizes on the FR and VR of the IPS. The scenario is summarised in Table 8.1.

Table 8.1. BESS analysis scenario details

Scenario	Frequency setpoint (Hz)	Voltage setpoint (p.u.)	Switching time (s)	Load type	Power factor (lagging)	Load size (MW)	BESS size (MVA)
8.3.1	50.15	0.90	5	CCL	0.9	10	10, 20, 30, 40, 50
8.3.2	50.15	0.90	5	CCL	0.9	20	10, 20, 30, 40, 50
8.3.3	50.15	0.90	5	CCL	0.9	30	10, 20, 30, 40, 50
8.3.4	50.15	0.90	5	CCL	0.9	40	10, 20, 30, 40, 50
8.3.5	50.15	0.90	5	CCL	0.9	50	10, 20, 30, 40, 50

8.3 SCENARIO 3: TRANSIENT SIMULATION RESULTS

8.3.1 The connection of 10MW load (BESS sizes from 10MVA to 50MVA)

The results within this section provide insight into the support provided by BESS. The intention here is to compare the results from Chapter 6 to highlight the positive contribution provided and the adverse risks associated with the deployment of BESS within the SA IPS during system restoration. The scenarios analysed provide an idealistic view for the deployment of BESS as the rate of response, limited by the inverter system, is not factored into the simulation. Again, the FR and VR are important as they provide insight into the stability support provided by BESS within the SA IPS when deployed early within the frequency band. The results show the FR, followed by the VR varying the load and BESS sizes within the simplified model employed.

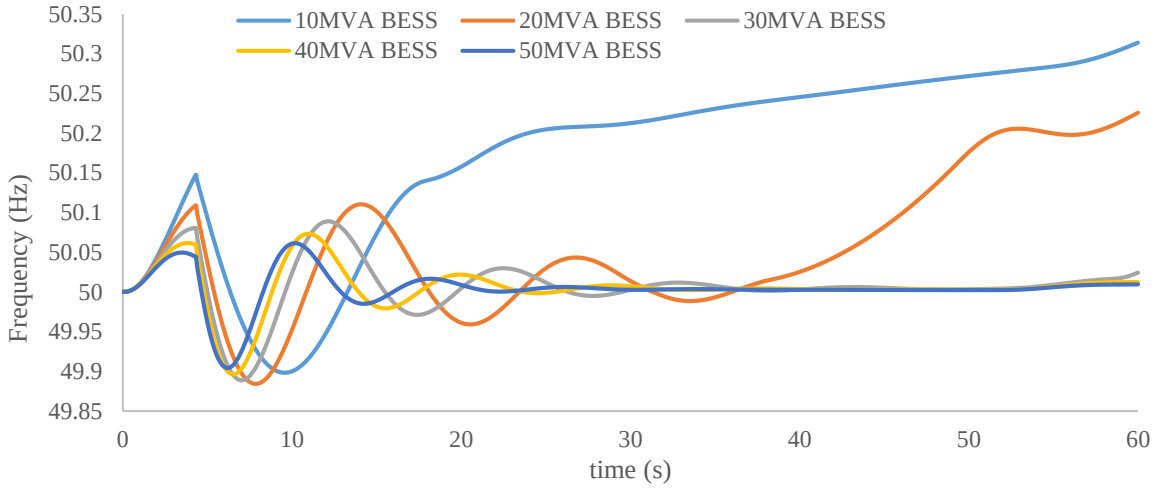

Figure 8.1. FR, after energising 10MW at varying BESS capacities

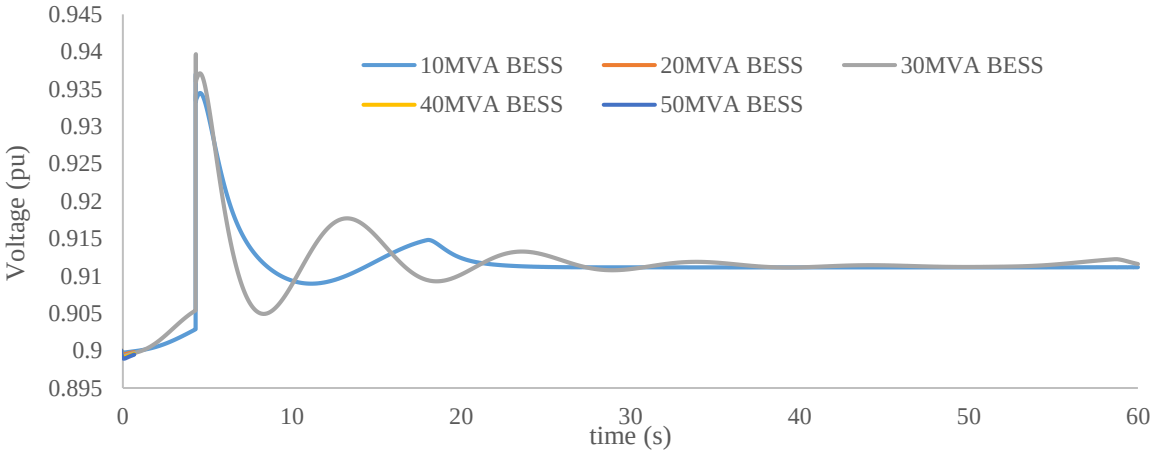

Figure 8.2. Source VR after energising 10MW at varying BESS capacities

From Figure 8.1, with a 10MW load connected, the IPS comfortably handles the load's size under all BESS size scenarios. The maximum frequency drop from 50Hz is approximately 0.12Hz, resulting in no UFLS protection or other generator protection triggered. The results are significantly better when compared to the first restoration scenario considered due to the BESS support provided within the system. From Figure 8.2, the settling voltage has increased from the 0.90 p.u. setpoint to a stabilising setpoint of 0.911 p.u. for all BESS sizes. The result is similar to the voltage setpoint achieved under scenario 1. If there is uncertainty in the load's size, the connection of 10MW will always provide acceptable FR. However, the dampening support because of the small load connected may worsen the setpoint voltage as more of the transmission system is energised.

8.3.2 The connection of 20MW load (BESS sizes from 10MVA to 50MVA)

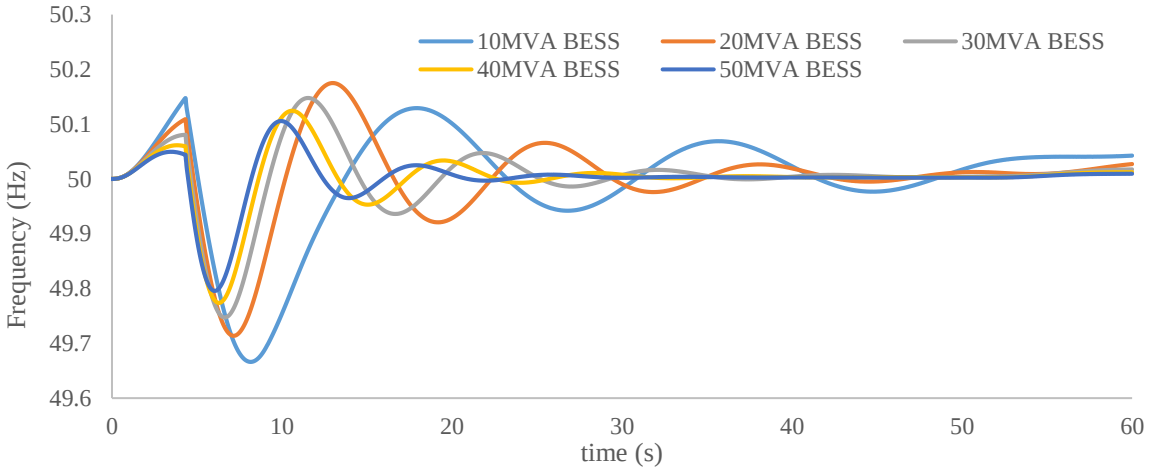

Figure 8.3. FR, after energising 20MW at varying BESS capacities

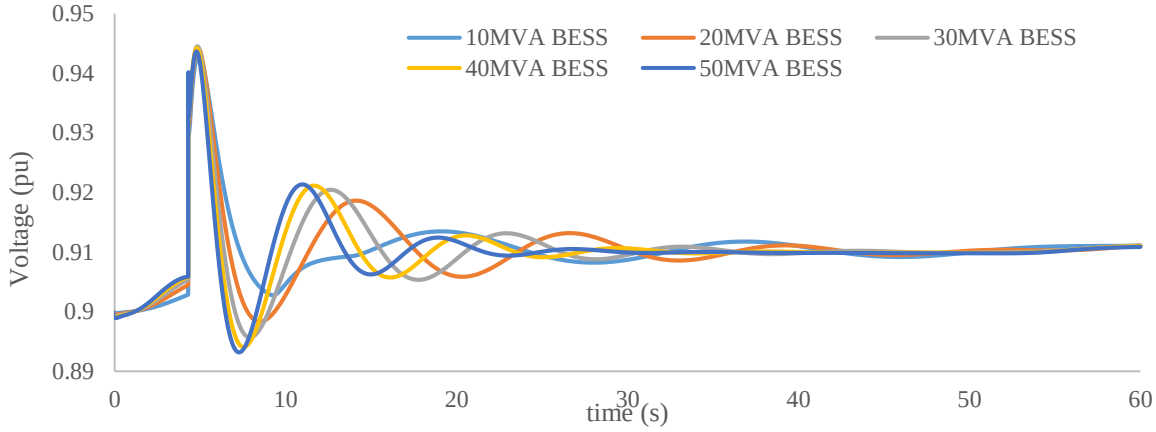

Figure 8.4. Source VR after energising 20MW at varying BESS capacities

From Figure 8.3, with a 20MW load connected, the IPS again comfortably handles the load size under all BESS size installations. The maximum frequency drop from 50Hz is approximately 0.34Hz, with again no IPS protection triggered. The frequency dip also does not trigger a UFLS incident within the IPS. Frequency stabilization correlates to the BESS size, with the more significant sizes providing a faster stabilization over the simulated period. From Figure 8.4, the voltage dip becomes more pronounced, with the drop being 0.7% when measuring from the voltage setpoint of 0.90 p.u. for the largest 50MVA BESS size. The settling voltage has slightly increased from 0.90 p.u. to 0.910 p.u. for all BESS sizes. The connection of 20MW provides an acceptable FR but may provide challenges as the IPS become extended.

8.3.3 The connection of 30MW load (BESS sizes from 10MVA to 50MVA)

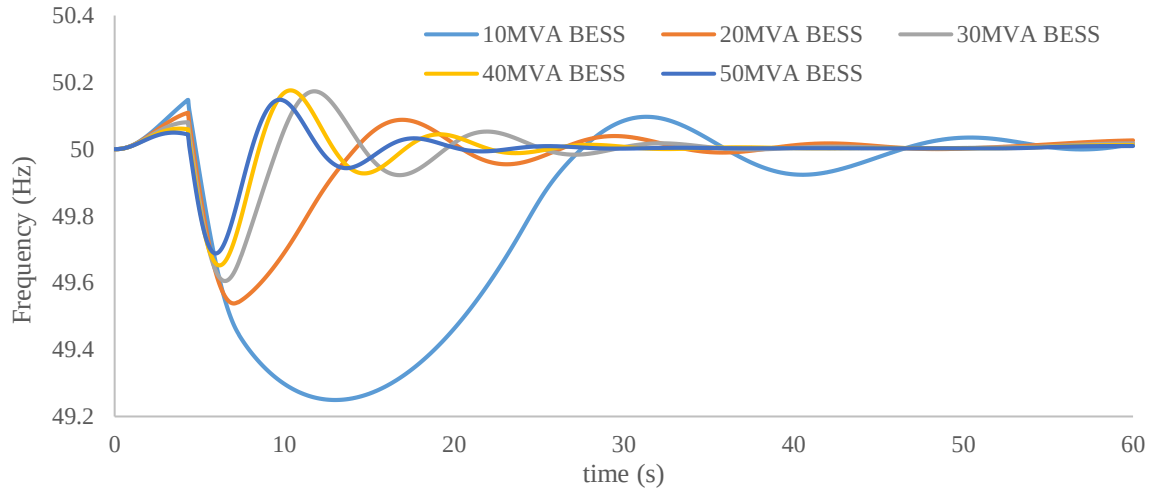

Figure 8.5. FR, after energising 30MW at varying BESS capacities

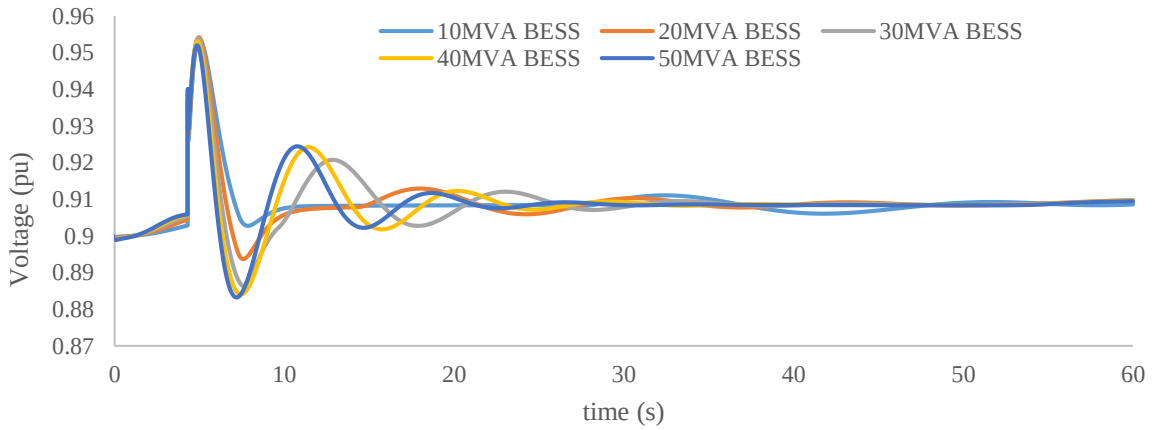

Figure 8.6. Source VR after energising 30MW at varying BESS capacities

Under Figure 8.5, with a 30MW load connected, the IPS again comfortably handles the connected load under all BESS size installations. In this scenario, the maximum frequency drop from 50Hz is approximately 0.76Hz under the BESS size of 10MVA. The FR becomes riskier for the 10MVA BESS size scenario, and a UFLS incident may be triggered within the IPS. Under Figure 8.6, the voltage dip more than doubles to 1.86% when measuring from a voltage setpoint of 0.90 p.u. for a 50MVA BESS size. The settling voltage is 0.908 p.u., and the improved dampening is due to the inductive compensation provided by the inductive load at 0.90 power factor. Under this scenario, 30MW of load provides an acceptable FR and VR, and some dampening is observed with the increased load size.

8.3.4 The connection of 40MW load (BESS sizes from 10MVA to 50MVA)

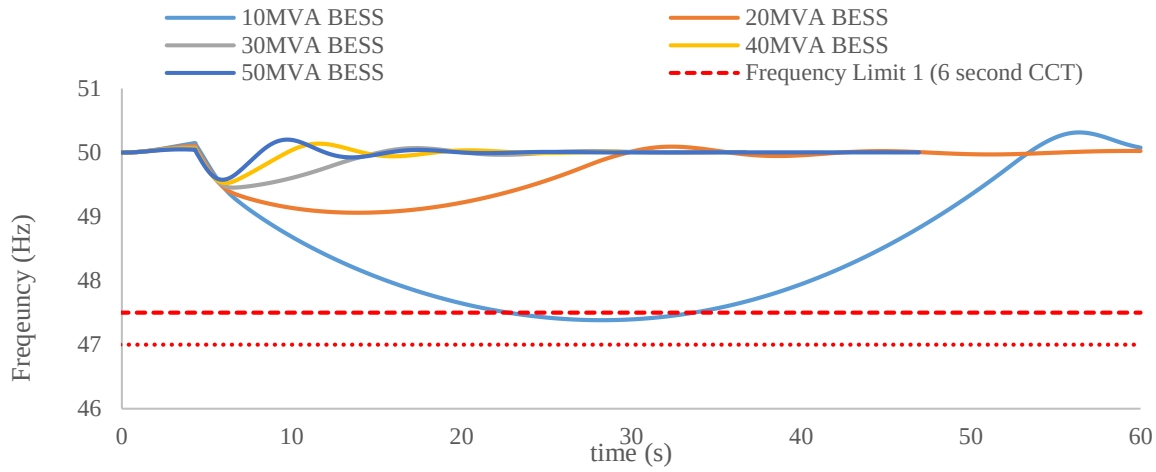

Figure 8.7. FR, after energising 40MW at varying BESS capacities

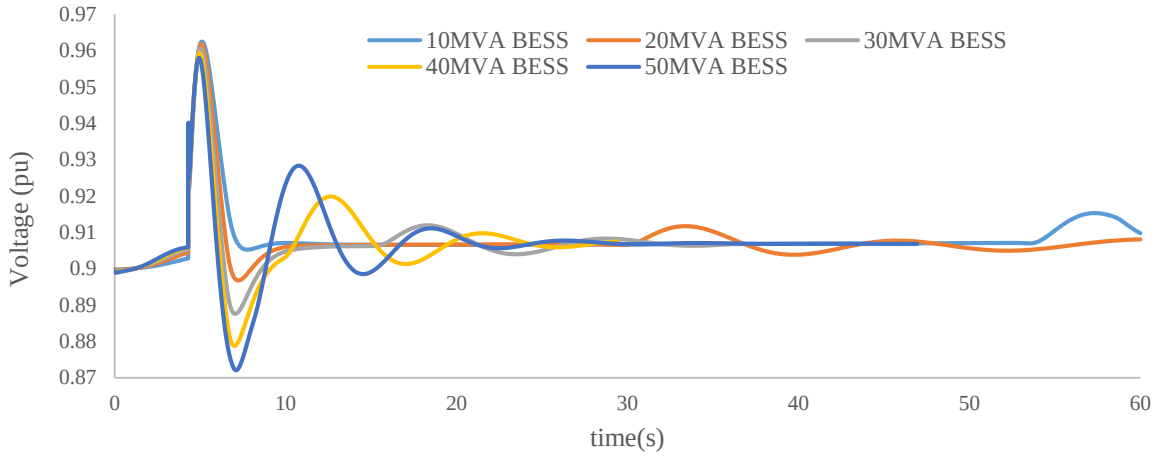

Figure 8.8. Source VR after energising 40MW at varying BESS capacities

From the result in Figure 8.7, with a 40MW load connected, the IPS has challenges managing the FR for the 10MVA BESS size installation. In this scenario, the maximum frequency drop from 50Hz is approximately 2.62Hz for the BESS size of 10MVA. The frequency recovery, once passing the 47.5Hz mark, takes too long to recover. The generation system would disconnect under the 10MVA BESS scenario because the frequency is below 47.5Hz for more than 6 seconds. Under this scenario, the more considerable sizes for BESS (≥20MVA) provides an enhanced response. From the results presented in Figure 8.8, the voltage dip increased to 3.11% when measuring from the voltage setpoint of 0.90 p.u. for the 50MVA BESS size. The settling voltages are 0.906 p.u. for all BESS sizes due to the increased load.

8.3.5 The connection of 50MW load (BESS sizes from 10MVA to 50MVA)

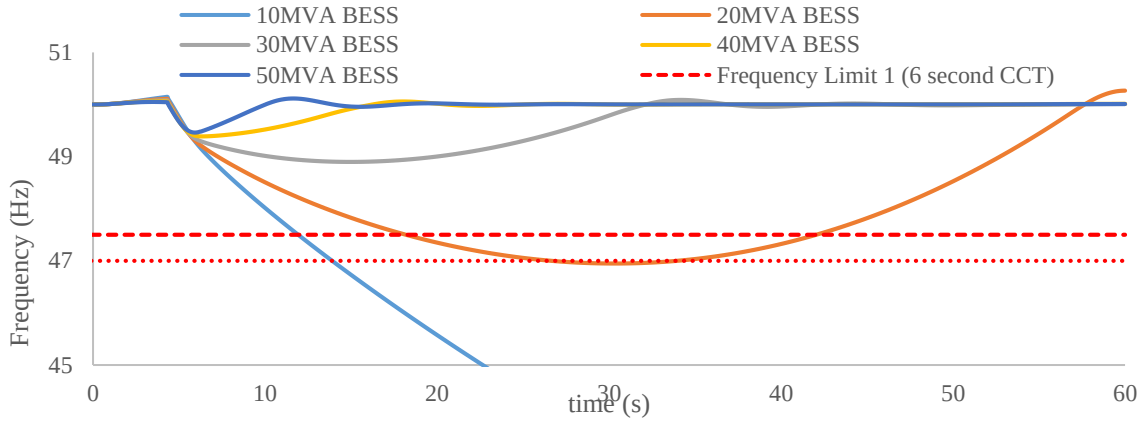

Figure 8.9. FR, after energising 50MW at varying BESS capacities

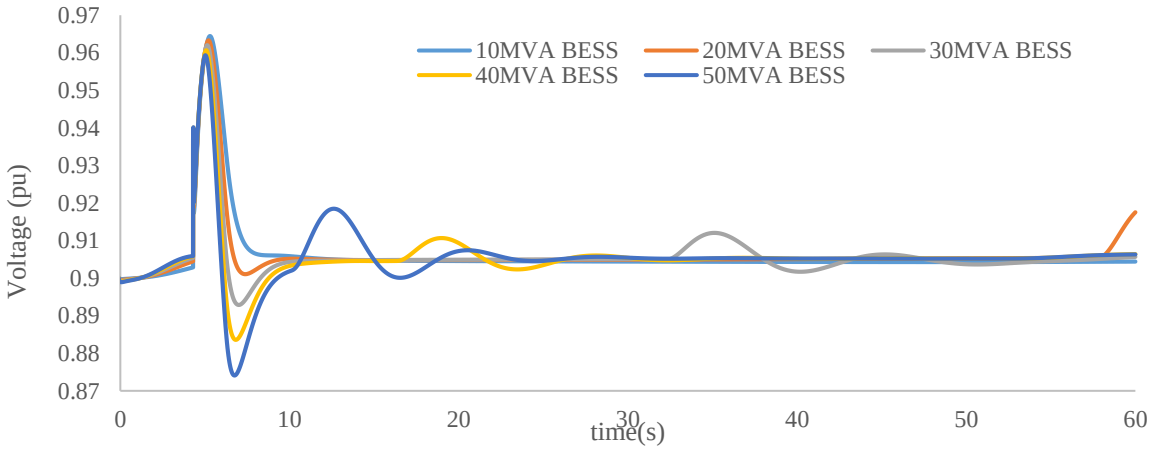

Figure 8.10. Source VR after energising 50MW at varying BESS capacities

Under Figure 8.9, the larger load size of 50MW significantly affects the smaller BESS sizes of 10MVA and 20MVA. Under this scenario, the mentioned smaller sizes do not support the IPS during the energization period. The frequency collapses for the 10MVA BESS resource, and a breach at 47.0 Hz for the 20MVA BESS system is observed. The collapse is due to the BESS being wholly discharged and becoming a load as maximum compensation is provided during the inertial response period. The generation plant now provides power to the BESS system and connected load. For the 20MVA BESS, the 47Hz frequency dip results in a unit trip. For the more considerable BESS sizes (≥30MVA), the generation station will adequately recover the frequency to the required 50Hz. From Figure 8.10, the voltage dip at the station has a depth of 2.8% when measuring from the 0.90 p.u. mark. The drop indicates the maximum amount of

energy injected to assist with quicker stabilization when compared to the 40MVA and 30MVA BESS size. A larger BESS size would increase the dip depth and duration.

8.4 CHAPTER SUMMARY

BESS's connection is not straightforward and should be studied on a case-by-case basis as the system goes through the system restoration stage. Under the investigated scenarios, the frequency remains sensitive for smaller BESS sizes (≤20MVA), and the voltage impact does not provide a straightforward response. A natural operational instruction would be to use the more significant BESS systems, providing better support. As the load increases, the smaller size BESS becomes inadequate to support the system frequency and would assist more localized systems within the distribution networks. A balance between the increase in load and system voltage needs to be determined proactively.

CHAPTER 9 RESULTS OF THE FOURTH RESTORATION SCENARIO

9.1 CHAPTER OVERVIEW

This section analyses a small portion of the SA IPS (11-bus system) to determine if the principles identified under scenario 1, 2 and 3 provides acceptable FR and VR responses under the three corridor restoration scenarios investigated for this section. The restoration proceeds from the blackstart facility as with the previously analysed scenarios. Due to information confidentiality, substation names and lines do not reflect within the simulation model. Section 9.2 discuss the details of the fourth scenario considered. The section unpacks the detailed steps followed when simulating the corridor energisation. Section 9.3 provide the transient results and the analysis of the results for each of the figures presented. Section 9.4 provide the Ferranti impact based on the steady-state voltage for various voltage scenarios considered.

9.2 THE FOURTH SCENARIO CONSIDERED

Scenario 4 divides into three restoration scenarios. These restoration steps split this way to provide insight into the gradual restoration, demonstrating the IPS' impact with and without BESS connected to the IPS. The BESS size is 50MVA at 0.90 p.f. operating in Q-control mode, supporting the reactive power requirements for restoration. The source voltage setpoint is 0.95 p.u. providing adequate support to the IPS. The reasons for selecting a 0.95 p.u. setpoint is demonstrated under section 9.4 under the steady-state voltage analysis of IPS when thoroughly energising all connected loads in the scenario. Voltage setpoints of 1.00 p.u., 0.95 p.u. and 0.90 p.u. are used in the assessment. The scenario assesses the effect of the energised system after the entire system is rebuilt and when the IPS is at its most extended length, providing the worst-case scenario with the minimum load added or with no CCL connected to the IPS.

All transformer tap settings in the assessment are set to the lowest possible setting with the automatic on-load tap adjustment disabled, disabling reactive power management from the reactive power compensation devices within the IPS. Due to the setting adjustments, voltage and reactive power management are managed from one supply source to mitigate the potential exaggeration of Ferranti risks that will creep in during the simulation when transformers connected on the IPS automatically adjusts at EHV and HV busbars to contractual setpoint values. It is essential to understand that the IPS is designed to carry a load under normal operating conditions that usually dampen the Ferranti risk. The national load is generally supplied from the interconnected generating stations that support the generator during consumption. The combined restoration switching activity is captured in Table 9.1.

Table 9.1. The combined restoration sequence

Restoration step	Name	Time (s)
1st restoration step	Line 1	4.5
1st restoration step	Line 2	6
1st restoration step	Substation C - Load 1 (50MW)	7
1st restoration step	Line 5 + Substation F - Load 1 (25MW)	55
1st restoration step	Substation F (Gen 1)	75
2nd restoration step	Line 3	80
2nd restoration step	Line 4 + Substation E - Load 1 (55MW)	100
3rd restoration step	Line 7	125
3rd restoration step	Substation G (Gen1)	130
3rd restoration step	Substation G - LD 1 (30 MW)	150
3rd restoration step	Line 6	160

9.3 SCENARIO 4: TRANSIENT AND STEADY-STATE RESULTS

9.3.1 Scenario 4.1: The first restoration step

The results from this section demonstrate the implementation of the restoration principles established under chapters 6, 7 and 8. The first restoration sequence energises lines 1 and 2, with load from substation C amounting to 50MW. In addition, line 5, substation F with a load of 25MW, adds to the power system within this restoration sequence. The energised load and asset are further supported by adding a generator to the IPS. The restoration is iteratively solved until stability is achieved. The restoration's timing is solved using a waiting period for frequency recovery above 50Hz for more extensive and smaller loads. The results show the

FR, followed by the VR, load response with and without BESS connected. Lastly, the charge and discharge rates are presented for the BESS over the simulation period.

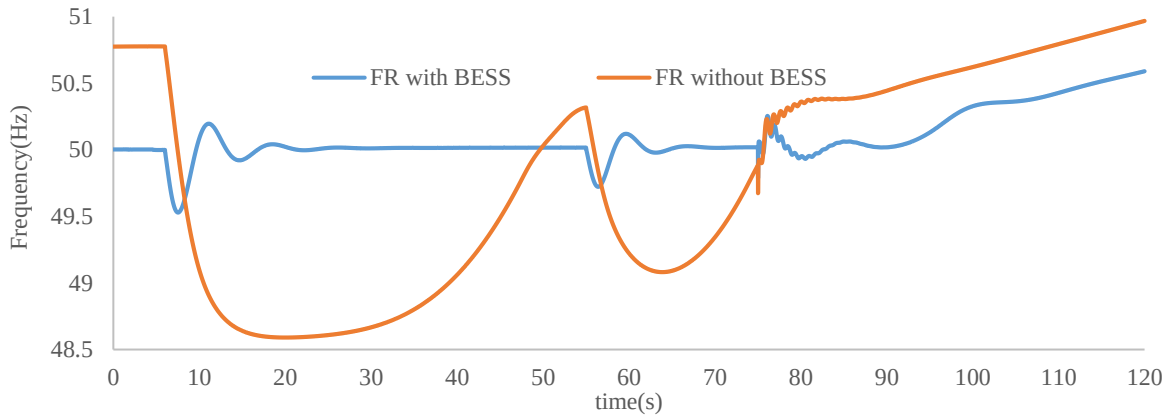

Figure 9.1. FR for the first restoration step of the SA IPS

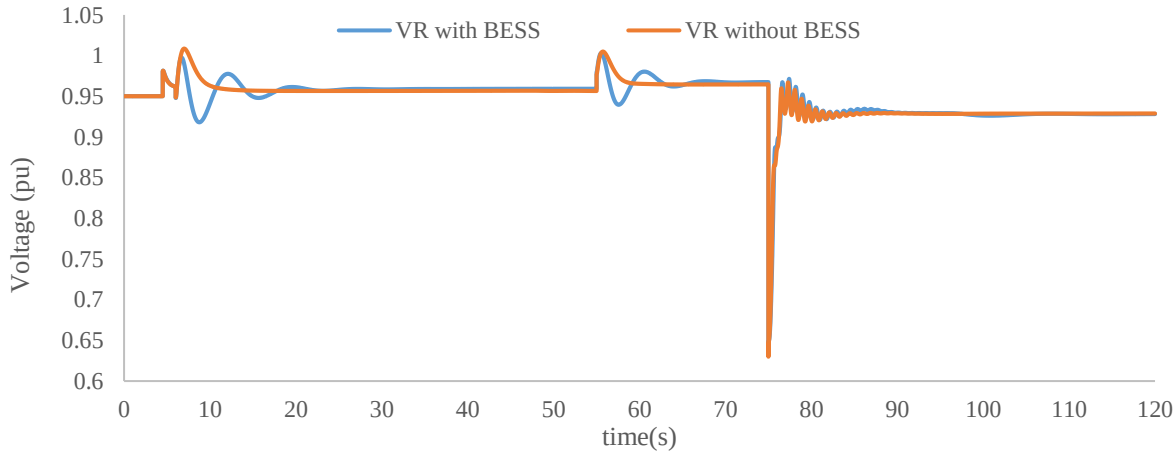

Figure 9.2. VR for the first restoration step of the SA IPS

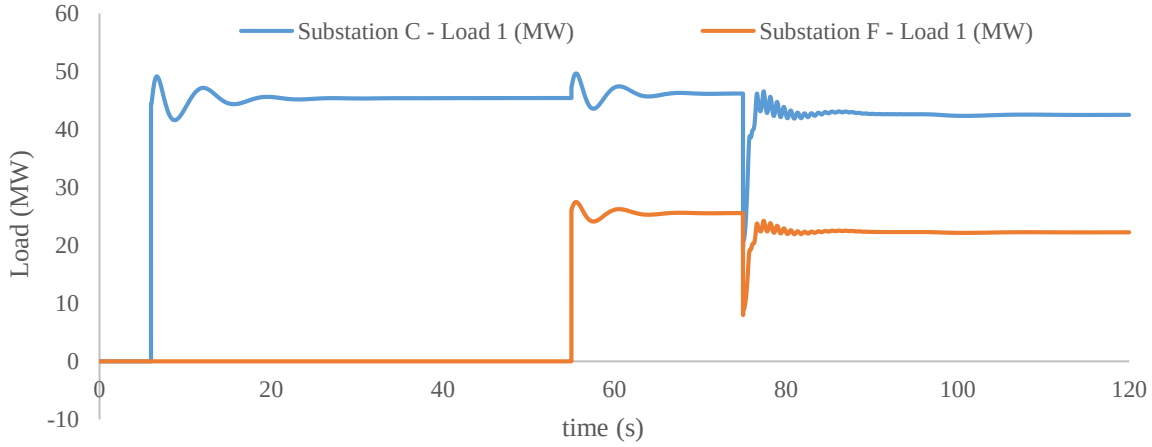

Figure 9.3. Load energisation response with and without BESS

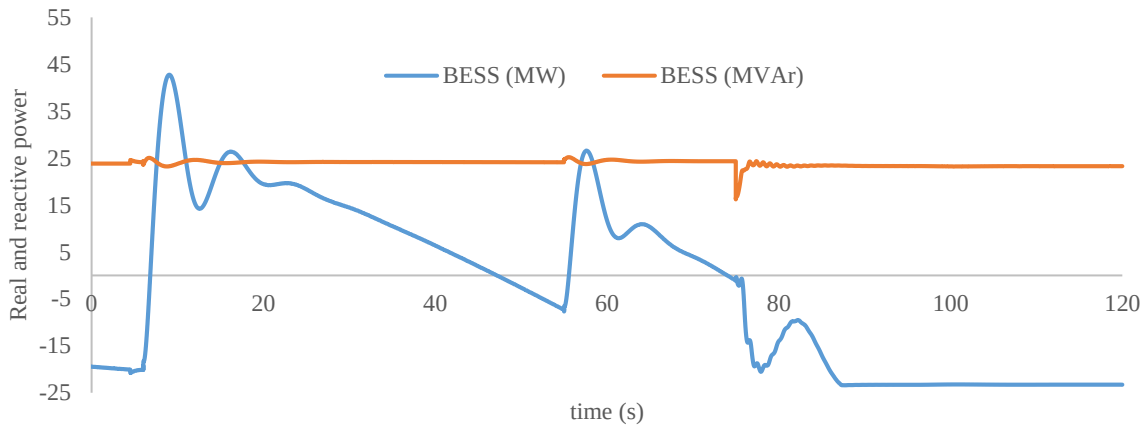

Figure 9.4. BESS response for real and reactive power

In the first scenario analysed, in Figure 9.1, with the frequency adjusted to 50.85Hz, the frequency remains within safe operating limits. With the BESS connected, the FR is far more superior when compared to the scenario with the BESS not connected. The frequency recovers adequately within the grid code specified limits. During a real-world incident, the high rise in frequency is actively managed and will not go beyond the grid code specified limits.

In Figure 9.2, a significant voltage dip experienced (Z2-type dip) lasting 1120ms after approximately 75 seconds. The generators electrical power increase is inversely proportional to the load and unit energized (observed under Figures 9.1, 9.2 and 9.3). A dip primarily arises due to the transformer inrush current connected to the energizing station (Substation F). Due to transformer energisation, the internal inrush characteristics worsen the voltage dip. The dip can be limited by adjusting the voltage at the energising station to a much lower tap setting, which will affect the customer voltage initially, but can be adjusted as the restoration progresses.

From Figure 9.3, there are no significant oscillations experienced due to the voltage dependency factored into the simulation. For both scenarios (with and without BESS), the load stabilizes adequately. In Figure 9.4, the BESS continuously charges and discharges real power and continuously dispatches reactive power. The charge and discharge periods are not reflective of a real-world charging scenario. It is essential to do the charging where the system security risk is low (optimal periods) to optimize the charging and dispatching of the BESS resource. A total combined load of approximately 75MW adds to the IPS within 55 seconds, and the frequency and voltage achieve stability within 10 seconds.

9.3.2 Scenario 4.2: The second restoration step

The second restoration step is a continuation of the first restoration step. The energised corridor from the first restoration step extends by adding two additional lines, lines 3 and 4, with load from substation E amounting to 55MW. The restoration is again iteratively solved until stability is achieved, using a waiting period for frequency recovery above 50Hz after more extensive and smaller loads connected to the power system. The results show the FR, followed by the VR, load response with and without BESS and charge and discharge rates for BESS over the simulation period.

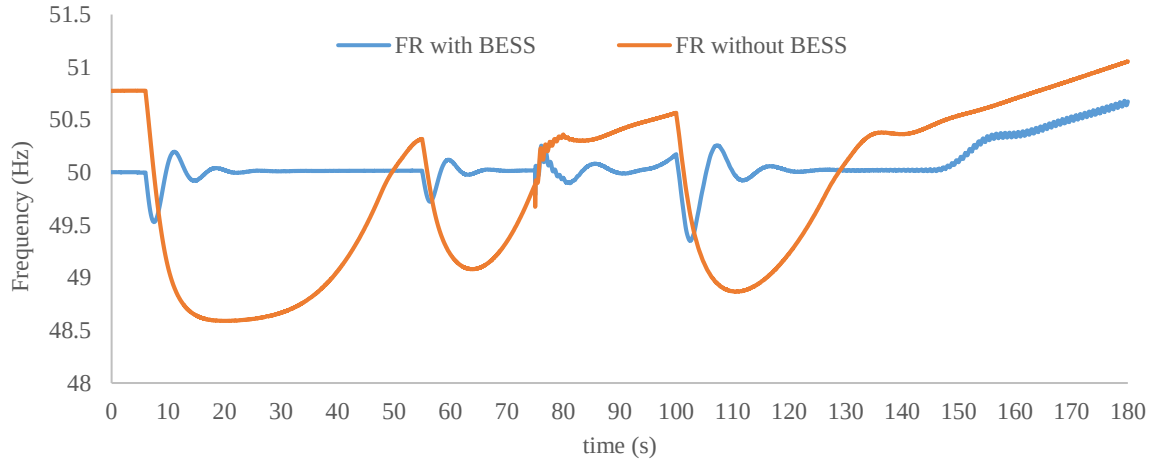

Figure 9.5. FR for the second restoration step of the SA IPS

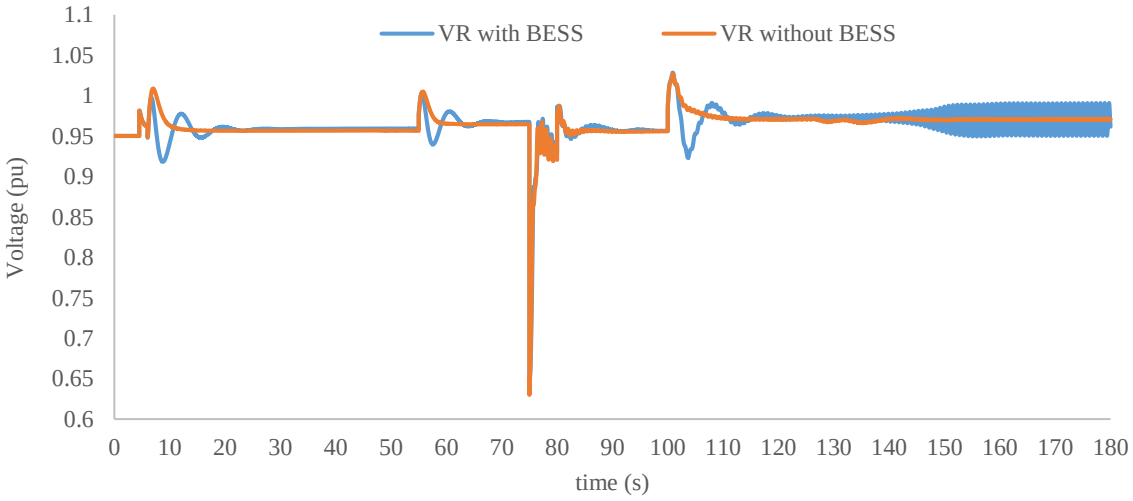

Figure 9.6. VR for the second restoration step of the SA IPS

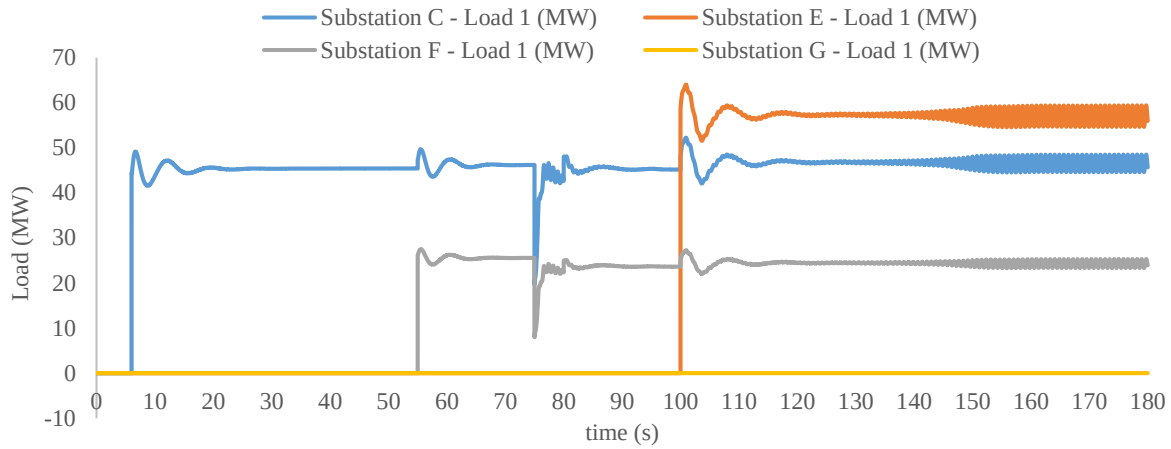

Figure 9.7. Load response with BESS

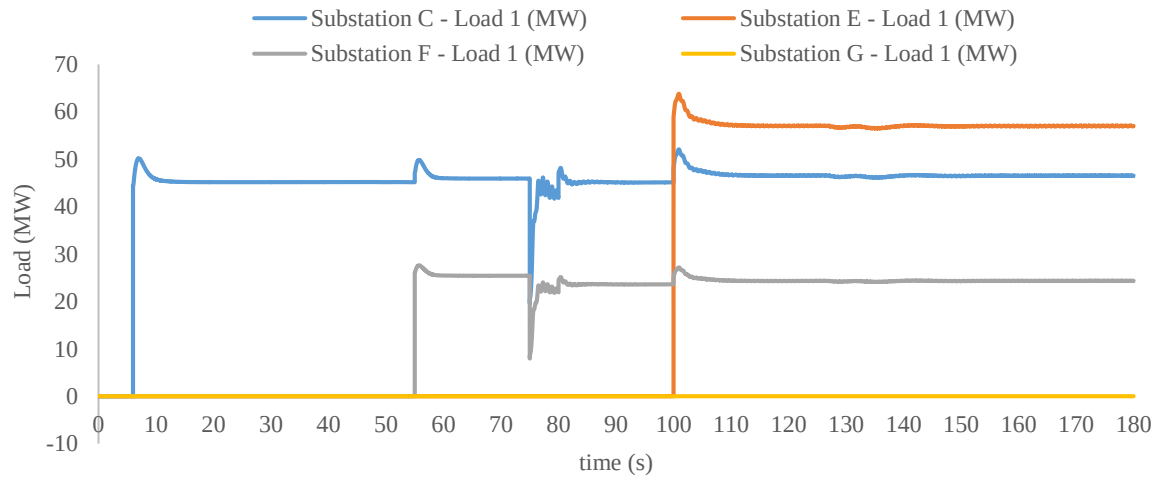

Figure 9.8. Load energisation response without BESS

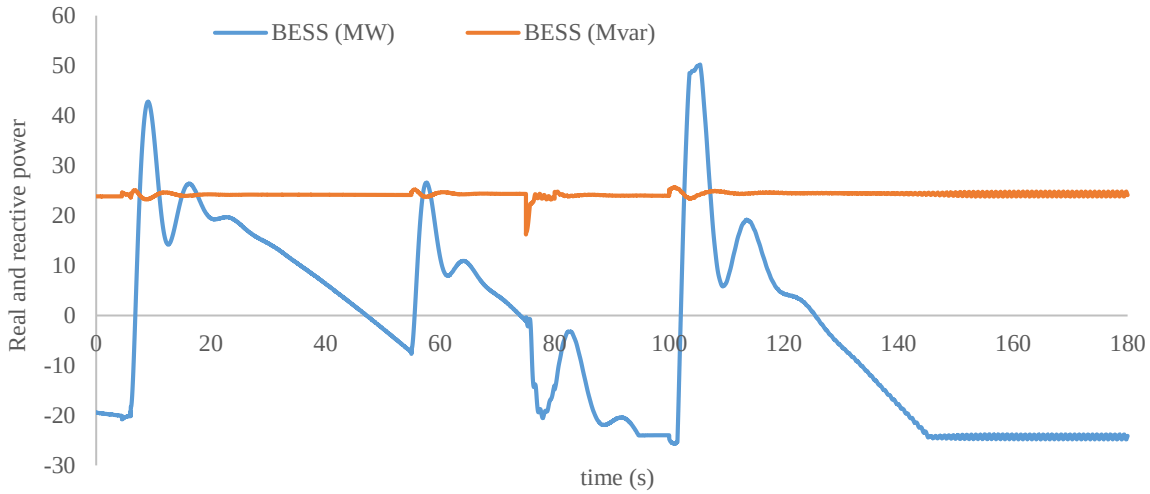

Figure 9.9. BESS response for real and reactive power

The second grid restoration scenario is a follow-on from the previous assessment to demonstrate continuation. In Figure 9.5, based on the load selection and the resources

dispatched, the frequency recovers adequately within specified grid code requirements. In the BESS connected response, the frequency is more durable, and recovery is far more superior when compared to the scenario without BESS connected.

From Figures 9.6 and 9.7, with the BESS connected, due to the charge and discharge patterns observed in Figure 9.9 for the BESS resource, voltage oscillations exist as the system is dealing with a more load connected, experiencing a charged state from 100 seconds. Disconnecting the BESS beyond 100 seconds resolves the oscillation challenges. Figure 9.8, due to the BESS being disconnected, the load response is positive, with the TGOV5 system connected. An additional 55MW adds to the 75MW from scenario one at 100 seconds. Figure 9.6 shows an increase in the settling voltage due to the capacitive contribution of the lines connected. The load connected helps manage the voltage rise risk. This result demonstrates that as more generators are connected, a gradual increase in load is possible.

9.3.3 Scenario 4.3: The third restoration step

The third restoration step continues the first and second restoration steps. The energised corridor further extends by adding two additional lines, lines 6 and 7, a generator and a load amounting to 30MW at substation G. The results show the FR, followed by the VR, load response with and without BESS and charge and discharge rates for BESS over the simulation period.

Figure 9.10. FR for the third restoration step of the SA IPS

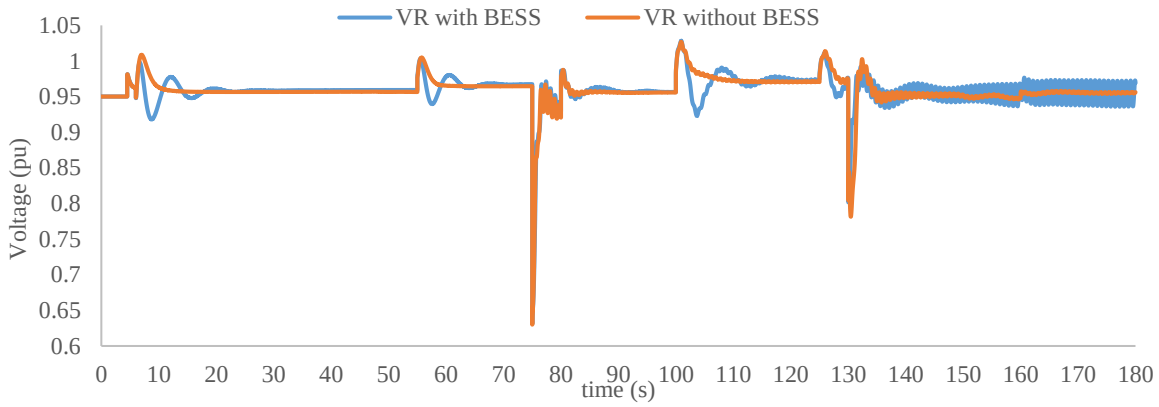

Figure 9.11. VR for the third restoration step of the SA IPS

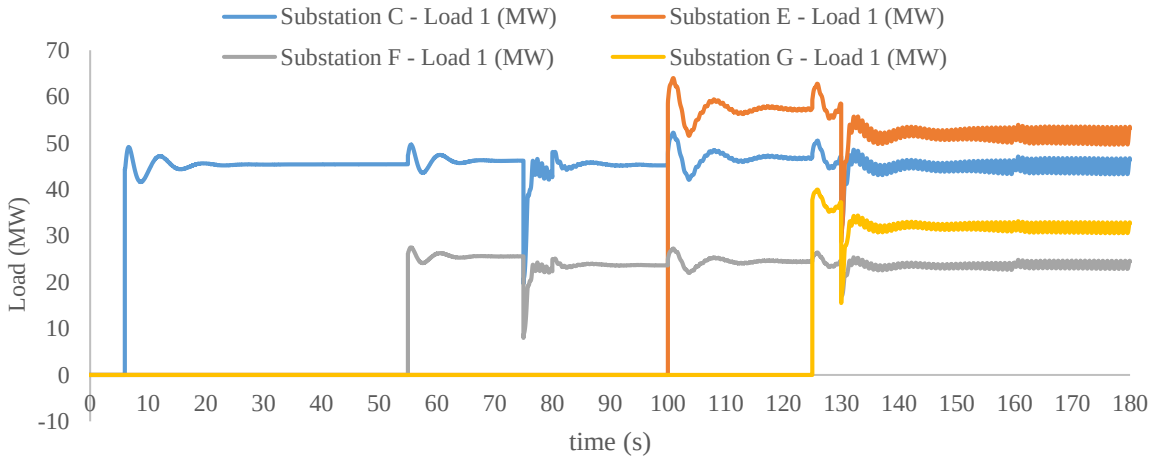

Figure 9.12. Load response with BESS

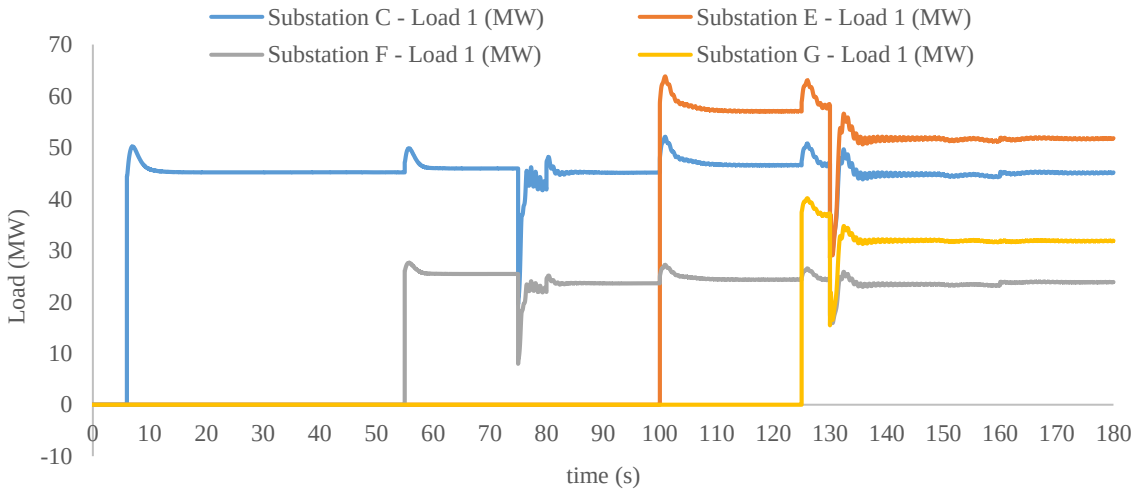

Figure 9.13. Load response without BESS

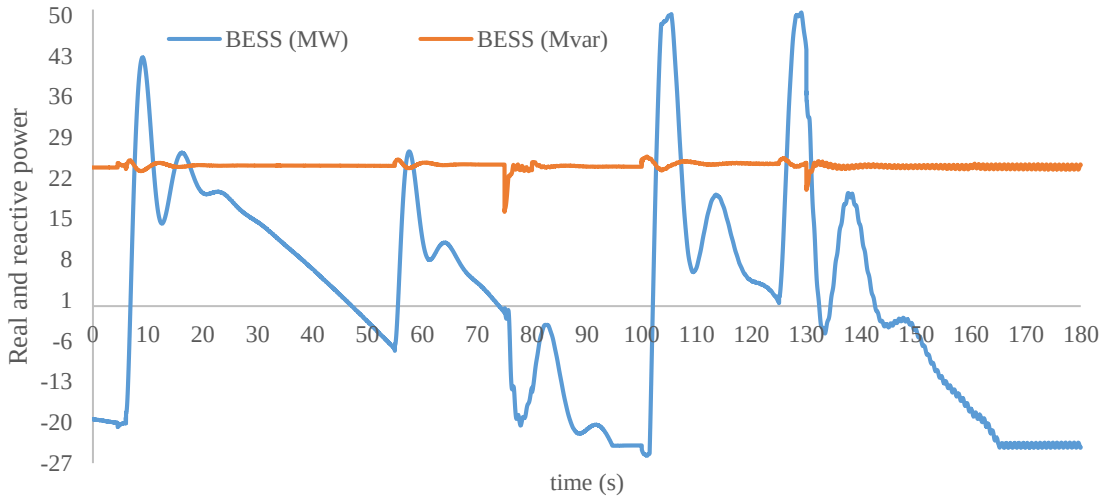

Figure 9.14. BESS response for real and reactive power

The third restoration scenario adds 30MW to the 130MW connected to the IPS. From Figure 9.10, with BESS connected, the response is again superior to the scenario without BESS. For both cases considered, the FR is within acceptable limits. In Figure 9.11, voltage oscillations exist beyond 140 seconds (seen in Figures 9.11 and 9.12) with BESS connected to the IPS.

Even though the load added was adequately spaced, voltage oscillations exist due to the combination of load and transmission lines connected to stabilise the IPS. Figure 9.13 demonstrates that without BESS support, an adequate load response is achieved. In addition, the BESS system requires support from the generators connected due to the charging pattern observed beyond 140 seconds observed in Figure 9.14.

In some instances, the FR, VR and load response becomes unstable, and this is due to the BESS used a load (charge state). The results demonstrate that additional load is added, which results in the unstable oscillation seen. When the frequency reaches an unstable operating criterion, this is due to the power system stabiliser being disabled. Realistically, there will be active frequency, voltage and reactive power management during a blackout scenario, and the unstable frequency response and voltage response will not occur.

9.4 THE STEADY-STATE VOLTAGE RESPONSE

In this section, the IPS steady-state voltage is analysed, analysing dampening through the connection of load and without energising any load at sending end voltages of 1.00 p.u., 0.95

p.u. and 0.90 p.u. The section intends to demonstrate the overall Ferranti impact on the IPS as assets with load connects to the IPS. A summary of the results is captured in Figure 9.15.

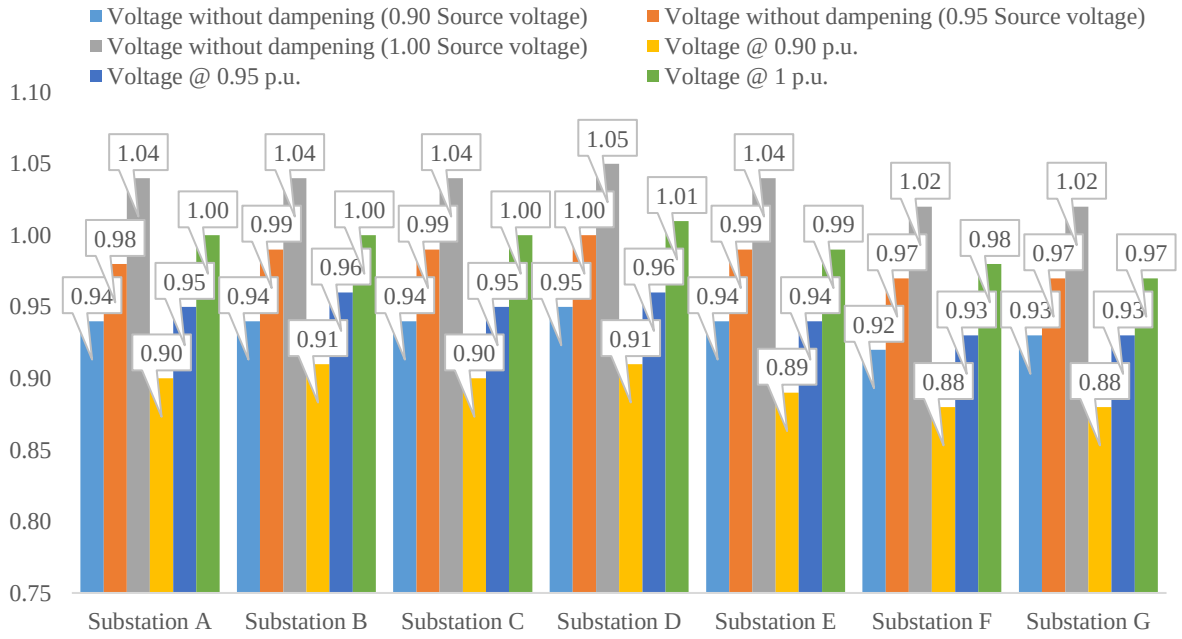

Figure 9.15. Steady-state voltage after energising all stations within the SA IPS

From the results under Figure 9.15, it is evident that there is an impact from the extended network energised, and careful consideration should be taken when selecting the sending end source voltage. The steady-state voltage response analyses confirm IPS security. The undampened scenario demonstrates a voltages increase of 5%. Under scenario two, recommendations were that line lengths below 120km. Under the worst-case scenario (source voltage setting of 1.00 p.u.), using dampening from the connected load, better optimisation is also achieved for the extended IPS.

9.5 CHAPTER SUMMARY

Applying the principles obtained from scenarios one, two and three to scenario four proves effective from the results presented. It is advisable to simulate the restoration steps beforehand before proceeding with restoration activities, as the impact is unknown if not simulated proactively, especially when considering the BESS resource connected. BESS charging will not be done during risky steady-state periods. The result obtained can be applied to a more extensive interconnected power system, using the principle of frequency recovery above 50Hz before connecting the optimal amount of load to the IPS. The deployment of BESS, considering the rate of response of the inverter system and is not factored into the simulation.

The limitation can also be observed during the charge times, which is unrealistic. However, it does provide a capability assessment.

CHAPTER 10 CONCLUSION AND SCOPE FOR FUTURE WORK

10.1 CONCLUSION

Power system restoration is a complex task that requires cross-regional coordination, balancing and managing the IPS risks associated with the three stages of restoration. There are challenges with the frequency bias resulting from the lack of inertia within the IPS due to the absence of sufficient generation resources due to the large scale interruption. The lack of generation resources energised has a significant impact on the transfer of power within the IPS due to the absence of reactive power resources.

After performing the scenario analysis, the maximum load that may connect to the TGOV5 system is 50MW, with the frequency adjusted to 50.85Hz, selecting power factors ranging from 0.98 pf to 0.85 pf lagging. For a frequency adjustment of 50.40Hz, the maximum allowable load that may connect to the IPS is 32MW. For each of the scenarios analysed, the frequency recovers adequately within specified grid code requirements. The TSO will most likely run the frequency no higher than 50.40Hz as this is a safer operating criterion. However, a frequency setpoint of 50.85Hz is possible when carefully coordinating the restoration activities. The most challenging experience is the preparation of the power system, which may take a considerable amount of time, based on the size of most of the transmission stations and the number of distribution stations used to support the dampening of the system frequency. Other than this, once the IPS is ready for the connection of load, verification of the load size through simulation assist with comfortably coordinating

restoration activities. It is vital to have the normalized linking aligned to a power system restoration scenario as far as possible as this would speed up switching activities for the system preparation stage.

The source voltage setpoint is to be kept at a minimum of 0.9 p.u. to ensure the effective management of the system voltages, and if voltage increases are required, it must be done from the source end or more localised. It is essential to adjust the voltage to nominal tap or lower, to limit the inrush when closing a circuit breaker onto a higher voltage adjustment. Locally adjusting the voltage ensures a quality supply to connected customers. Voltage management will be dynamic and requires active control that is difficult to achieve within a simulation.

Dampening through adjusting the load power factor, manages the source voltage rise at the various station. The lower power factor improves the source voltage settling time as the source tap changer is already set to the minimum. A further decrease in sending end voltage will affect the downstream MV distribution network voltage. Slight increases in the sending end voltage will always occur as the network corridor extends (more capacitive) as load connect to the IPS. The addition must be carefully monitored and actively managed.

With UFLS relays armed and connected, disabling armed UFLS relays is a prudent step during the preparation stage for system restoration. The system's frequency will continuously operate within the 51 and 48Hz bandwidths. It is best to keep the armed relays disconnected and to reconnect the relays strategically as the system achieves a stable interconnection to avoid nuisance tripping.

From the utilisation of BESS, the more significant BESS resources (ranging from 30MVA to 50MVA) provide better frequency and load management support during system restoration for the load size considered. The intention is to energise the most considerable load to stabilise the upstream generator and return power to consumers as fast as possible. Smaller BESS sizes cater to the connection of smaller load sizes to the IPS.

Lastly, it is vital to be cognisant of the charge and discharge of the BESS resource. A depleted BESS resource negatively affects the IPS, and disconnecting the resource is recommended and charging should be done during less risky operational periods. It is vital to confirm the simulation outcome as it may not be straightforward.

10.2 SCOPE FOR FUTURE WORK

The restoration efficiency improves by adding automation to the simulation process to speed up restoration studies during an incident. The restoration procedure can be completed in advance using simulation models with multiple plausible scenarios. In addition, certified islanding facilities can support localised restoration islands, and it is a credible option for enhanced grid resilience following the typical top-down restoration philosophy. It will be an additional consideration for IPS resilience enhancement. Furthermore, the extensive analysis of load models supports accurate results in the simulation assessment.

REFERENCES

[1] S. Lee, *Interconnected power system dynamics tutorial*, 3rd ed. Palo Alto, USA: EPRI, 2009.

[2] P. S. Kundur, *Power system stability and control*. Toronto, Ontario, Canada: McGraw-Hill, 2014.

[3] P. S. Kundur, *Power system stability and control volume*, 1st ed. Toronto, Ontario, Canada: McGraw-Hill, 2004.

[4] P. Hines, J. Apt, and S. Talukdar, "Trends in the history of large blackouts in the United States," in *IEEE Power Energy Soc. Gen. Meet. Convers. Deliv. Electr. Energy 21st Century*, Pittsburgh, Pennsylvania, USA, Jul. 2008, vol. 15213, pp. 1–8.

[5] B. A. Carreras, V. E. Lynch, D. E. Newman, and I. Dobson, "Blackout mitigation assessment in power transmission systems," in *36th Annu. Hawaii Int. Conf. Syst. Sci.*, Big Island, Hawaii, USA, Jan. 2003, pp. 1–10.

[6] M. Vaiman, K. Bell, Y. Chen, B. Chowdhury, I. Dobson, P. Hines, M. Papic, S. Miller, and P. Zhang, "Risk assessment of cascading outages: Methodologies and challenges," *IEEE Trans. Power Syst.*, vol. 27, no. 2, pp. 631–641, May 2012.

[7] I. Dobson, D. E. Newman, B. A. Carreras, and V. E. Lynch, "An initial complex systems analysis of the risks of blackouts in power transmission systems," in *Power Syst. Commun. Infrastructures Futur.*, Beijing, China, May 2002, pp. 1–7.

[8] C. Luo, J. Yang, and Y. Sun, “Risk assessment of power system considering frequency dynamics and cascading process,” *Energies*, vol. 11, no. 2, pp. 1–16, Jan. 2018.

[9] Y. Tang, J. Yan, C. Li, S. Luo, and L. He, “China’s valuable experiences in defending large-scale and long-time blackouts,” in *Asia-Pacific Power Energy Eng. Conf.*, Hong Kong, China, Dec. 2013, pp. 1–5.

[10] M. Banafer and M. Biswal, “Investigation of power system cascading failure and the causes,” in *2nd Int. Conf. Energy, Power Environ. Towar. Smart Technol.*, Shillong, India, Mar. 2019, pp. 1–5.

[11] L. H. Fink and K. Carlsen, “Operating under stress and strain,” *IEEE Spectr.*, vol. 15, no. 3, pp. 48–53, Mar. 1978.

[12] G. Andersson, P. Donalek, R. Farmer, N. Hatziargyriou, I. Kamwa, P. Kundur, N. Martins, J. Paserba, P. Pourbeik, J. Sanchez-Gasca, R. Schulz, A. Stankovic, C. Taylor, and V. Vittal, “Causes of the 2003 major grid blackouts in North America and Europe, and recommended means to improve system dynamic performance,” *IEEE Trans. Power Syst.*, vol. 20, no. 4, pp. 1922–1928, Nov. 2005.

[13] A. Atputharajah and T. K. Saha, “Power system blackouts - Literature review,” in *4th Int. Conf. Ind. Inf. Syst.*, Peradeniya, Sri Lanka, Dec. 2009, pp. 460–465.

[14] I. Dobson, B. A. Carreras, V. E. Lynch, and D. E. Newman, “Complex systems analysis of series of blackouts: Cascading failure, critical points, and self-organisation,” *Chaos*, vol. 17, no. 2, pp. 1–13, Apr. 2007.

[15] J. Chen, J. S. Thorp, and M. Parashar, “Analysis of electric power system disturbance data,” in *Proc. Hawaii Int. Conf. Syst. Sci.*, Maui, USA, Jan. 2001, pp. 1–8.

[16] I. Dobson, J. Chen, J. S. Thorp, B. A. Carreras, and D. E. Newman, “Examining criticality of blackouts in power system models with cascading events,” in *Proc.*

Annu. Hawaii Int. Conf. Syst. Sci., Big Island, Hawaii, USA, Jan. 2002, pp. 1–10.

[17] B. A. Carreras, V. E. Lynch, I. Dobson, and D. E. Newman, "Complex dynamics of blackouts in power transmission systems," *Chaos*, vol. 14, no. 3, pp. 643–652, Jun. 2004.

[18] M. Velay, M. Vinyals, Y. Besanger, and N. Retiere, "An analysis of large-scale transmission power blackouts from 2005 to 2016," in *53rd Int. Univ. Power Eng. Conf.*, Glasgow, UK, Sep. 2018, pp. 1–6.

[19] Z. Bo, O. Shaojie, Z. Jianhua, S. Hui, W. Geng, and Z. Ming, "An analysis of previous blackouts in the world: Lessons for China's power industry," *Renew. Sustain. Energy Rev.*, vol. 42, pp. 1151–1163, Oct. 2015.

[20] M. Adibi, P. Clelland, L. Fink, H. Happ, R. Kafka, J. Raine, D. Scheurer, and F. Trefny, "Power system restoration - A task force report," *IEEE Trans. Power Syst.*, vol. 2, no. 2, pp. 271–277, May 1987.

[21] R. G. Farmer and E. H. Allen, "Power system dynamic performance advancement from history of North American blackouts," in *IEEE PES Power Syst. Conf. Expo.*, Atlanta, Georgia, USA, Dec. 2006, pp. 293–300.

[22] L. L. Lai, H. T. Zhang, C. S. Lai, F. Y. Xu, and S. Mishra, "Investigation on July 2012 Indian blackout," in *Int. Conf. Mach. Learn. Cybern.*, Tianjin, China, Jul. 2013, pp. 92–97.

[23] B. Li, P. Gomes, R. Baumann, W. Phillips, A. Guarini, M. Hayden, B. Jayasekara, M. Miller, R. Pestana, L. Vanfretti, R. Krebs, V. Sinagra, T. Smit, and N. Singh, "Lessons learnt from recent emergencies and blackout incidents," Jan. 2015. [Online]. Available: http://www.cigre.org.

[24] Y. Liu, "Analysis of Brazilian blackout on March 21st, 2018 and revelations to security for Hunan grid," in *4th Int. Conf. Intell. Green Build. Smart Grid*, Yichang,

China, Sep. 2019, pp. 422–426.

[25] S. M. Praminta, S. Wiguna, and A. Pramana, “Blackout restoration plan in Jakarta power grid,” in *2nd Int. Conf. Technol. Policy Electr. Power Energy*, Bandung, Indonesia, Sep. 2020, pp. 295–300.

[26] V. Suresh, K. Debnath, R. Sutradhar, and S. Mandal, “Near miss of blackout in Southern part of North Eastern grid of India,” in *3rd Int. Conf. Energy, Power Environ. Towar. Clean Energy Technol.*, Shillong, Meghalaya, India, Mar. 2021, pp. 1–5.

[27] G. Liang, S. R. Weller, J. Zhao, F. Luo, and Z. Y. Dong, “The 2015 Ukraine Blackout: Implications for False Data Injection Attacks,” *IEEE Trans. Power Syst.*, vol. 32, no. 4, pp. 3317–3318, Jul. 2017.

[28] A. Mar, P. Pereira, and J. F. Martins, “A survey on power grid faults and their origins: A contribution to improving power grid resilience,” *Energies*, vol. 12, no. 24, pp. 1–21, Dec. 2019.

[29] B. Chen and H. Chen, “Impact of cyber system failure on cascading blackout of power grid,” in *2nd IEEE Conf. Energy Internet Energy Syst. Integr.*, Beijing, China, Oct. 2018, pp. 18–22.

[30] J. Krupa and S. Burch, “A new energy future for South Africa: The political ecology of South African renewable energy,” *Energy Policy*, vol. 39, no. 10, pp. 6254–6261, Aug. 2011.

[31] A. Lawrence, “Energy decentralization in South Africa : Why past failure points to future success,” *Renew. Sustain. Energy Rev.*, vol. 120, no. 109659, pp. 1–8, Dec. 2019.

[32] I. Pretorius, S. Piketh, R. Burger, and H. Neomagus, “A perspective on South African coal fired power station emissions,” *J. Energy South. Africa*, vol. 26, no. 3, pp. 27–

40, Aug. 2015.

[33] B. Graeber, “Generation and transmission expansion planning in Southern Africa,” in *5th AFRICON Conf. Africa*, Cape Town, SA, Sep. 1999, vol. 2, pp. 983–988.

[34] Eskom, “Integrated report 31,” Mar. 2019. [Online]. Available: https://www.eskom.co.za/OurCompany/Investors/IntegratedReports/Pages/Annual_Statements.aspx.

[35] Eskom, “Medium-term system adequacy outlook,” Oct. 2018. [Online]. Available: https://www.eskom.co.za/Whatweredoing/SupplyStatus/Documents/MediumTermSystemAdequacyOutlook2018.pdf.

[36] M. . Van Harte, R. Koch, A. Nambiar, G. Hurford, T. Smit, S. Joseph, G. Loedolff, and U. Heideman, “Infrastructure resilience: Regional and national blackout planning,” in *CIGRE - South. Africa Reg. Conf.*, Somerset West, Western Cape, SA, Oct. 2015, pp. 1–9.

[37] S. Jain and P. K. Jain, “The rise The of Renewable Energy implementation in South Africa,” in *Energy Procedia*, Jul. 2017, vol. 143, pp. 721–726.

[38] NERSA, *The South African Grid Code: The system operation code*. National energy regulator of South Africa, 2014, pp. 1–24.

[39] M. M. Adibi, J. N. Borkoski, and R. J. Kafka, “Power system restoration - The second task force report,” *IEEE Trans. Power Syst.*, vol. 2, no. 4, pp. 927–932, Nov. 1987.

[40] NERSA, *ELECTRICITY SUPPLY — QUALITY OF SUPPLY Part 2 : Voltage characteristics, compatibility levels, limits and assessment methods*. National energy regulator of South Africa, 2003, pp. 1–33.

[41] J. A. Bohlmann and R. Inglesi-Lotz, “Analysing the South African residential sector’s energy profile,” *Renew. Sustain. Energy Rev.*, vol. 96, pp. 240–252, Aug. 2018.

[42] NERSA, *The South African grid code: The network code*. National energy regulator of South Africa, 2014, pp. 1–61.

[43] NERSA, *Electricity supply - Quality of supply part 9: Load reduction practices, system restoration practices, and critical & essential load requirements under system emergencies*. National energy regulator of South Africa, 2019, pp. 1–103.

[44] L. Musaba, P. Naidoo, and A. Chikova, "Southern African power pool plan development," in *IEEE Power Eng. Soc. Gen. Meet.*, Montreal, Quebec, Canada, Jun. 2006, pp. 1–3.

[45] R. Grünbaum and J. Samuelsson, "Series capacitors facilitate long distance AC power transmission," in *IEEE Russ. Power Tech*, St. Petersburg, Russia, Jun. 2005, pp. 1–6.

[46] N. Petcharaks, C. Yu, and C. Panprommin, "A study of Ferranti and energisation overvoltages case of 500kV line in Thailand," in *High Volt. Eng. Symp.*, London, United Kingdom, Aug. 1999, pp. 291–294.

[47] B. Gou, H. Zheng, W. Wu, and X. Yu, "The statistical law of power system blackouts," in *38th North Am. Power Symp.*, Carbondale, Illinois, USA, Sep. 2006, pp. 495–501.

[48] M. Parihar and M. K. Bhaskar, "Review of power system blackout," *Int. J. Res. Innov. Appl. Sci.*, vol. 3, no. 6, pp. 1–7, Sep. 2018.

[49] R. Moreno, M. A. Ríos, and A. Torres, "Security schemes of power systems against blackouts," in *IREP Symp. - Bulk Power Syst. Dyn. Control - VIII*, Rio de Janeiro, Brazil, Aug. 2010, pp. 1–6.

[50] B. Carreras, D. Newman, I. Dobson, and A. Poole, "Evidence for self-organised criticality in a time series of electric power system blackouts," *IEEE Trans. Circuits Syst.*, vol. 51, no. 9, pp. 1733–1740, Sep. 2004.

[51] R. Yan, N. Al-Masood, T. Kumar Saha, F. Bai, and H. Gu, "The anatomy of the 2016

South Australia blackout: A catastrophic event in a high renewable network," *IEEE Trans. Power Syst.*, vol. 33, no. 5, pp. 5374–5388, Sep. 2018.

[52] A. L. J. Janssen, A. Kubis, J. M. Willieme, K. Aprosin, Q. Zhuang, G. Poggi, S. McGuinness, L. N. . De Villiers, S. Suganuma, S. Temtem, K. Jones, S. Yoshimoto, and T. Geraerds, "System conditions for and probability of out-of-phase," Jan. 2018.

[53] O. Samuelsson and S. Lindahl, "Discussion of 'Definition and classification of power system stability,'" *IEEE Trans. Power Syst.*, vol. 19, no. 2, pp. 1387–1401, May 2004.

[54] Z. Daria and K. Sroka, "The characteristics and main causes of power system failures basing on the analysis of previous blackouts in the world," in *Int. Interdiscip. PhD Work.*, Poland, May 2018, pp. 257–262.

[55] K. Sroka and D. Złotecka, "The risk of large blackout failures in power systems," *Arch. Electr. Eng.*, vol. 68, no. 2, pp. 411–426, Feb. 2019.

[56] L. H. Fink, K. L. Liou, and C. C. Liu, "From generic restoration actions to specific restoration strategies," *IEEE Trans. Power Syst.*, vol. 10, no. 2, pp. 237–244, May 1995.

[57] P. Pradhan, T. Deki, P. Wangmo, D. Dorji, D. Phuntsho, and C. Dorji, "Simulation and optimization of blackstart restoration plan in Bhutan using DIgSILENT," in *2nd Int. Conf. Recent Adv. Eng. Comput. Sci.*, Chandigarh, India, Dec. 2015, pp. 1–6.

[58] M. M. Adibi and D. P. Milanicz, "Estimating restoration duration," *IEEE Trans. Power Syst.*, vol. 14, no. 4, pp. 1493–1498, Nov. 1999.

[59] J. J. Ancona, "A framework for power system restoration following a major power failure," *IEEE Trans. Power Syst.*, vol. 10, no. 3, pp. 1480–1485, Aug. 1995.

[60] M. M. Adibi and L. H. Fink, "Power system restoration planning," *IEEE Trans. Power Syst.*, vol. 9, no. 1, pp. 22–28, Feb. 1994.

[61] M. M. Adibi and R. J. Kafka, “Power system restoration issues,” *IEEE Comput. Appl. Power*, vol. 4, no. 2, pp. 19–24, Apr. 1991.

[62] S. Liu, “Development of power system restoration tool based on generic restoration milestones,” Palo Alto, California, USA, Dec. 2010.

[63] IEEE, *Design of Reliable Industrial and Commercial Power Systems*, vol. 493. New York, USA: IEEE, 2007.

[64] Republic of South Africa, *Disaster Management Act 57*, vol. 451, no. 24252. Parliament of the Republic of South Africa, 2003, pp. 1–32.

[65] D. Złotecka and K. Sroka, “The characteristics and main causes of power system failures basing on the analysis of previous blackouts in the world,” in *Int. Interdiscip. PhD Work.*, Poland, May 2018, pp. 257–262.

[66] B. Hoseinzadeh, F. F. Da Silva, and C. L. Bak, “Power system stability using decentralized under frequency and voltage load shedding,” in *IEEE Power Energy Soc. Gen. Meet.*, National Harbor, Maryland, USA, Oct. 2014, pp. 1–5.

[67] M. Nilsson, L. Söder, and Z. Yuan, “Estimation of power system frequency response based on measured and simulated frequencies,” in *IEEE Power Energy Soc. Gen. Meet.*, Boston, Massachusetts, USA, Jul. 2016, pp. 1–5.

[68] M. M. Adibi and L. H. Fink, “Overcoming restoration challenges associated with major power disturbances,” *IEEE Power and Energy Magazine*, vol. 4, no. 5, pp. 68–77, Sep. 2006.

[69] J. W. Feltes, S. Member, C. Grande-moran, and S. Member, “Black start studies for system restoration,” in *Power Energy Soc. Gen. Meet. - Convers. Deliv. Electr. Energy 21st Century*, Pittsburgh, Pennsylvania, USA, Jul. 2008, pp. 1–8.

[70] M. M. Adibi, L. H. Fink, C. J. Andrews, F. Arsanjani, M. W. Lanier, J. M. Miller, T. A. Volkmann, and J. Wrubel, “Special consideration in power system restoration. The

second working group report," *IEEE Trans. Power Syst.*, vol. 7, no. 4, pp. 1419–1427, Nov. 1992.

[71] M. M. Adibi and N. Martins, "Power system restoration dynamics issues," in *IEEE Power Energy Soc. Gen. Meet. - Convers. Deliv. Electr. Energy 21st Century*, Pittsburgh, Pennsylvania, USA, Jul. 2008, pp. 1–8.

[72] M. A. Van Harte, R. Koch, A. Nambiar, S. Joseph, I. Tshwagong, L. Naidoo, and U. Heideman, "Power system resilience – enablers supporting an effective blackout response," in *CIGRE - South. Africa Reg. Conf.*, Somerset West, Western Cape, SA, Nov. 2017, pp. 1–9.

[73] M. A. Van Harte, R. Koch, A. Nambiar, S. Joseph, I. Tshwagong, L. Naidoo, and U. Heideman, "Power system resilience – enablers supporting an effective blackout response," in *CIGRE - South. Africa Reg. Conf.*, Somerset West, Western Cape, SA, Aug. 2017, pp. 1–9.

[74] P. Jamborsalamati, M. Moghimi, M. J. Hossain, S. Taghizadeh, J. Lu, and G. Konstantinou, "A framework for evaluation of power grid resilience case study: 2016 South Australian blackout," in *IEEE Int. Conf. Environ. Electr. Eng. IEEE Ind. Commer. Power Syst. Eur.*, Palermo, Italy, Jun. 2018, pp. 1–6.

[75] M. M. Adibi, "Special consideration in power system restoration," *IEEE Trans. Power Syst.*, vol. 9, no. 1, pp. 15–21, Feb. 1994.

[76] M. M. Adibi, R. W. Alexander, and D. P. Milanicz, "Energizing high voltage and extra-high voltage lines during restoration," *IEEE Trans. Power Syst.*, vol. 14, no. 3, pp. 1121–1126, Aug. 1996.

[77] T. Funakoshi, K. Furukawa, T. Kawachino, S. Takasaki, T. Shimojo, K. Hirayama, T. Sogabe, T. Shimamura, H. Hashimoto, and S. Nohara, "Transformer overvoltage problems and countermeasures at black Start," in *IEEE Power Eng. Soc. Gen. Meet. Conf. Proc.*, Toronto, Ontario, Canada, Jul. 2003, pp. 581–588.

[78] D. Lindenmeyer, H. W. Dommel, A. Moshref, and P. Kundur, "Framework for black start and power system restoration," in *Can. Conf. Electr. Comput. Eng.*, Halifax, Nova Scotia, Canada, May 2000, pp. 153–157.

[79] K. P. Haggerty, "Dynamics of heating and cooling loads: Models, simulation, and actual utility data," *IEEE Trans. Power Syst.*, vol. 5, no. 1, pp. 243–249, Feb. 1990.

[80] J. Law, L. Elliott, D. Minford, and M. Storms, "Measured and predicted cold load pick up and feeder parameter determination using the harmonic model algorithm," *IEEE Trans. Power Syst.*, vol. 10, no. 4, pp. 1756–1764, Nov. 1995.

[81] N. D. Hatziargyriou and M. Papadopoulos, "Cold load pickup studies in extended distribution networks," in *6th Mediterr. Electrotech. Conf.*, LJubljana, Slovenia, May 1991, pp. 1404–1407.

[82] M. M. Adibi and R. J. Kafka, "Power system restoration issues," *IEEE Comput. Appl. Power*, vol. 19, no. 91, pp. 31–36, Apr. 1991.

[83] H. D. Chiang, F. F. Wu, and P. P. Varaiya, "Foundations of direct methods for power system transient stability analysis," *IEEE Trans. Circuits Syst.*, vol. 34, no. 2, pp. 160–173, Feb. 1987.

[84] S. G. Abhyankar and A. J. Flueck, "Simulating voltage collapse dynamics for power systems with constant power load models," in *IEEE Power Energy Soc. Gen. Meet. Convers. Deliv. Electr. Energy 21st Century*, Pittsburgh, Pennsylvania, USA, Jul. 2008, pp. 1–6.

[85] V. Yari, S. Nourizadeh, and A. M. Ranjbar, "Determining the best sequence of load pickup during power system restoration," in *9th Int. Conf. Environ. Electr. Eng.*, Prague, Czech Republic, May 2010, pp. 1–4.

[86] H. W. K. M. Amarasekara, L. Meegahapola, A. P. Agalgaonkar, and S. Perera, "Impact of renewable power integration on VQ stability margin," in *Australas. Univ.*

Power Eng. Conf., Hobart, Tasmania, Australia, Sep. 2013, pp. 1–6.

[87] M. M. Adibi, D. P. Milanicz, and T. L. Volkmann, "Remote cranking of steam electric stations," *IEEE Trans. Power Syst.*, vol. 11, no. 3, pp. 1613–1618, Aug. 1996.

[88] W. Sun, C. C. Liu, and L. Zhang, "Optimal generator start-up strategy for bulk power system restoration," *IEEE Trans. Power Syst.*, vol. 26, no. 3, pp. 1357–1366, Aug. 2011.

[89] M. M. Adibi, "Remote blackstart of steam electric station," in *IEEE Power Eng. Soc. Summer Meet.*, Chicago, Illinois, USA, Jul. 2002, pp. 1229–1232.

[90] M. M. Adibi, D. P. Milanicz, and T. L. Volkmann, "Optimizing generator reactive power resources," *IEEE Trans. Power Syst.*, vol. 14, no. 1, pp. 319–326, Feb. 1999.

[91] M. M. Adibi and D. P. Milanicz, "Reactive capability limitation of synchronous machines," *IEEE Trans. Power Syst.*, vol. 9, no. 1, pp. 29–40, Feb. 1994.

[92] M. Power, C. Roggatz, C. Norlander, E. Diskin, S. Power, M. Kranhold, A. Probst, R. Belhomme, A. Bose, J. Gaudin, D. Moneta, D. Ilisiu, R. Schwerdfeger, N. Singh, J. Reilly, T. Hearne, D. Nnabuife, E. Kaempf, M. Sanchez Llorente, *et al.*, "System operation emphasizing DSO/TSO interaction and coordination," Jun. 2018.

[93] Q. Liu, M. Cao, and D. Wang, "The analysis of the reactive power ancillary service of regional grid," in *Int. Conf. Electron. Commun. Control*, Ningbo, China, Sep. 2011, pp. 2332–2335.

[94] P. Pourbeik, R. Boyer, K. Chan, G. Chown, J. Feltes, C. Grande-Moran, L. Gérin-Lajoie, F. Langenbacher, D. Leonardo, L. Lima, L. Hajagos, L. Hannett, W. Hofbauer, F. Modau, M. Patel, S. Patterson, S. Sterpu, A. Schneider, and J. Undrill, "Dynamic models for Turbine-Governors in power system studies," IEEE Power & Energy Society, New York, USA, Jan. 2013.

[95] M. M. Adibi, R. A. Polyak, I. A. Griva, L. Mili, and S. Ammari, "Optimal transformer

tap selection using modified barrier-augmented Lagrangian method," *IEEE Trans. Power Syst.*, vol. 18, no. 1, pp. 251–257, Feb. 2003.

[96] M. M. Adibi, D. P. Milanicz, and T. L. Volkmann, "Asymmetry issues in power system restoration," *IEEE Trans. Power Syst.*, vol. 14, no. 3, pp. 1085–1092, Aug. 1999.

[97] V. León-Martínez, J. Montañana-Romeu, J. Giner-García, A. Cazorla-Navarro, J. Roger-Folch, and M. A. Graña-López, "Power quality effects on the measurement of reactive power in three-phase power systems in the light of the IEEE standard 1459-2000," in *9th Int. Conf. Electr. Power Qual. Util.*, Barcelona, Spain, Oct. 2007, pp. 1–6.

[98] S. Lee, *EPRI Power systems dynamics tutorial without Q/A section*, 1018866th ed. Palo Alto, California, USA: EPRI, 2009.

[99] R. N. Nayak, Y. K. Sehgal, and S. Sen, "EHV transmission line capacity enhancement through increase in surge impedance loading level," in *IEEE Power India Conf.*, New Delhi, India, Apr. 2006, pp. 1–4.

[100] F. Edström, J. Rosenlind, P. Hilber, and L. Söder, "Modeling impact of cold load pickup on transformer aging using ornstein-uhlenbeck process," *IEEE Trans. Power Deliv.*, vol. 27, no. 2, pp. 590–595, Apr. 2012.

[101] K. McKenna and A. Keane, "Residential load modelling of price-based demand response for network impact studies," *IEEE Trans. Smart Grid*, vol. 7, no. 5, pp. 2285–2294, Sep. 2016.

[102] H. Qu and Y. Liu, "General model for determining maximum restorable load," in *IEEE Power Energy Soc. Gen. Meet.*, San Diego, California, USA, Jul. 2012, pp. 1–6.

[103] E. Agneholm and J. Daalder, "Cold load pick-up of residential load," in *IET Proc.* -

Gener. Transm. Distrib., Feb. 2000, vol. 147, no. 1, pp. 44–50.

[104] T. Babnik, S. Gagperir, A. Gubina, and F. Gubina, "Influence of load behavior on service restoration," in *Int. Conf. Electr. Power Eng.*, Budapest, Hungary, Aug. 1999, pp. 116–116.

[105] K. P. Schneider, E. Sortomme, S. S. Venkata, M. T. Miller, and L. Ponder, "Evaluating the magnitude and duration of cold load pick-up on residential distribution feeders using multi-state load models," *IEEE Trans. Power Syst.*, vol. 31, no. 5, pp. 3765–3774, Sep. 2016.

[106] M. M. Adibi, P. M. Hirsh, and J. A. Jordan, "Solution methods for transient and dynamic stability," *Proc. IEEE*, vol. 62, no. 7, pp. 951–959, Jul. 1974.

[107] M. M. Adibi and D. P. Milanicz, "Protective system issues during restoration," *IEEE Trans. Power Syst.*, vol. 10, no. 3, pp. 1492–1497, Aug. 1995.

[108] T. W. K. Mak, C. Coffrin, P. Van Hentenryck, I. A. Hiskens, and D. Hill, "Power system restoration planning with standing phase angle and voltage difference constraints," in *Power Syst. Comput. Conf.*, Wroclaw, Poland, Aug. 2014, pp. 1–8.

[109] O. P. Veloza and R. H. Cespedes, "Vulnerability of the Colombian electric system to blackouts and possible remedial actions," in *IEEE Power Eng. Soc. Gen. Meet.*, Montreal, Quebec, Canada, Jun. 2006, pp. 1–7.

[110] M. Rampokanyo and P. Ijumba-Kamera, "Power system inertia in an inverter-dominated network," *J. Energy South. Africa*, vol. 30, no. 2, pp. 80–86, May 2019.

[111] G. Chown, J. Wright, R. van Heerden, and M. Coker, "System inertia and rate of change of frequency (RoCoF) with increasing non-synchronous renewable energy penetration," in *CIGRE - 8th South. Africa Reg. Conf.*, Somerset West, Western Cape, South Africa, Nov. 2017, pp. 214–219.

[112] NERC, "Frequency response standard background document," Nov. 2012. [Online].

Available: https://www.nerc.com/pa/Stand/Project 200712 Frequency Response DL/Bal-003-1-Background_Document-Clean-2013_FILING.pdf.

[113] K. P. Schneider, N. Radhakrishnan, C. C. Liu, and J. Xie, "Improving primary frequency response to support networked microgrid operations," *IEEE Trans. Power Syst.*, vol. 34, no. 1, pp. 1–10, Jan. 2019.

[114] NERC, "Balancing and frequency control," Jan. 2011. [Online]. Available: https://www.nerc.com/docs/oc/rs/NERC Balancing and Frequency Control 040520111.pdf.

[115] N. Tephiruk and K. Hongesombut, "System identification of an interconnected power system with an energy storage system for robust stability improvement," in *IEEE Innov. Smart Grid Technol.*, Bangkok, Thailand, Nov. 2015, pp. 1–5.

[116] H. L. Nguyen, "Newton-Raphson method in complex form," *IEEE Trans. Power Syst.*, vol. 12, no. 3, pp. 1355–1359, Aug. 1997.

[117] A. M. Eltamaly, Y. Sayed, and A. N. A. Elghaffar, "Optimum Power Flow Analysis By Newton Raphson," *Ann. Fac. Eng. Hunedoara – Int. J. Eng.*, vol. 4, pp. 51–58, Dec. 2018.

[118] DIgSILENT GmbH, *DIgSILENT PowerFactory 2018 user manual*. 2018.

[119] F. M. Hughes, "Improvement of turbogenerator transient performance by control means," *Proc. IEEE*, vol. 120, no. 2, pp. 233–240, Feb. 1973.

[120] Y. K. Wu and K. T. Tang, "Frequency support by BESS – Review and analysis," in *5th Int. Conf. Power Energy Syst. Eng.*, Nagoya, Japan, Sep. 2018, vol. 156, pp. 187–198.

[121] C. Wannasut and K. Hongesombut, "A study of BESS application for the diferral of power distribution system investment," in *Int. Conf. Inf. Sci. Electron. Electr. Eng.*, Sapporo, Japan, Apr. 2014, vol. 3, pp. 1624–1628.

[122] Y. P. Gusev and P. V. Subbotin, “Using battery energy storage systems for load balancing and reactive power compensation in distribution grids,” in *Int. Conf. Ind. Eng. Appl. Manuf.*, Sochi, Russia, Mar. 2019, pp. 1–5.

[123] K. Qing, Q. Huang, S. Chen, W. Hu, and J. W. Henan, “Optimized operating strategy for a distribution network containing BESS and renewable energy,” in *IEEE PES Innov. Smart Grid Technol.*, Chengdu, China, May 2019, pp. 1593–1597.

[124] N. Zagoras, K. Balasubramaniam, I. Karagiannidis, and E. B. Makram, “Battery Energy Storage Systems,” in *North Am. Power Symp.*, Charlotte, North Carolina, Oct. 2015, pp. 1–6.

[125] Z. A. Obaid, L. M. Cipcigan, M. T. Muhssin, and S. S. Sami, “Control of a population of battery energy storage systems for frequency response,” *Int. J. Electr. Power Energy Syst.*, vol. 115, no. March 2019, pp. 1–8, 2020.

[126] A. P. Tellez, “Modelling aggregate loads in power systems,” KTH Royal Institute of Technology, 2017.

[127] U. Eminoglu and M. H. Hocaoglu, “A new power flow method for radial distribution systems including voltage dependent load models,” *Electr. Power Res. Inst.*, vol. 76, no. 1–3, pp. 106–114, Sep. 2005.

[128] M. H. Haque, “Load flow solution of distribution systems with voltage dependent load models,” *Electr. Power Syst. Res.*, vol. 36, no. 3, pp. 151–156, Mar. 1996.

ADDENDUM A CALCULATION MODELS AND PARAMETERS

A.1 - CALCULATION PARAMETERS FOR CCL AND CPL

Frequency (Hz)	Scenario	Settling power (MW)	Voltage (p.u.)	CCL setpoint (MW)	CCL Peak load (MW) (measured)	CCL Lowest frequency (Hz) (measured)	CPL setpoint (MW)	CPL Peak load (MW) (measured)	CPL Low frequency (Hz) (measured)	Frequency difference (Hz)
50.4	1	20	0.9	23.971	21.117	49.567	21.805	20.497	49.582	0.015
50.4	2	30	0.9	36.089	32.587	48.151	32.764	31.136	48.176	0.025
50.4	3	32	0.9	38.532	34.967	47.538	34.964	33.299	47.574	0.036
50.4	4	34	0.9	40.961	37.357	46.725	37.157	35.465	46.771	0.046
50.4	1	20	1.0	19.386	20.971	49.557	19.688	20.484	49.582	0.025
50.4	2	30	1.0	29.163	32.333	48.156	29.576	31.103	48.176	0.020
50.4	3	32	1.0	31.132	34.558	47.545	31.56	32.26	47.574	0.029

Frequency (Hz)	Scenario	Settling power (MW)	Voltage (p.u.)	CCL setpoint (MW)	CCL Peak load (MW) (measured)	CCL Lowest frequency (Hz) (measured)	CPL setpoint (MW)	CPL Peak load (MW) (measured)	CPL Low frequency (Hz) (measured)	Frequency difference (Hz)
50.4	4	34	1.0	33.088	36.888	46.735	33.538	35.42	46.771	0.036
50.8	1	20	0.9	23.971	21.12	50	21.806	20.5	50	0.000
50.8	2	30	0.9	36.095	32.606	49.829	32.766	31.153	49.86	0.031
50.8	3	40	0.9	48.330	44.747	49.238	43.772	42.058	49.301	0.063
50.8	4	42	0.9	50.788	47.187	49.075	45.978	44.256	49.145	0.070
50.8	5	44	0.9	53.245	49.600	48.887	48.183	46.448	48.965	0.078
50.8	6	46	0.9	55.719	52.002	48.654	50.395	48.640	48.741	0.087
50.8	7	48	0.9	58.214	54.398	48.217	52.618	48.640	48.318	0.101
50.8	8	50	0.9	60.638	56.702	47.553	54.808	52.986	47.649	0.096
50.8	9	52	0.9	63.133	59.048	46.757	57.028	55.158	46.857	0.100

A.2 - TRANSMISSION LINE PARAMETERS

Name	Rated voltage(kV)	Rated current (kA)	Nominal Frequency (Hz)	R' (AC,20°C) (Ohm/km)	X' (Ohm/km)	L' (mH/km)	R0' (Ohm/km)	X0' (Ohm/km)	L0' (mH/km)
1x2BEAR 50 510 2x104E	400	1.042	50	0.0577	0.331538	1.055318	0.422251	1.002066	3.189675
1x2BEAR 50 U40 2x104E	400	1.042	50	0.057238	0.33394	1.062964	0.413505	1.00663	3.204203
1x2BERSFORT 50 515 2x104E	400	1.93	50	0.022561	0.322201	1.025598	0.378828	0.994891	3.166836
1x2DINOSAUR 50 501 2x104E	400	1.876	50	0.029532	0.315632	1.004688	0.438774	0.940225	2.992829
1x2GOAT 50 510 2x104E	400	1.236	50	0.047286	0.328377	1.045256	0.411837	0.998905	3.179613
1x2ZEBRA 50 510 2x104E	400	1.42	50	0.036271	0.326053	1.037859	0.400822	0.996581	3.172216
1x3BEAR 50 524 2x104E	400	1.563	50	0.038068	0.296727	0.944511	0.367527	1.039034	3.307348
1x3BERSFORT 50 503 2x104E	400	2.895	50	0.015777	0.286358	0.911506	0.375169	0.959898	3.05545
1x3DINOSAUR 50 503 2x104E	400	2.814	50	0.016283	0.285768	0.909628	0.375676	0.959309	3.053575
1x3KINGBIRD 50 527 2x104E	400	1.758	50	0.030919	0.196939	0.626877	0.34679	1.206581	3.840667
1x3TERN 50 515 2x104E	400	1.995	50	0.026058	0.293407	0.933944	0.382325	0.966097	3.075182
1x4BEAR 50 433 2x104E	400	2.084	50	0.029552	0.252585	0.804003	0.411811	0.949637	3.022789
1x4WOLF 50 515 2x104E	400	1.452	50	0.048012	0.283038	0.900938	0.404278	0.955728	3.042177
1x4ZEBRA 50 433 2x104E	400	2.84	50	0.018838	0.249842	0.795272	0.401097	0.946894	3.014057

Name	Rated voltage(kV)	Rated current (kA)	Nominal Frequency (Hz)	R' (AC,20°C) (Ohm/km)	X' (Ohm/km)	L' (mH/km)	R0' (Ohm/km)	X0' (Ohm/km)	L0' (mH/km)
2x2DINOSAUR 50 513 2x104E	400	1.876	50	0.023929	0.328364	1.045215	0.685576	1.72734	5.498294

A.3 - BESS INVERTER CONTROL MODULE

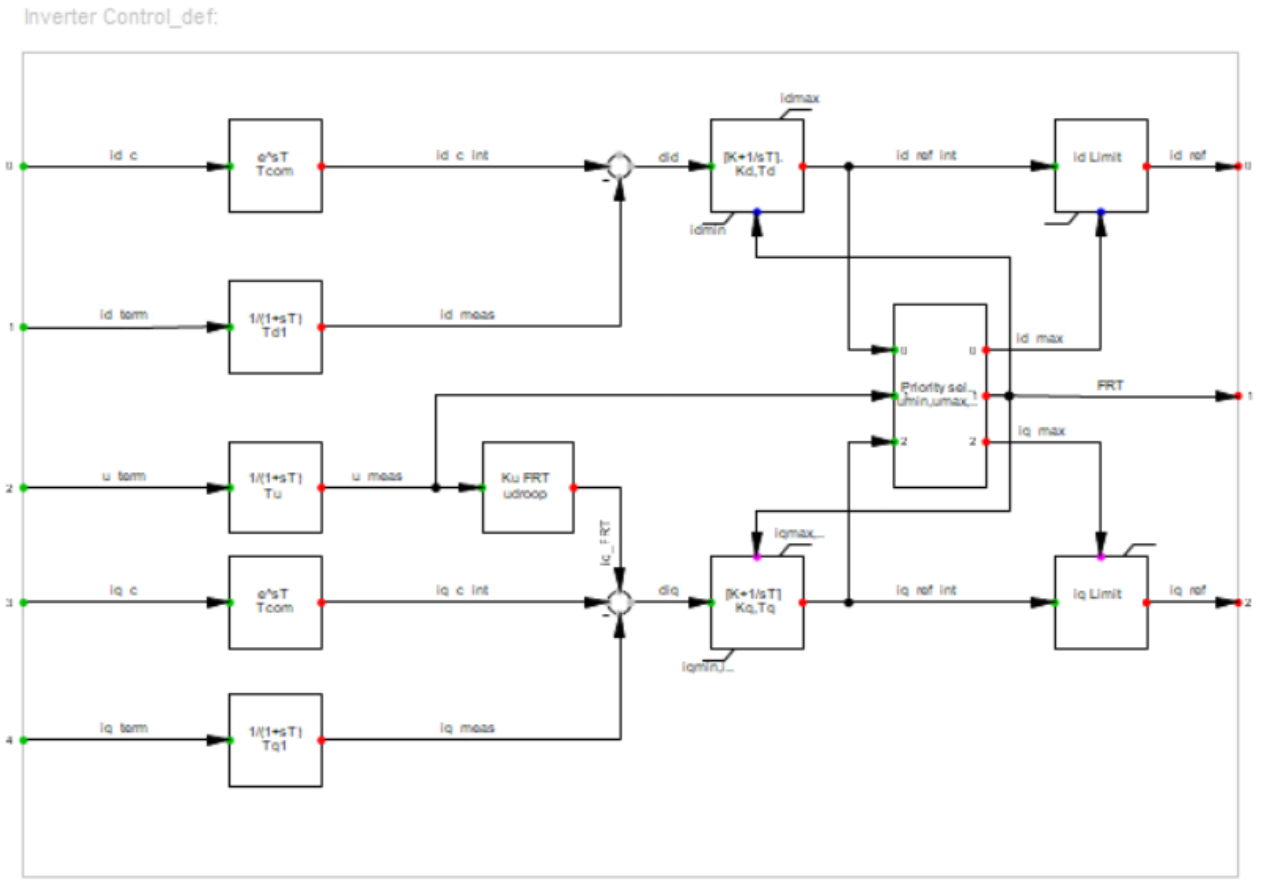

A.4 - GENERATOR PARAMETERS

Name	Local Controller	Active power (MW)	Reactive power (Mvar)	Apparent power (MVA)	power factor	cos(phi) (ind, cap)	Angle (degrees)	Min. Voltage Setpoint (p.u.)	Max. Voltage Setpoint (p.u.)
Blackstart Gen 1	constv	641	0	641	1	ind.	0	0.9	1.1
Substation F Gen 1	constv	303	0	303	1	ind.	0	0.9	1.1
Substation G Gen 1	constv	135	0	135	1	ind.	0	0.9	1.1

A.5 - DEFAULT PARAMETERS FOR THE TGOV5

Parameter	Description	Value
B	The frequency bias for load reference control [p.u.]	0.05
C_1	The pressure drop coefficient	0.2
C_2	The gain for pressure error bias	0
C_3	The adjustment to the pressure set point	1
C_b	The boiler storage time constant [s]	750
C_{max}	The maximum controller output [p.u.]	1.2
C_{min}	The minimum controller output [p.u.]	0.1
D_{pe}	The deadband in the pressure error signal for load reference control [p.u. of pressure]	0.001
K	Controller gain [p.u.]	5
K_1	High pressure turbine factor [p.u.]	0.3
K_{10}	The gain of anticipation signal from the main steam flow	0.1
K_{11}	The gain of anticipation signal from load demand	0.1
K_{12}	The gain for pressure error bias	0.02
K_{13}	The gain between MW demand and pressure setpoint	0.02
K_{14}	Inverse of load reference servomotor time constant [s]	5
K_2	High-pressure turbine factor [p.u.]	0
K_3	Intermediate pressure turbine factor [pu]	0.25
K_4	Intermediate pressure turbine factor [p.u.]	0
K_5	Medium pressure turbine factor [p.u.]	0.3
K_6	Medium pressure turbine factor [p.u.]	0
K_7	Low-pressure turbine factor [p.u.]	0.15
K8	Low-pressure turbine factor [p.u.]	0
K_9	The adjustment to the pressure drop coefficient as a function of drum pressure	0
K_I	The feedback gain from the load reference (0 or 1)	1
K_i	The controller integral gain [p.u.]	0.02
K_{mw}	The gain of the MW transducer (0 or 1)	1
L_{max}	The maximum load reference [p.u.]	1

Parameter	Description	Value
L_{min}	The minimum load reference [p.u.]	0.2
PNhp	HP turbine rated power (=0->PNhp=PgnnHP) [MW]	0
PNlp	LP turbine rated power (=0->PNhp=PgnnHP) [MW]	0
P_{sp}	The initial throttle pressure set point	1
R_{max}	The load reference positive rate of change limit [p.u./s]	0.3
R_{min}	The load reference negative rate of change limit [p.u./s]	-0.3
T_1	Governor time constant [s]	0.2
T_2	Governor derivative time constant [s]	1
T_3	Servo time constant [s]	0.6
T_4	High pressure turbine time constant [s]	0.6
T_5	Intermediate pressure turbine time constant [s]	0.5
T_6	Medium Pressure Turbine Time Constant [s]	0.8
T_7	Low Pressure Turbine Time Constant [s]	1
T_d	The time delay in the fuel supply system [s]	60
T_f	The fuel and air system time constant [s]	25
T_i	The controller proportional lead time constant [s]	90
T_{mw}	The MW transducer time constant [s]	10
T_r	The controller rate lead time constant [s]	60
T_{ri}	The inherent lag associated with lead TR [s]	6
T_w	Fuel flow time constant [s]	7
U_c	Valve Closing Time [p.u./s]	-0.3
U_o	Valve Opening Time [p.u./s]	0.3
V_{max}	Maximum Gate Limit [p.u.]	1
V_{min}	Minimum Gate Limit [p.u.]	0